INORGANIC CHEMISTRY
FRONTIERS

REVIEW

View Article Online
View Journal | View Issue



Cite this: *Inorg. Chem. Front.*, 2025, **12**, 897

# Anticancer iridium(III) cyclopentadienyl complexes

Pavel Štarha

Received 30th September 2024,
Accepted 11th December 2024

DOI: 10.1039/d4qi02472a

rsc.li/frontiers-inorganic

Platinum-based anticancer drugs have been highly effective at treating various cancers. While they have shown significant promise, their potential limitations have motivated researchers to explore other noble metal-based compounds, including iridium (Ir) complexes. Among these, half-sandwich Ir(III) cyclopentadienyl (Ir–Cp$^x$) complexes have emerged as promising new anticancer compounds. This relatively new area of bioinorganic chemistry has made significant progress since its inception in 2007, although no representative has yet entered clinical trials. Recent studies over the past 5–10 years have significantly advanced our understanding of the stability, speciation, intracellular localization, target organelles and molecular targets involved in the mechanisms of action (MoAs) of these compounds. This comprehensive review provides the reader with an overview of anticancer Ir–Cp$^x$ complexes and diverse chemical, biochemical and biological methods used for their research and development. Structure–activity relationships (SARs) and mechanisms of action (MoAs) are discussed with respect to anticancer activity and in comparison with their structurally similar ruthenium(II), rhodium(III) and osmium(II) analogues. Considerable attention is paid to *in vivo* anticancer activity and related aspects, such as drug delivery strategies, multi-component drugs or photodynamic therapy.



## 1. Introduction

Iridium (Ir) is a d-block noble metal, belonging to group 9 and period 6 of the periodic table and having atomic number 77.[1] Ir is considered to be one of the rarest elements on Earth and is known for being highly inert and non-corrosive. Iridium, as one of the platinum (Pt) metals, typically occurs together with platinum and the other platinum metals in the same deposits (alloys, sulfides). It is used in various alloys (*e.g.*, for hardening, corrosion resistance and heat resistance) or catalysts (methanol carbonylation in the Cativa process using the $[Ir(CO)_2I_2]^-$ complex).[2] Iridium-based catalysts have been widely used in various processes, such as C–H bond activation or asymmetric hydrogenation.[3–5]

In the periodic table, Ir is positioned next to Pt, the complexes of which (*e.g.*, cisplatin, carboplatin or oxaliplatin) have been used for the treatment of various types of cancer for more than forty years.[6,7] Even Rosenberg's initial study on cisplatin identified several non-platinum compounds as having similar biological effects to those of cisplatin. Among them, the ruthenium(III) complex $[RuCl(NH_3)_4(OH)]Cl$ seems to be the first non-platinum complex reported to have anticancer activity. Later, Ru became a prominent d-block metal in the fields of bioinorganic and bioorganometallic chemistry,[8,9] because several complexes have entered clinical trials as new anticancer metallodrugs.[10–12]

Following early studies on bioactive Ru complexes and the relative success of this type of compound, complexes of osmium,[13] rhodium[14] and iridium[15] were introduced into the field of bioinorganic chemistry a couple of years later. Nowadays, Ru, Os, Rh and Ir complexes[9,16,17] are accepted as prospective candidates for the research and development of new metallodrugs (Fig. 1).[18] Regarding iridium, the first complexes bioanalysed in the 1970 and 80s were $(NH_4)_2[Ir^{IV}Cl_6]$ (**1**)[15] and $[Ir^I(\eta^4\text{-cod})(acac)]$ (**2**)[14,19] (Fig. 1); cod = cycloocta-1,5-diene, Hacac = pentane-2,4-dione. Especially Ir(I) complexes have been investigated in depth, because their metal centre is isoelectronic with Pt(II), which is involved in conventional Pt anticancer drugs. Later, other Ir oxidation states and structural types were introduced, such as octahedral polypyridyl (*e.g.*, *fac*-$[IrCl_3(dmso)(phen)]$ (**3**))[20] or cyclometalated (*e.g.*, $[Ir(biq)(ppy)_2]$ (**4**))[21] Ir(III) complexes or pseudo-octahedral half-sandwich Ir(III) cyclopentadienyl complexes (*e.g.*, $[Ir(\eta^5\text{-Cp}^*)Cl(dppz)]CF_3SO_3$ (**5**)),[22] as new anticancer agents (Fig. 1); dmso = dimethyl sulfoxide, phen = 1,10-phenanthroline, biq = 2,2′-biquinoline, Hppy = 2-phenylpyridine, HCp* = 1,2,3,4,5-pentamethylcyclopenta-1,3-diene, dppz = dipyrido[3,2-*a*:2′,3′-*c*]phenazine. Other types of Ir complexes have also been reported as having anticancer properties *in vitro*.[23,24] Although anticancer complexes have been the subject of extensive research, significantly fewer compounds have been studied for their antimicrobial or other biological properties.[25]

In contrast to Pt-based drugs, non-platinum half-sandwich metallodrugs of Ru, Os, Rh and Ir do not primarily target DNA and kill the cancer cells through a different mechanism of

*Department of Inorganic Chemistry, Faculty of Science, Palacky University Olomouc, 17. listopadu 12, 77146 Olomouc, Czech Republic. E-mail: pavel.starha@upol.cz; Tel: +420 585 634 348*

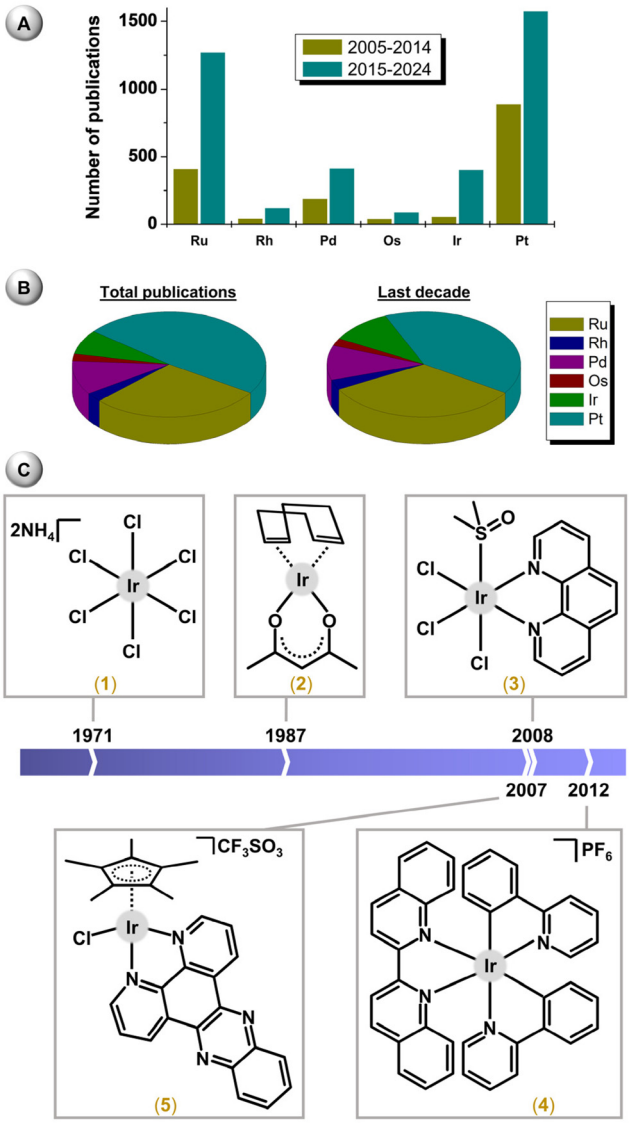


**Fig. 1** (A) Absolute and (B) relative number of scientific publications dealing with anticancer complexes of platinum metals. (C) Chronology of the pioneering works on iridium anticancer compounds **1**–**5**.

action (MoA).[8,18,26] Together with the different structures and differences in chemistry between classical Pt drugs and non-platinum half-sandwich complexes, this gives much potential for the latter to be a new type of biologically active compound. In this review, the history of anticancer Ir(III) cyclopentadienyl (Ir–Cp$^x$) complexes is briefly recapitulated, and the design strategies, current knowledge regarding the structure–activity relationships (SARs) and mechanisms of action (MoAs) and challenges in the field are discussed. It is worth noting that some reviews of biologically active Ir complexes can be found in the literature, but these have either been published quite a few years ago[16,27,28] or focus on a specific part of the topic, specifically anticancer apoptosis inducers,[29] complexes with C-donor ligands,[30] multi-targeted complexes[26] and multinuclear complexes.[31]

# 2. General properties

## 2.1. Structural types

The first antiproliferative activity studies on Ir–Cp$^x$ complexes were reported by Sheldrick and co-workers in 2007.[22] Among the four investigated complexes, [Ir($\eta^5$-Cp*)Cl(en)]$CF_3SO_3$ and [Ir($\eta^5$-Cp*)Cl(phen)]$CF_3SO_3$ were inactive ($IC_{50}$ > 100 μM) against MCF-7 breast carcinoma cells,[32,33] but co-studied analogues **5** (Fig. 1)[34] and [Ir($\eta^5$-Cp*)(dppn)(tmtu)]$(CF_3SO_3)_2$ (**6**; Fig. 2),[22] with more extended chelating ligands, revealed acute cytotoxicity in the MCF-7 breast and HT-29 colon cancer cell lines used; en = ethylene-1,2-diamine, dppn = benzo[*i*]dipyrido[3,2-*a*:2′,3′-*c*]phenazine, tmtu = 1,1,3,3-tetramethylthiourea. Earlier, these complexes were studied in depth for their ability to interact with DNA and its models (see section 5.4).[34–36]

These pioneering Ir–Cp$^x$ complexes represent one of two basic structural types. In general, their pseudo-octahedral geometry consists of $\eta^5$-coordinated arenyl (*i.e.*, substituted cyclopentadienyl, Cp$^x$) anions occupying three of the six positions, and three other coordination sites occupied either by three monodentate ligands or by a bidentate (chelating) ligand combined with a monodentate one (Fig. 3).

This categorization can be applied to both mononuclear and multinuclear complexes. Complexes containing three monodentate ligands usually belong to the family of dichlorido complexes of the general formula [Ir($\eta^5$-Cp$^x$)$Cl_2$(L)]$^{0/+}$, with two chlorido ligands and a third monodentate ligand (L) coordinated through various donor atoms (section 3.1). The second type is dominantly represented by chlorido complexes of the general formula [Ir($\eta^5$-Cp$^x$)Cl(L^L)]$^{0/+}$, where L^L symbolizes a bidentate-coordinated (*i.e.*, chelating) ligand (section 3.2). Only a few structurally different bioactive Ir–Cp$^x$ complexes have been reported to date (section 3.4).

## 2.2. Synthesis

For both structural types of the most studied (di)chlorido Ir(III) complexes (Fig. 3), dinuclear [Ir(μ-Cl)($\eta^5$-Cp$^x$)Cl]$_2$ compounds represent key intermediates, which are easily prepared from $IrCl_3 \cdot xH_2O$ either conventionally[37,38] or by microwave-assisted syntheses[39,40] (Scheme 1). A cyclopentadienyl ring is most

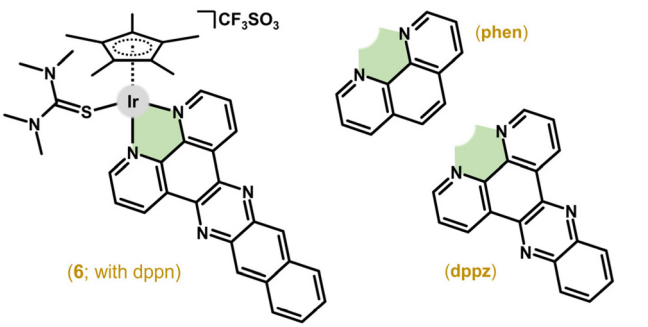


**Fig. 2** Structural formulas of the complexes [Ir($\eta^5$-Cp*)(dppn)(tmtu)]$(CF_3SO_3)_2$ (**6**), 1,10-phenanthroline (phen) and dipyrido[3,2-*a*:2′,3′-*c*]phenazine (dppz).

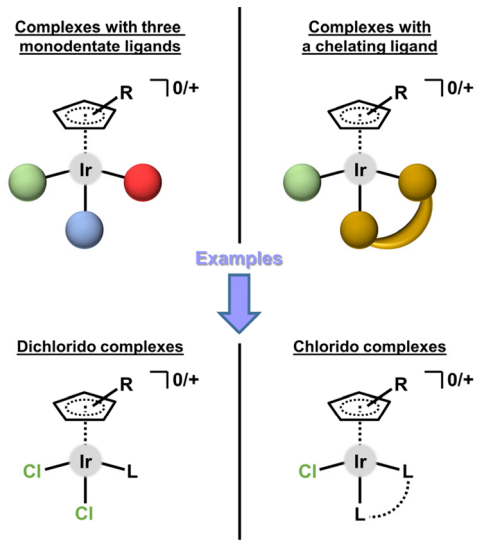


**Fig. 3** Two basic structural types of half-sandwich iridium(III) cyclopentadienyl complexes (Ir–Cp$^x$).

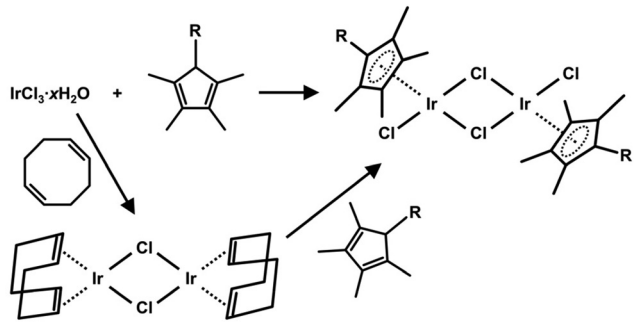


**Scheme 1** Synthesis of the most used dinuclear intermediate, [Ir(μ-Cl)(η$^5$-Cp$^x$)Cl]$_2$, for the synthesis of half-sandwich Ir(III) cyclopentadienyl complexes.

widely represented by Cp*,[22] followed by its arenyl derivatives with a more extended Cp$^x$ ring, such as (2,3,4,5-tetramethylcyclopenta-2,4-dien-1-yl)benzene (HCp$^{ph}$) or 4-(2,3,4,5-tetramethylcyclopenta-2,4-dien-1-yl)biphenyl (HCp$^{bph}$).[41] Alternatively to the abovementioned direct syntheses of [Ir(μ-Cl)(η$^5$-Cp$^x$)Cl]$_2$, $IrCl_3{\cdot}xH_2O$ can be transformed into the [Ir$^I$(μ-Cl)(η$^4$-cod)]$_2$ intermediate, which subsequently reacts with an appropriate Cp$^x$ derivative.[42]

Dimers [Ir(μ-Cl)(η$^5$-Cp$^x$)Cl]$_2$ are usually allowed to react with a stoichiometric amount or an excess of appropriate organic compound (pro-ligand), providing the [Ir(η$^5$-Cp$^x$)Cl$_2$(L)]$^{0/+}$ and [Ir(η$^5$-Cp$^x$)Cl(L^L)]$^{0/+}$ compounds. In the case of organic compounds coordinated as an electroneutral bidentate ligand, it is the chloride salt of an ionic complex, [Ir(η$^5$-Cp$^x$)Cl(L^L)]Cl, which is formed by this synthesis, and which typically undergoes further reaction to replace the chloride anion in the outer coordination sphere,[22] for example, with hexafluorophosphate,[41] to get compounds of the general formula [Ir(η$^5$-Cp$^x$)Cl(L^L)]PF$_6$.

Chlorido complexes [Ir(η$^5$-Cp$^x$)Cl(L^L)]$^{0/+}$ are frequently used as an intermediate for the synthesis of congeners bearing different monodentate ligands (see section 3.4).[36] To exemplify, halogenido,[43] py-[44] or pta-containing[45] complexes can be mentioned in this context; py = pyridine, pta = 1,3,5-triaza-7-phosphaadamantane. In most cases, complexes bearing a monodentate ligand different from the chlorido one (*e.g.*, Br, I, py or pta) are prepared by dehalogenation using a silver(I) salt (*e.g.*, nitrate or triflate), followed by the addition of an excess of appropriate pro-ligand (salt, organic compound *etc.*).[36,43–45] Halogenido (bromido and iodido) complexes can also be prepared from appropriate [Ir(μ-Br)(η$^5$-Cp$^x$)Br]$_2$ or [Ir(μ-I)(η$^5$-Cp$^x$)I]$_2$ dimers,[46] which can be prepared from their chlorido analogues.[47,48]

Regarding [Ir(μ-Cl)(η$^5$-Cp*)Cl]$_2$, it proved to be more cytotoxic in several human cancer cell lines (*e.g.*, IC$_{50}$ = 4.2 μM in A2780 ovarian carcinoma cells) than similar arene (for Ru and Os) and Cp* (for Rh) dimers used for the preparation of anticancer half-sandwich complexes of the abovementioned platinum metals.[49]

## 3. Structural classification and *in vitro* antiproliferative activity

The structural type of the half-sandwich Ir–Cp$^x$ complex is accepted and proves to be a suitable one for the development of new anticancer compounds. It is noteworthy that this structural type, while pharmacologically promising, cannot be considered as having general toxicity, because numerous representatives are reported to be inactive in various cancer cells.[34,50–52]

In this section, Ir–Cp$^x$ complexes, which have been studied for their *in vitro* antiproliferative activity, are comprehensively overviewed and discussed with respect to their composition, specifically the type of ligand (monodentate *vs.* chelating), the donor set of ligands used or the nuclearity of complexes.

### 3.1. Mononuclear complexes with three monodentate ligands

Among the first complexes of this type reported in 2010, only [Ir(η$^5$-Cp*)Cl$_2$(mpta$^+$)]CF$_3$SO$_3$ (7; Fig. 4A), containing a P-donor ligand, 1-methyl-1,3,5-triaza-7-phosphaadamantane (mpta), showed some antiproliferative activity (IC$_{50}$ = 349 μM) against A2780 cells, which was comparable with the Ru reference drug [Ru(η$^6$-pcym)Cl$_2$(pta)] (RAPTA-C; IC$_{50}$ = 353 μM); pcym = 1-methyl-4-(1-methylethyl)benzene.[53] Other complexes, [Ir(η$^5$-Cp*)Cl$_2$(pta)], [Ir(η$^5$-Cp*)Cl(pta)$_2$]PF$_6$ and [Ir(η$^5$-Cp*)Cl(mpta$^+$)(pta)](CF$_3$SO$_3$)(PF$_6$), were essentially inactive (IC$_{50}$ > 500 μM). The last two compounds represent a different structural type with only one chlorido ligand and two monodentate ligands. Additional studies proved a different ability to inhibit the cysteine (Cys) protease cathepsin B with IC$_{50}$ = 2.5 μM for RAPTA-C, 6.5 μM for the Os analogue [Os(η$^6$-pcym)Cl$_2$(pta)] and >300 μM for both [Ir(η$^5$-Cp*)Cl$_2$(pta)] and [Rh(η$^5$-Cp*)Cl$_2$(pta)].

Dichlorido complexes with diphenylphosphano-functionalized methyl-phenyl sulfides, sulfoxides, and sulfones were in

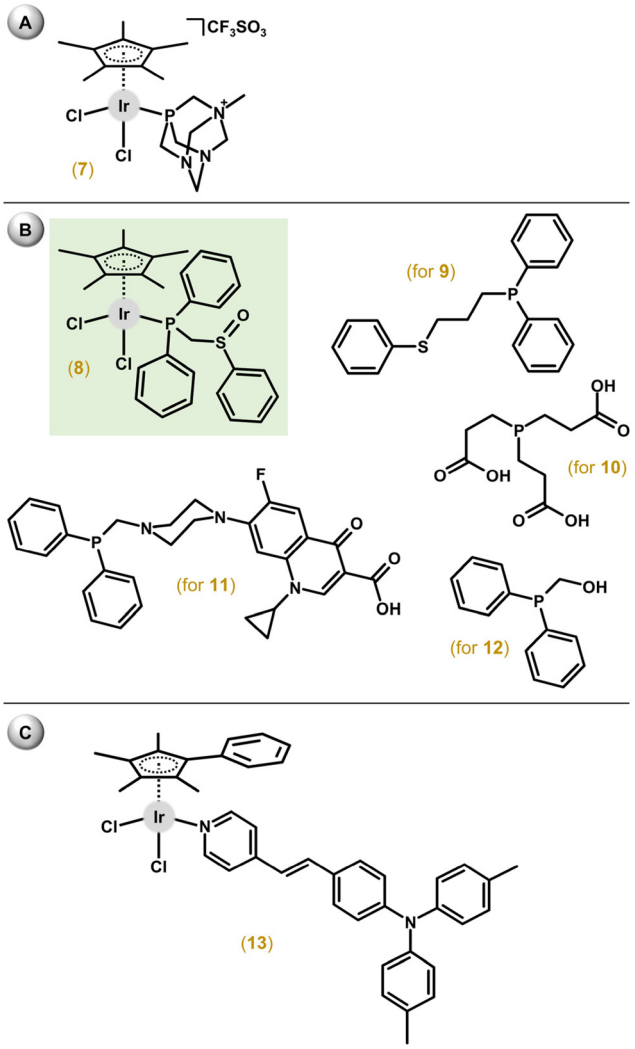


**Fig. 4** Structural formulas of (A) ionic complex $[Ir(\eta^5\text{-}Cp^*)Cl_2(mpta^+)]CF_3SO_3$ (**7**), (B) electroneutral complex $[Ir(\eta^5\text{-}Cp^*)Cl_2(phs^1)]$ (**8**) and P-donor ligands $phs^2$, tcep, psf and poh involved in analogues **9–12**, respectively, and (C) complex **13** with monodentate N-donor ligand from (B).

most cases less potent than cisplatin for the panel of cell lines.[54] Only the $[Ir(\eta^5\text{-}Cp^*)Cl_2(phs^1)]$ (**8**) complex exceeded cisplatin against 8505C ($IC_{50}$ = 3.5 μM, RA = 1.4) and SW480 ($IC_{50}$ = 2.3 μM, RA = 1.4) cells; $phs^1$ = diphenyl[(phenylsulfinyl) methyl]phosphane, 8505C = thyroid carcinoma, SW480 = colon carcinoma, RA = relative activity calculated as $IC_{50}$(reference drug)/$IC_{50}$(complex). While apoptosis and autophagy were detected in 8505C cells, the lower level of ROS/RNS was found in 8505C cells treated with **8** compared with non-treated cells. The same research team developed a series of analogues involving similar ligands with a longer alkyl chain (propyl).[55] Among them, the $[Ir(\eta^5\text{-}Cp^*)Cl_2(phs^2)]$ (**9**) complex exceeded the cytotoxic efficacy of cisplatin ($IC_{50}$ = 0.2–0.6 μM, RA = 4.0–25.0); $phs^2$ = diphenyl[3-(phenylsulfanyl)propyl]phosphane (Fig. 4B). Apoptosis was identified in 8505C cells as the cell death mechanism. The $[Ir(\eta^5\text{-}Cp^*)Cl_2(tcep)]$ (**10**) complex was more active ($IC_{50}$ = 7.8 μM) towards MDA-MB-231 triple-negative breast cancer cells than its Rh analogue ($IC_{50}$ = 67 μM) and cisplatin ($IC_{50}$ = 61 μM); tcep = tris(2-carboxyethyl) phosphane (Fig. 4B).[56]

Another series of dichlorido complexes were derived from various phosphane ligands.[57–62] The $[Ir(\eta^5\text{-}Cp^*)Cl_2(pcfx)]$ (**11**; Fig. 4B) complex exceeded ($IC_{50}$ = 11.8 μM) the antiproliferative activity of cisplatin ($IC_{50}$ > 100 μM) against DU-145 human prostate carcinoma,[57] a cell line that was also highly sensitive to various congeners of **11**;[58,59] pcfx = phosphane bearing fluoroquinolone ciprofloxacin. Complex **11** was highly selective towards cancer cells over HEK-293 normal ones. Additionally, these phosphane-derived complexes were effective against various multicellular (3D) tumour spheroids (see section 5.9). Other complexes, which contained (diphenylphosphanyl) methanol (poh for **12**; Fig. 4B) or its 4,4-bismethoxy derivative, showed only moderate (*e.g.*, $IC_{50}$ = 22.5 μM in A549 lung cancer cells for **12**) or even no cytotoxic activity.[59,61,62]

A series of complexes with triphenylamine-modified pyridines used as a monodentate N-donor ligand were designed to act as luminescent compounds for the intracellular tracking studies.[63] Hit complex **13** (Fig. 4C) showed moderate antiproliferative activity (*e.g.*, $IC_{50}$ = 26.7 μM in A549 cells) and high fluorescence (quantum yield of 15.2%) allowing advanced *in-cell* and *in vivo* biological studies.

Numerous complexes of this type bearing monodentate N-,[64–66] S-[67,68] or C-donor[69–72] ligands showed no significant cytotoxicity. Similarly, an advanced metal–peptide conjugate coordinating numerous $\{Ir(\eta^5\text{-}Cp^*)Cl_2\}$ moieties through benzimidazolium groups of a peptide was not effective against the human cancer cell lines used (nor were Ru/pcym, Rh/Cp* and Os/pcym analogues).[73]

### 3.2. Mononuclear complexes with a chelating ligand

This section is devoted to mononuclear Ir–$Cp^x$ complexes with a bidentate-coordinated chelating ligand of a different donor set, which is used here for the classification of these compounds.

**3.2.1. Complexes with an N,N-donor ligand.** This structural type is discussed above, as introduced for the first representatives of Ir–$Cp^x$ complexes (**5**, **6**) developed in the field.[22,34–36] The research of Sheldrick and co-workers, dealing with bidentate (chelating) N,N-donor ligands (*e.g.*, phen or dppz; Fig. 2), was soon followed by other research groups using either N,N-donor ligands (section 3.2.1) or ligands offering a different donor set (section 3.2.2–3.2.7).

In 2010, Therrien and co-workers reported an inactive Ir complex with 2-(1,3-thiazol-2-yl)pyridine.[74] The next year, Sadler *et al.* reported the anticancer activity and basic mechanistic studies of previously reported Cp* complexes with en, bpy, phen and pico ligands[32,33,75] and their $Cp^{ph}$ and $Cp^{bph}$ congeners; bpy = 2,2′-bipyridine, Hpic = pyridine-2-carboxylic (2-picolinic) acid.[41] The $[Ir(\eta^5\text{-}Cp^{bph})Cl(phen)]PF_6$ (**14**; $IC_{50}$ = 0.7 μM) and $[Ir(\eta^5\text{-}Cp^{bph})(bpy)Cl]PF_6$ (**15**; $IC_{50}$ = 0.6 μM) complexes reached even higher activity than cisplatin ($IC_{50}$ = 1.2 μM) (Fig. 5). The antiproliferative activity against A2780

 

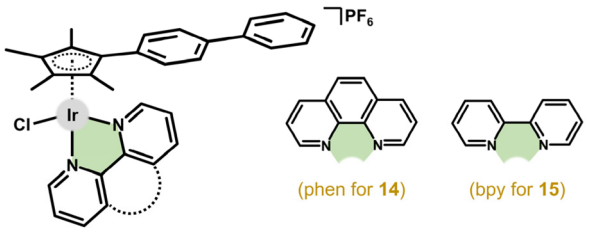


**Fig. 5** The general structural formula of complexes **14** and **15**.

cells increased with the size of the $Cp^x$ ligand (section 4.2). Interestingly, the hydrolysis rate, lipophilicity and cellular accumulation also proved to be $Cp^x$-size dependent and correlated with antiproliferative activity. Other properties (*e.g.*, interactions with DNA or intracellular distribution) were investigated for $[Ir(\eta^5\text{-}Cp^x)Cl(phen)]PF_6$ and these are discussed in more detail below.[76,77] Despite its moderate antiproliferative activity in A2780 cells,[41] the $[Ir(\eta^5\text{-}Cp^{ph})(bpy)Cl]PF_6$ complex was later reported to be inactive against A549 and HeLa cells.[78]

Following this cutting-edge work,[41] various phen and bpy derivatives have been used for the synthesis of analogous Ir–$Cp^x$ complexes.[79] Regarding bpy complexes, $[Ir(\eta^5\text{-}Cp^{bph})(bpy^1)Cl]PF_6$ (**16**; $IC_{50}$ = 7.3 μM; RA = 2.0) containing 4,4′-dinitro-2,2′-bipyridine ($bpy^1$; Fig. 6) was *ca.* 2-fold more cytotoxic than **15** ($IC_{50}$ = 14.3 μM) in A549 cells and exceeded the potency of other co-studied Ir–$Cp^{bph}$ complexes containing bpy derivatives with electron-donating groups –$NH_2$ (**17**; Fig. 6), –OH or –$OCH_3$ ($IC_{50}$ = 14.9–35.2 μM).[80] This suggests a positive effect of the substitution of the chelating ligand (bpy in this work) by the electron-withdrawing groups on the resulting antiproliferative activity. Another improvement to the antiproliferative activity was reached by the substitution of the bpy ring for one triphenylamine substituent (**18**; Fig. 6), which was not the case for similar complexes bearing two of these substituents on both pyridines of bpy (**19**; Fig. 6).[81,82]

Ir complexes involving bpy derivatives bearing the antimalarial drug artemisinin were, with respect to the bound organic drug, studied especially for their antimicrobial activity (section 7.1).[83] Their antiproliferative activity was examined against human cancer cell lines, where the best performing complex, $[Ir(\eta^5\text{-}Cp^{bph})(bpy^2)Cl]PF_6$ (**20**), exceeded cisplatin; $bpy^2$ = 4-methyl-4′-carboxy-2,2′-bipyridine dihydroartemisinin ester (Fig. 6). A similar synthetic strategy for the biofunctionalization of Ir–bpy-based cyclopentadienyl complexes was also reported elsewhere (section 6.2).[84]

Complexes with bpy-based ligands derived from rhodamine were shown to target lysosomes of the treated cancer cells.[85] The use of a bpy derivative bearing a biologically relevant sulfonamide substituent led to an Ir compound that was inactive in cancer cells.[86] A set of substituents used for bpy derivatization indicated that the resulting biological activity was connected to lipophilicity, because derivatization with more lipophilic substituents (phenyl and especially nonyl in **21**; Fig. 6) led to markedly higher antiproliferative activity than in the case of poorly effective or even inactive complexes bearing

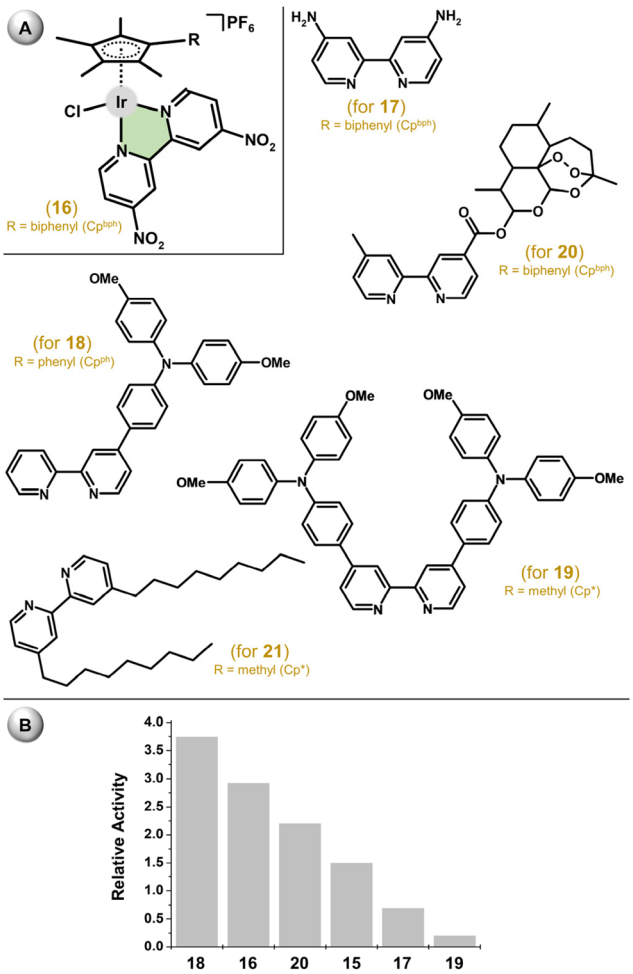


**Fig. 6** (A) The structural formula of complex **16** and bpy-based ligands of analogues **17–21**, and (B) comparison of the *in vitro* antiproliferative activity of **15–20** against the A549 lung carcinoma cell line (given as relative activity). Complex **15** (see Fig. 5) is given for comparative purposes. Complex **21** was not tested in A549 cells.

more polar substituents (*e.g.*, amine or methylene alcohol) on the bpy moiety.[87] Remarkably, the nonyl substituted complex, $[Ir(\eta^5\text{-}Cp^*)(bpy^3)Cl]PF_6$ (**21**; Fig. 6), was *ca.* 40-fold more effective ($IC_{50}$ = 2.0 μM) against the HT-29 colon cancer cells than cisplatin; $bpy^3$ = 4,4′-dinonyl-2,2′-bipyridine.

For the complexes with phen-based ligands, a series of compounds were derived from previously studied $[Ir(\eta^5\text{-}Cp^*)Cl(phen)]^+$.[33,41,88] This compound ($PF_6^-$ salt) was reported to be inactive in A2780 cells ($IC_{50}$ > 100 μM),[41] but later it showed decent cytotoxicity in the same cells ($IC_{50}$ = 29.0 μM).[88] More importantly, its potency was improved by phen derivatization ($IC_{50}$ = 0.2 μM for $[Ir(\eta^5\text{-}Cp^*)Cl(bphen)]PF_6$) as well as by using different $Cp^x$ rings (*e.g.*, $IC_{50}$ = 0.02 μM for $[Ir(\eta^5\text{-}Cp^{bph})Cl(bphen)]PF_6$ (**22**; Fig. 7); bphen = bathophenanthroline). In addition to nanomolar *in vitro* potency, **22** also showed high anticancer (and antiangiogenic) activity *in vivo* (section 5.9).

A series of Ru, Rh and Ir complexes were developed with various bithiazole ligands.[89] Their antiproliferative activity was

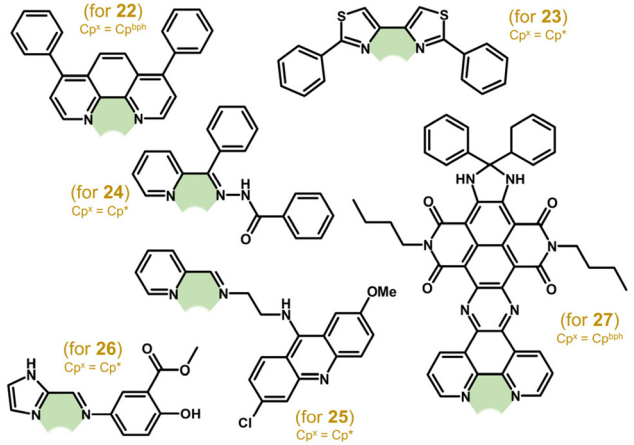


Fig. 7 Structural formulas of ligands L^L of $[Ir(\eta^5\text{-}Cp^x)Cl(L\text{^}L)]^+$ complexes **22–27**, where $Cp^x$ = Cp* or $Cp^{bph}$.

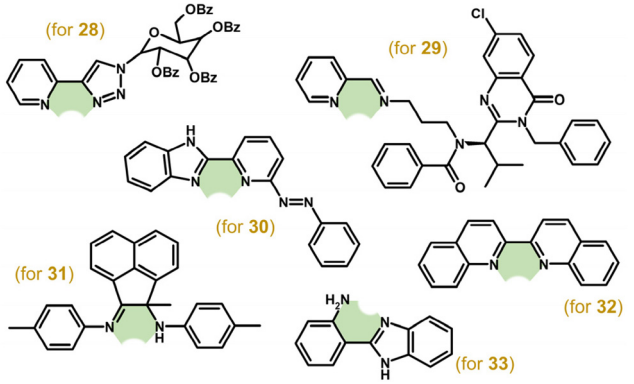


Fig. 8 Structural formulas of ligands L^L of $[Ir(\eta^5\text{-}Cp^*)Cl(L\text{^}L)]^+$ complexes **28–33**; Bz = benzyl.

studied towards two MDA-MB-231 and T47D breast carcinoma cells, where Ir complex **23** containing 2,2′-diphenyl-4,4′-bithiazole (Fig. 7) was the most potent one. Ir complexes with benzhydrazone derivatives (*e.g.*, **24**; Fig. 7) were comparably effective against $HCT116^{+/+}$ (p53 wild type) and $HCT116^{-/-}$ (p53 null) cell lines and even more cytotoxic than cisplatin towards $HCT116^{-/-}$ cells, although their activity was lower when compared with free benzhydrazones.[90] An organic intercalator, acridine, was used for the synthesis of the ligand *N*-(6-chloro-2-methoxyacridin-9-yl)-*N*′-[pyridin-2-ylmethylidene] ethane-1,2-diamine ($L^{acr}$) and its Ir, Ru, Rh and Os complexes, as well as for complexes containing a similar N,O-ligand (see section 3.2.2).[91] The $[Ir(\eta^5\text{-}Cp^*)Cl(L^{acr})]BPh_4$ (**25**; Fig. 7) complex was more cytotoxic but less selective than cisplatin. A similar design – a bioactive substituent (mesalazine in this work) linked to a heterocycle through the Schiff bond – was applied for a series of Ir complexes, such as $[Ir(\eta^5\text{-}Cp^*)Cl(L^{mes})]Cl$ (**26**; Fig. 7).[92] Although the antiproliferative activity of **26** was in the low micromolar range (*e.g.*, $IC_{50}$ = 3.5 μM in HepG2 cells), it was less effective than some co-studied Ru complexes.

Other complexes followed the pioneering complexes of Sheldrick and co-workers, because they contained dppz derivatives (including dppn)[93] or similar imidazo[4,5-*f*][1,10]phenanthroline derivatives.[94,95] Although these complexes interacted with DNA (similarly to **5**, **6**), they also disrupted mitochondria despite their cytoplasmic localization. A very recently reported complex, $[Ir(\eta^5\text{-}Cp^{bph})Cl(ndi)]PF_6$ (**27**; Fig. 7), also contained a phen-based ligand (ndi), this time modified by naphthalene diimide, which was used to improve the photochemical behaviour of **27** to treat hypoxic tumours.[96] In this regard, **27** was studied *in vitro* for its photocytotoxicity under normoxic and hypoxic conditions and *in vivo* after laser activation in tumours (section 5.9).

Although a large series of Ir–Cp* complexes with various *C*- and *N*-glycosyl azoles (1,2,3-triazole, 1,3,4-oxadiazole and 1,2,4-oxadiazole were used) were prepared, only complex **28** (Fig. 8) was effective against some of the human cancer cell lines used (*e.g.*, $IC_{50}$ = 1.6 μM in A2780 cells).[97] Other highly cytotoxic complexes containing imino-pyridyl bases,[98–101] imino-quinolines/naphthyridines,[102] diimines,[103] rhodamine- or naphthalimide-modified bpy-based ligands,[104,105] lonidamine-based amides,[106] a kinesin spindle protein (KSP) inhibitor ispinesib-derived ligand,[107–109] 1,3,4-thiadiazoles[110] or aza derivatives of 2-(pyridin-2-yl)-1*H*-benzimidazole[111] were prepared and studied for their antiproliferative activity. Among them, for example, ispinesib-derived complex **29** (Fig. 8) showed submicromolar activity in various human cancer cell lines (*e.g.*, $IC_{50}$ = 0.27 μM in A549 cells).[109] Complex **30** (Fig. 8) was, as the first example of such studies, investigated in mixtures of relevant intracellular small biomolecules (NADH, GSH, ascorbic acid; section 6.1.1).[111]

Very recently, Guo, Liu and co-workers demonstrated that the type of very similar N,N-donor ligand (pyridyl-imine *vs.* pyridyl-amido) could affect the resulting cytotoxicity.[112] Specifically, complexes containing widely used pyridyl-imine ligands exhibited moderate cytotoxicity ($IC_{50}$ = 23.2–29.8 μM in A549 cells), while the 16-electron pyridyl-amido complex was inactive ($IC_{50}$ > 100 μM). The same research group reported an interesting coordination mode for a series of Ir compounds, represented by Cp* complex **31**, containing hybrid $sp^2$-N/$sp^3$-N donor (*i.e.*, imine–amine) chelating ligands (Fig. 8).[113] These compounds were found to be cytotoxic, which contrasted with structurally similar analogues with a diimine-type chelating ligand.[103]

The $[Ir(\eta^5\text{-}Cp^*)(biq)Cl]PF_6$ (**32**; Fig. 8) complex was studied, together with its Ru analogue, for its photochemical and photobiological properties (section 6.3).[114] An interesting series of complexes involving various N,N- (*e.g.*, 2-(1*H*-benzimidazol-2-yl)aniline in **33**; Fig. 8), C,N- and N,O-donor ligands was developed, but complexes with N,N-donor ligands exhibited the lowest antiproliferative activity (section 4.3).[115]

Numerous other Ir chlorido complexes containing a chelating N,N-donor ligand showed little to no cytotoxicity (usually significantly less than the reference drug used).[64,65,116–142] Also of interest, a non-cytotoxic complex, $[Ir(\eta^5\text{-}Cp^*)(bpy)Cl]Cl$, later

proved to be a selective chemosensitizer for cancer cells treated with platinum-based drugs (section 6.4).[143]

**3.2.2. Complexes with an N,O-donor ligand.** Probably the first Ir–Cp$^x$ complex, [Ir($\eta^5$-Cp*)Cl(qui)] (**34**; Fig. 9), involving an N,O-donor chelating ligand was derived from a well-known pharmacological moiety, quinolin-8-ol (Hqui).[144] **34** was effective against human melanoma and glioblastoma cell lines (*e.g.*, $ID_{50}$ = 0.8 μM in SK-Mel cells). In the same year, the [Ir($\eta^5$-Cp*)Cl(nqo)] (**35**; Fig. 9) complex was developed and proved to have much stronger activity against the cancer cells used (*e.g.*, $IC_{50}$ = 2.2 μM in HeLa cells) than cisplatin ($IC_{50}$ = 25.0 μM), but only low selectivity towards cancer cells ($IC_{50}$ = 5.0 μM against HUVEC human umbilical-vein endothelial cells); Hnqo = 1-nitrosonaphthalen-2-ol (1,2-naphthoquinone-1-oxime).[145] This pioneering investigation proposed a different MoA for **35** in comparison with that of cisplatin. Recently, **34** was followed by a series of Ir–Cp$^x$ complexes containing 2-[2-(4-nitrophenyl)ethenyl]quinolin-8-ol.[146] Although the best-performing Ir complex **36** (Fig. 9) exceeded the potency of cisplatin (*e.g.*, $IC_{50}$ = 5.6 μM in HeLa cells), it has not been studied in detail because it was outperformed by the co-studied Ru congener.

The [Ir($\eta^5$-Cp$^{bph}$)Cl(pic)] (**37**; Fig. 9) complex showed moderate antiproliferative activity against A2780 cells ($IC_{50}$ = 16.3 μM), which was markedly lower than that for cisplatin ($IC_{50}$ = 1.2 μM) and analogues with phen and bpy (section 4.3).[41] Later, **37** ($IC_{50}$ = 31.3 μM in A549 cells) was derivatized on pic by various substituents (*e.g.*, halogeno, carboxy or hydroxy), leading in most cases to improved antiproliferative activity, as exemplified by [Ir($\eta^5$-Cp$^{bph}$)Cl(pic$^1$)] (**38**; Fig. 9) with $IC_{50}$ = 4.4 μM in A549 cells; Hpic$^1$ = 5-(trifluoromethyl)pyridine-2-carboxylic acid.[147]

McGowan and co-workers developed a series of complexes with different donor atoms (*i.e.*, N,N-, N,O- and O,O-ligands; section 4.3), including the [Ir($\eta^5$-Cp*)Cl(fpb)] (**39**; Fig. 9) complex with 1-(3-fluorophenyl)-3-(phenylamino)but-2-en-1-one (Hfpb).[116] This complex was less effective (*e.g.*, $IC_{50}$ = 5.1 μM in HT-29 cells) than cisplatin ($IC_{50}$ = 2.4 μM). Its derivatization by reducing the ligand size (–N–H instead of –N–phenyl) and changing the donor set (N,O-donor fpb *vs.* O,O-donor 1-(3-fluorophenyl)-3-hydroxybut-2-en-1-oate) did not lead to improved antiproliferative activity.[148] In contrast, using a different position and/or substituent than 3-fluoro of **39**[116] led, in some cases, to higher potency compared with cisplatin.[149] For example, the [Ir($\eta^5$-Cp*)Cl(dcpb)] (**40**; Fig. 9) complex with 1-(2,4-dichlorophenyl)-3-(phenylamino)but-2-en-1-one (Hdcpb) showed much higher antiproliferative activity ($IC_{50}$ = 2.8 μM) than cisplatin ($IC_{50}$ = 8.1 μM) in HCT116 p53$^{-/-}$ cells; this was connected to significant selectivity towards the cancer cells mentioned over the ARPE-19 normal retinal epithelial cells used ($IC_{50}$ > 100 μM).

Complexes with various benzohydrazones bearing the fluorenyl substituent (*e.g.*, **41**; Fig. 9) showed moderate cytotoxicity in HeLa cells.[150] Acridine was used for the derivatization of 2-[(imino)methyl]phenol within complex **42** (Fig. 9).[91] This complex, analogous to co-studied ionic **25** with an N,N-ligand, was highly potent towards the HL60 cancer cells used but not selective towards the cancer cells mentioned over FG0 normal skin fibroblasts. Similar complexes derived from different 2-[(imino)methyl]phenol-based ligands,[151] as well as complexes containing 2-[(alkyl/aryl-substituted imino)methyl]phenols or pyridylphosphinates[46,121,152,153] were markedly less effective or even inactive towards human cancer cell lines.

**3.2.3. Complexes with a C,N-donor ligand.** As the above-mentioned complexes demonstrate, even seemingly very small structural changes can result in effective switching on/off of a biological effect. This was also demonstrated in pioneering work from 2011, in which replacing N,N-chelating bpy in the inactive [Ir($\eta^5$-Cp*)(bpy)Cl]$^+$ complex (Fig. 3)[41] with the C,N-chelating deprotonated 2-phenylpyridine (ppy) switched on the antiproliferative activity for the electroneutral [Ir($\eta^5$-Cp*)Cl(ppy)] complex (**43**; Fig. 10) against A2780 cells ($IC_{50}$ = 10.8 μM).[154] This success triggered follow-up research on compounds involving ppy-derived C,N-ligands. It was demonstrated that the position and type of substituent on the ppy pyridine and phenyl rings critically influenced the outcome of

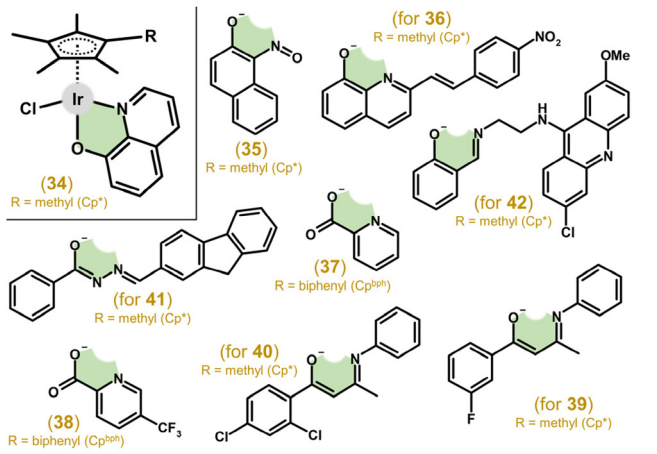


**Fig. 9** Structural formulas of N,O-donor ligands (HL) of representative [Ir($\eta^5$-Cp$^x$)Cl(L)] complexes **34**–**42**, where Cp$^x$ = Cp* or Cp$^{bph}$.

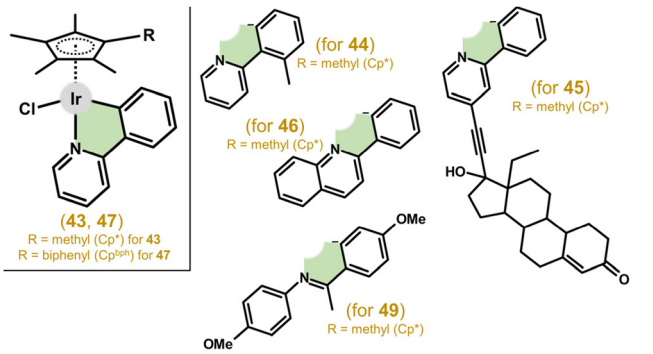


**Fig. 10** Structural formulas of complex **43**, containing deprotonated 2-phenylpyridine (ppy), and its analogues (**44**–**47**, **49**) involving different ionic C,N-donor ligands.

such structural modification, as even positional isomers exhibited different antiproliferative effects, with [Ir($\eta^5$-Cp*)Cl(mppy)] (**44**; Fig. 10) as the best performing within the studied group of analogues ($IC_{50}$ = 1.2 μM in A2780 cells, *i.e.*, 10× more active than **43**); Hmppy = 2-(2-methylphenyl)pyridine.[155] Ruiz *et al.* modified **43** by introducing a lipophilic steroidal ppy conjugate with a levonorgestrel group, 17-α-[2-phenylpyridyl-4-ethynyl]-19-nortestosterone ($Hppy^{LEV}$), involved in complex **45** (Fig. 10) that was twice as active ($IC_{50}$ = 5.4 μM) as the non-steroidal parent molecule **43** in A2780 cells, while being equally active in cisplatin-resistant A2780Cis cells.[156] Another innovative derivatization of ppy involves a steroidal backbone based on androsterone.[157] The prepared steroidal complexes showed potent activity in, *e.g.*, the RT112 human bladder carcinoma cell line and its cisplatin-resistant variant with very low resistance factors (RF = 0.5–1.2), while retaining promising selectivity with respect to somatic fibroblasts.

Complexes with 2-(*p*-tolyl)pyridine, 2-phenylquinoline (for complex **46**; Fig. 10), and 2-(2,4-difluorophenyl)pyridine showed promising potency in A2780 cells with $IC_{50}$ values from 2.5 to 6.5 μM, and exceeded the potency of **43**.[158] Another improvement to the antiproliferative activity of **43** was reached by a $Cp^x$ ring extension, as exemplified by the [Ir($\eta^5$-$Cp^{bph}$)Cl(ppy)] complex (**47**) in section 4.2. Other analogues of **43** were reported in which ppy was derived from substitution with rhodamine dyes with the aim of preparing a prospective theranostic agent.[159] The complexes had good fluorescent properties; however, they exhibited only moderate antiproliferative activity and no selectivity to cancer cells compared with normal cells. Furthermore, triphenylamine, carbazole and their derivatives, as efficient fluorescent materials, were also introduced as substituents for ppy, resulting in complexes with higher activity than that of cisplatin in A549, HeLa and HepG2 cell lines.[160,161] These complexes also showed the ability to prevent the migration of cancer cells, as revealed in a study on prospective antimetastatic agents (section 6.4). Unfortunately, no selectivity with respect to healthy cells was found. Other complexes derived from the ppy ligand are discussed below (section 3.4), as they contain a different monodentate ligand (*e.g.*, pyridine) than the chlorido one, and therefore, represent another structural type.[44,162,165]

Following the success of ppy-based complexes, other organic scaffolds have been investigated as C,N-chelating ligands for Ir–$Cp^x$ complexes. Ru(II), Rh(III) and Ir(III) complexes involving various 2-phenylbenzimidazoles were prepared.[166] All complexes showed significant anticancer activity on all tested cell lines in low micromolar ranges. The Ir complex [Ir($\eta^5$-Cp*)($bzim^1$)Cl] (**48**; section 7.3) was the most potent one of all the tested congeners, with, *e.g.*, $IC_{50}$ = 1.0 μM in HT-29 cells; $Hbzim^1$ = methyl 1-butyl-2-phenyl-1*H*-benzimidazole-5-carboxylate. Notably, all the tested complexes were also significantly active in A2780Cis cells (RF = 0.6–1.1; 9.7 for cisplatin). Based on these positive results, further derivatization of the 2-phenylbenzimidazole core was performed on the phenyl ring (*e.g.*, $CH_3$, F, $CF_3$, $NO_2$ or phenyl),[167] to extend the SAR study. The highest efficiency towards a panel of cancer cell lines was observed for a complex with a phenyl ring as the substituent (*i.e.*, 2-(biphenyl-4-yl)-1*H*-benzimidazole derivative) with the best results achieved on both A2780 and A2780Cis cell lines with $IC_{50} \approx 1.2$ μM.

Schiff bases represent other C,N-donor ligands used in Ir–$Cp^x$ cyclometalated complexes. Complexes with substituted benzylidene(4-*tert*-butylphenyl)amines were comparably or slightly less active than cisplatin against A549 cells ($IC_{50} \approx$ 20 μM).[168] Complexes (*e.g.*, **49** in Fig. 10) with ketimine Schiff bases based on aniline and acetophenone/2-acetonaphthone derivatives were found to be significantly active in K562 cells ($IC_{50}$ = 0.3–4.8 μM), all outperforming cisplatin ($IC_{50}$ = 5.9 μM).[169] SAR analysis revealed that electron-donating groups in the *para*-position of the aromatic rings favourably contributed to the activity of the complexes, while electron-withdrawing groups decreased the activity.

Other works employed various N-heterocyclic carbenes (NHC) as C,N-chelating ligands. The study of complexes involving imidazole-based imine-NHC presented compounds with promising anticancer activity.[170,171] For these compounds, enlarging the substituents on the aniline and imidazole rings, as well as on the $Cp^x$ arenyl ligand, leads to higher anticancer efficiency. On the other hand, low selectivity compared to healthy cells was found for this class of complexes, with the best results found for [Ir($\eta^5$-$Cp^{bph}$)Cl($nhc^n$)]$PF_6$, where $nhc^n$ = a 1-(phenylimino)methylimidazol-2-ylidene core substituted with methyl, phenyl or isopropyl (for **50** in Fig. 11) groups, with *ca.* 25 times higher activity than cisplatin in the A549 cell line ($IC_{50}$ = 0.9 *vs.* 21.3 μM) and a selectivity index ($IC_{50}$(BEAS-2B)/$IC_{50}$(A549)) of *ca.* 5.4 (SI = 2.0 for cisplatin).[171] In the follow-up study with benzimidazole-appended imidazole-based carbenes, the complexes showed no improvement over the abovementioned ones.[172]

Triazolyl-functionalized NHCs based on (benz)imidazole were also used as ligands in Ir(III), Rh(III), Ru(II) and Os(II) complexes.[173] The complexes were inactive in HCT116, NCI-H460, SiHa and SW480 cells except for the Ir(III) ones, achieving moderate activity with the lowest $IC_{50}$ = 10 μM in NCI-H460 cells for **51** (Fig. 11). The same research team achieved a significant improvement in antiproliferative activity by introducing a ferrocene moiety into the C,N-carbene ligand structure (*e.g.*, **52**

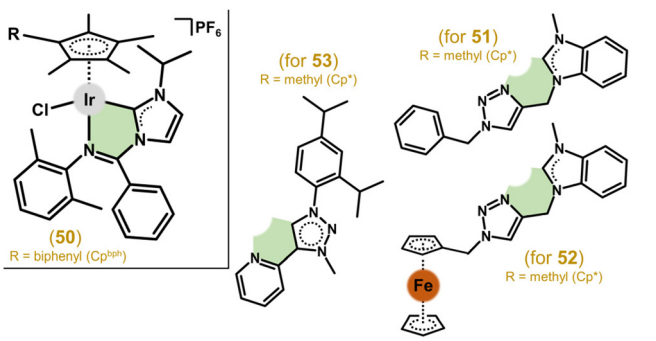


**Fig. 11** Structural formulas of complexes **50–53** containing N-heterocyclic carbenes (NHC) as C,N-chelating ligands.

 

in Fig. 11).[174] Another class of carbenes as C,N-donor ligands includes pyridyl functionalized mesoionic carbenes of the 1,2,3-triazol-5-ylidene type. Some complexes (*e.g.*, **53** in Fig. 11) reached low micromolar $IC_{50}$ values (*e.g.*, 2.0 μM in HeLa cells) while being non-toxic in normal primary keratinocytes.[175]

Complex **54** (Fig. 12) with 1-benzyl-4-phenyl-1*H*-1,2,3-triazole showed potent efficacy in A549 cells ($IC_{50}$ = 4.7 μM), which was comparable to auranofin, while being moderately active in other tested cancer cell lines (*e.g.*, HeLa).[176] 1-Phenyloxazoline derivatives (Hphox) were also investigated as ligands, for example, in complex **55** (Fig. 12) with low-micromolar potency in HeLa cells.[177] As a continuation of this study, complexes bearing either a fluorescent and lipophilic BODIPY entity (**56**)[178] or a bioorthogonal azido probe (**57**)[179] were reported by the same research group (Fig. 12). **56** was less active in HeLa cells ($IC_{50}$ = 8.6 μM) than its predecessors (**55**) and showed low selectivity to cancer cells.[178]

Another study reporting complexes of this type was in the field of photodynamic therapy (PDT), because even chlorido complexes but especially their analogues bearing a monodentate heterocyclic N-donor ligand (*e.g.*, imidazole) exhibited higher antiproliferative activity when irradiated than in the dark (see section 6.3).[180] The authors used π-expansive ligands, such as 4,9,16-triazadibenzo[*a*,*c*]naphthacene (pbpn; Fig. 12), in a highly phototoxic complex [Ir(η$^5$-Cp*)Cl(pbpn)] (**58**).

Bidentate 7-azaindole derivatives with N1-phenyl/thiophen-2-yl substituents (*e.g.*, **59**; Fig. 12) also coordinate in the C,N-fashion in Ir(III) complexes, which were either inactive or moderately active in A2780 and A2780Cis cells.[181]

### 3.2.4. Complexes with an N,X-donor ligand (X = S or P)

*3.2.4.1. N,S-Donor ligands.* Inspired by Ru half-sandwich complexes with thiosemicarbazone (TSC)-based N,S-chelating ligands, Ir(III), Rh(III) and Ru(II) complexes involving pyrenyl-derived TSC were reported in 2015.[182] Iridium complexes (*e.g.*, **60** in Fig. 13) showed low antiproliferative activity in cancer cells (*e.g.*, A549 or MCF-7 cell lines), while achieving some selectivity, as $IC_{50}$ values were up to 6.2-times higher in normal HEK-293 cells.

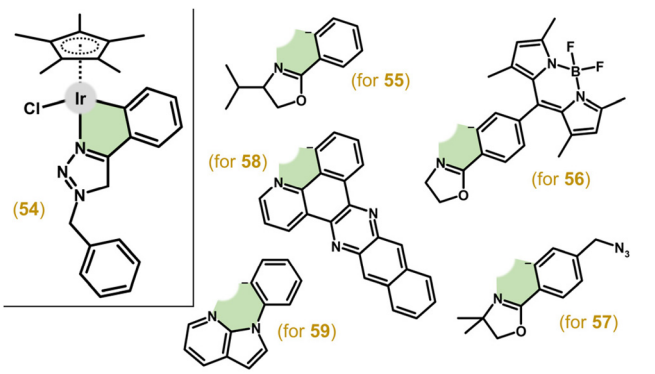


**Fig. 12** Structural formulas of complex **54** and C,N-donor ligands involved in its analogues **55–59**.

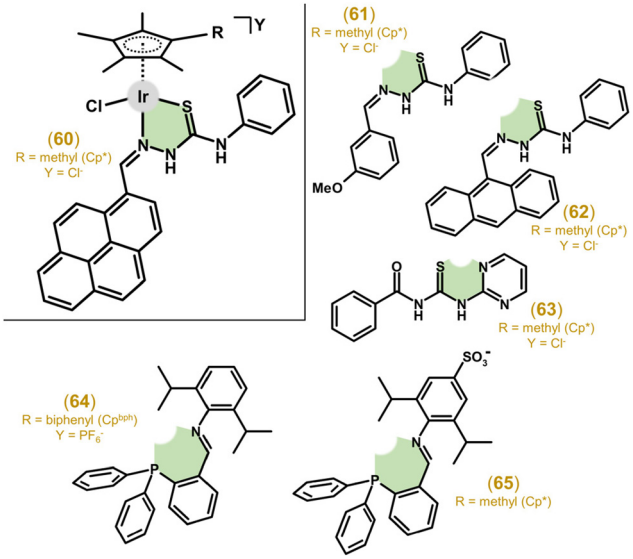


**Fig. 13** Structural formulas of complex **60**, N,S-donor ligands involved in analogues **61–63** and N,P-donor ligands involved in complexes **64** and **65**.

Other work, focusing on substituted benzaldehyde-*N*4-phenylthiosemicarbazones as ligands, describes complex **61** (Fig. 13) with promising antiproliferative activity (*e.g.*, $IC_{50}$ = 3.6 μM *vs.* 15.0 μM for cisplatin in HeLa cells) and significantly improved selectivity for cancer cells (SI of up to 26).[183] In a follow-up study, Su *et al.* developed TSC complexes for dual chemo- and photodynamic therapy by introducing a photosensitizer moiety (*e.g.*, 9-anthraldehyde for **62**; Fig. 13) into the TSC ligand (see section 6.3 for more details).[184]

Thiourea was used as a basic scaffold for N,S-coordinating ligands. Ir–Cp* cationic complexes with *N*-phenyl-*N*′-pyridyl/pyrimidyl thiourea showed rather low anticancer activity, significantly lower than cisplatin in, *e.g.*, the HCT116 cell line.[185] When benzoyl(2-pyrimidyl/4-picolyl)thiourea ligands were used instead, a notable improvement in activity and selectivity were observed, with the best results of $IC_{50}$ = 1.4 μM (2.8 μM for cisplatin) in HCT116 cells and SI ≈ 13 obtained for **63** (Fig. 13).[67] The introduction of N,S-ligands based on (benz)imidalole-2-thione appended with 1-benzyl-1,2,3-triazole led to Ir–Cp* complexes without relevant antiproliferative activity.[186] The complex involving N,S-coordinated *N*-(4-fluorophenyl)pyridine-2-carbothioamide showed a low antiproliferative effect, generally lower than that of its Ru/Os(II) and Rh(III) analogues.[187]

*3.2.4.2. N,P-Donor ligands.* Liu and co-workers systematically studied organometallic complexes with various P,X-donor ligands (X = P, O or N), including triphenylphosphane-imine based N,P-ligands.[188] Most of the complexes (*e.g.*, **64** in Fig. 13) showed good anticancer activity towards A549 cells ($IC_{50}$ = 4.7 μM), higher than the clinical drug cisplatin ($IC_{50}$ = 21.3 μM). Similar complexes involving N,P-donor phosphane-imines, this time prepared as zwitterionic compounds, exhibited moderate potency (*e.g.*, $IC_{50}$ = 14.7 μM in A549 cells for **65**;

Fig. 13)[189] and exceeded inactive analogues containing N,N-donor pyridyl-imines.[101] These investigations suggested the positive effect of phosphorus on cytotoxicity.

### 3.2.5. Complexes with an O,X-donor ligand (X = O, S, Se, P, C)

*3.2.5.1. O,O-Donor ligands.* As already mentioned, in 2012 McGowan and co-workers presented a series of complexes involving ligands with different donor atoms (*i.e.*, N,N-, N,O- and O,O-ligands). Therein, the first anticancer Ir–Cp$^{x}$ complex involving an O,O-donor ligand (**66**; Fig. 14) was reported with deprotonated 2-hydroxy-1,4-napthoquinone. However, **66** was less active than cisplatin ($IC_{50}$ = 20 μM *vs.* 2.4 μM) in HT-29 cells.[116]

Similarly, using the O,O-donor benzoylacetone derivative did not result in an active compound (**67**; Fig. 14), compared to more effective complexes with N,O-donor analogues (section 4.3).[148] Unfortunately, even using an extended diketonato ligand with intrinsic biological activity, *i.e.*, curcumin and its derivatives, complexes (*e.g.*, **68** in Fig. 14) with a moderate effect and no selectivity in A2780 and A2780Cis cells were obtained.[45] The following study, which evaluated the influence of various substitutions on curcumin, resulted in complexes again with a low anticancer effect in HepG2 and HeLa cancer cells, yet in comparison with normal cells, some selectivity was observed.[190] Another study also chose anticancer active chelating O,O-ligands, specifically, a naturally occurring β-diketone dibenzoylmethane and its derivatives, including synthetic avobenzone used in cosmetics.[191,192] Similarly to previous works, the results also did not identify the complexes (*e.g.*, **69** in Fig. 14) as being effective with significantly lower activity in A2780 and A2780Cis cell lines than cisplatin and the starting β-diketones.

*3.2.5.2. O,S- and O,Se-donor ligands.* In an effort to increase the stability of anticancer organometallic complexes, Keppler and colleagues used thiomaltol as an O,S-chelating ligand and prepared the complexes and analogous 1-methylimidazole derivatives (section 3.4).[193] The Ir–Cp* complexes (*e.g.*, **70** in Fig. 15) studied were found to be less active in A549 and CH1/PA-1 cells than cisplatin, but were significantly more active towards SW480 cells ($IC_{50}$ = 0.7 μM *vs.* 3.5 μM for cisplatin).

Follow-up studies introduced thiopyridone and derivatives as O,S-chelating ligands.[194,195] These compounds (*e.g.*, **71** in Fig. 15) showed increased stability in an aqueous solution and higher antiproliferative activity (*e.g.*, $IC_{50}$ = 0.5 μM in SW480 cells for **71**) compared to their pyridone and thiomaltol parental compounds. This group then explored the effect of sulphur substitution with selenium when using selenopyridones as O,Se-donor ligands.[196] However, some complexes showed remarkable air sensitivity and the stable compounds (*e.g.*, **72** in Fig. 15) were significantly less active than their thiopyridone analogues.

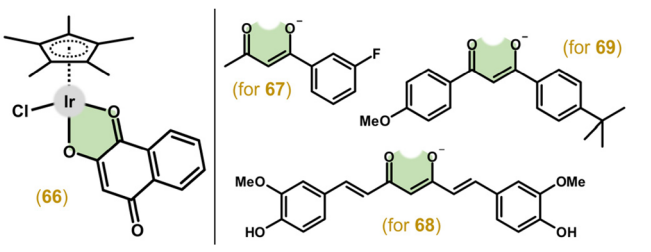


Fig. 14 Structural formulas of complex **66** and O,O-donor ligands involved in analogues **67–69**.

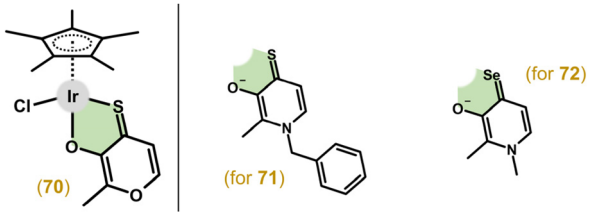


Fig. 15 Structural formulas of complex **70** and O,X-donor ligands involved in complexes **71** (X = S) and **72** (X = Se).

*3.2.5.3. O,P-Donor ligands.* Liu and collaborators explored Ir–Cp*/Cp$^{ph}$/$^{bph}$ complexes with O,P-donor phosphane phosphonic amide ligands, specifically [2-(dicyclohexylphospanyl) phenyl](phenyl)-phosphinic diisopropyl-amide. All the studied complexes (*e.g.*, **73** in Fig. 16) were significantly effective against HeLa and A549 cells; however, no selectivity was found.[197]

The follow-up work studied structurally similar complexes involving phosphane sulfonato O,P-ligands.[198] The electroneutral complexes (*e.g.*, **74** in Fig. 16) were investigated as prospective theranostics for their rich fluorescence properties and generally favourable anticancer activity against HeLa and A549 cell lines, which was in some cases significantly better than that of cisplatin. Selectivity to cancer cells over normal cells was also identified (the best SI was equal to *ca.* 3.3).

*3.2.5.4. C,O-Donor ligands.* The $IC_{50}$ values of the complexes (*e.g.*, **75** in Fig. 16), involving C,O-coordinated deprotonated 1-(2-hydroxyphenyl)-1*H*-benzimidazolium-based NHCs, towards A549 and HeLa cells ranged from 2.5 to 20.7 μM and 2.2 to 6.7 μM, respectively (cisplatin $IC_{50}$ = 21.3 and 7.5 μM).[199] The activity of the complexes increased with a higher number

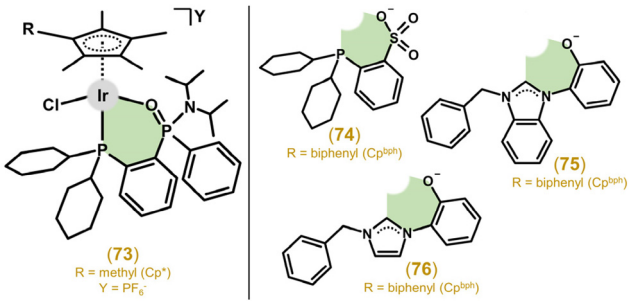


Fig. 16 Structural formulas of complex **73** and ligands involved in similar complexes **74** (with an O,P-donor ligand) and **75** and **76** (with C, O-donor ligands). Electroneutral complexes **74–76** do not contain any counter-anion (Y).

of phenyl groups in the complex molecule. Unfortunately, no selectivity to cancer cells over normal ones was found. Effective complexes, such as complex **76** (Fig. 16), were derived from imidazolium-based NHCs and studied for their anticancer activity even at the *in vivo* level (section 5.9).[200]

**3.2.6. Complexes with a P,X-donor ligand (X = P or S).** Together with the above-discussed highly-cytotoxic electroneutral dichlorido complexes with monodentate P-coordinated sulfides, sulfoxides, and sulfones (phs$^n$; section 3.1), their ionic monochlorido [Ir($\eta^5$-Cp*)Cl(phs$^n$)]$PF_6$ analogues (*e.g.*, **77** in Fig. 17) with the same ligands coordinated as chelating P,S-donor ligands, were also investigated.[54,55] A different coordination mode (*i.e.*, P- *vs.* P,S-donor) did not significantly impact the antiproliferative activity.

A follow-up study further investigated P,P-donor ligands involving two diphenylphosphano units with differing spacers between the P atoms.[201] The best anticancer activity was found for Ir–Cp$^{bph}$ complex **78** (Fig. 17) with the simplest studied spacer, *i.e.*, ethylene, with $IC_{50}$ = 2.3 μM in A549 cells (21.3 μM for cisplatin). This group continued their systematic research and next they reported on luminescent Ir–Cp*/Cp$^{bph}$ complexes with 1,2-bis(diphenylphosphano)benzene and 1,8-bis(diphenylphosphano)naphthalene as P,P-ligands.[202] The complexes displayed higher activity than cisplatin towards A549 and HeLa cancer cells, with the most potent complex, **79** (Fig. 17), being up to *ca.* 40 times more active than cisplatin against A549 cells. Their self-luminescence helped uncover their MoA linked to lysosomal damage. Other complexes (*e.g.*, **80**) involving P,P-coordinating 2,20-bis(diphenylphosphano)-1,10-binaphthyl (Fig. 17) were studied and proved to be significantly more active than cisplatin in A549 and HeLa cells.[203] Surprisingly, unlike in works involving complexes with N,N- and C,N-chelating ligands, an increase in activity was not observed for Ir–Cp$^{bph}$ compared to its Ir–Cp* analogue. Also, no selectivity over healthy cells was found.

**3.2.7. Complexes with a C,X-donor ligand (X = B or C).** The first work that introduced differently substituted 1,1′-methylenebis(1*H*-imidazol-3-ium)-based NHCs coordinated in a bidentate C,C-fashion was reported in 2017.[204] The anticancer activity could be tuned by varying the NHC and Cp$^x$ ligands, in the order of ph- > butyl- > ethyl- > methyl-substituted NHCs and Cp$^{bph}$ > Cp$^{ph}$ > Cp*. Complex **81** (Fig. 18) with a phenyl substituent on imidazole and a biphenyl substituent on the cyclopentadienyl ring was 3-times more potent than cisplatin against HeLa cells. Their intrinsic luminescence allowed their MoA to be studied in greater detail.[205]

Another group of C,C-ligands included 1-benzyl-3-methylimidazolium-based NHCs.[206] All the studied Ir(III) complexes (*e.g.*, **82** in Fig. 18) showed significantly higher antiproliferative activity ($IC_{50}$ values from 3.9 to 11.8 μM against A549 cells) than cisplatin ($IC_{50}$ = 21.3 μM). The abovementioned (section 3.1) dichlorido complexes involving C-coordinated imidazolium-based NHCs were co-studied with a chelated complex involving a mixed C,C-/C,B-coordination, which resulted in activity comparable to cisplatin in A2780 cells and better in A2780Cis cells for the complex involving the decaboranyl-imidazolium derivative as a B,C-donor NHC ligand.[71]

### 3.3. Multinuclear complexes

Multinuclear Ir cyclopentadienyl complexes containing two or more Ir atoms (homometallic complexes; section 3.3.1) or combining Ir with different metals (heterometallic complexes; section 3.3.2) have been described. Clearly, both designs offer an increase in the resulting biological activity of such multinuclear complexes through multiplication of (multiple metal centres in the molecule) or combining (different metal centres acting through different MoAs) biological effects.

**3.3.1. Homometallic complexes.** Multinuclear Ir cyclopentadienyl complexes, belonging to families of symmetrical[192,207–211] or unsymmetrical[135] dinuclear complexes, complexes of higher nuclearity[121,152,153,209,212–216] thiolato and chalcogenato complexes,[217–219] and metallacages,[220–224] have recently been comprehensively reviewed.[31] That is why only some examples of these compounds are discussed in this review together with complexes reported in the literature in the last few months.

The first multinuclear Ir–Cp$^x$ complexes, which were studied for their cytotoxic activity, were derived from complexes **5** and **6** (Figs. 1 and 2)[22] by the replacement of their monodentate ligands (*i.e.*, Cl for **5** and tmtu for **6**) by an appropriate N-donor bridging ligand (L = pyrazine (pyz) or 4,4′-bipyridine (bpy$^4$)).[207] Complexes, such as [$Ir_2$(μ-dpeb)($\eta^5$-Cp*)$_2$(dppz)$_2$](C$F_3SO_3$)$_4$ (**83**; Fig. 19), were highly cytotoxic against MCF-7 and HT-29 cell lines ($IC_{50}$ = 0.1–3.8 μM).[208] Improved antiproliferative activity was reached by analogues

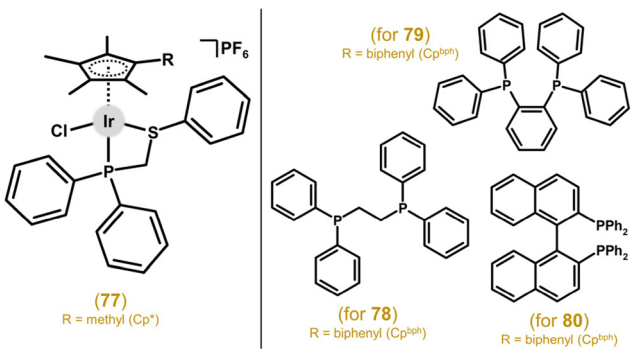


**Fig. 17** Structural formulas of complex **77** and P,P-donor ligands involved in complexes **78**–**80**.

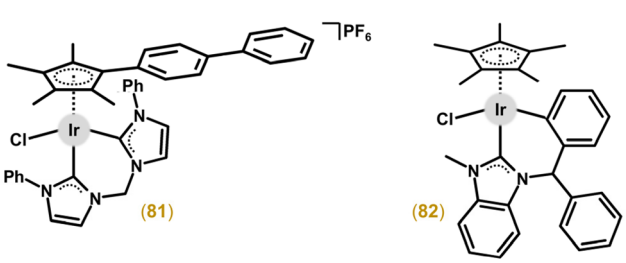


**Fig. 18** Structural formulas of complexes **81** and **82**.

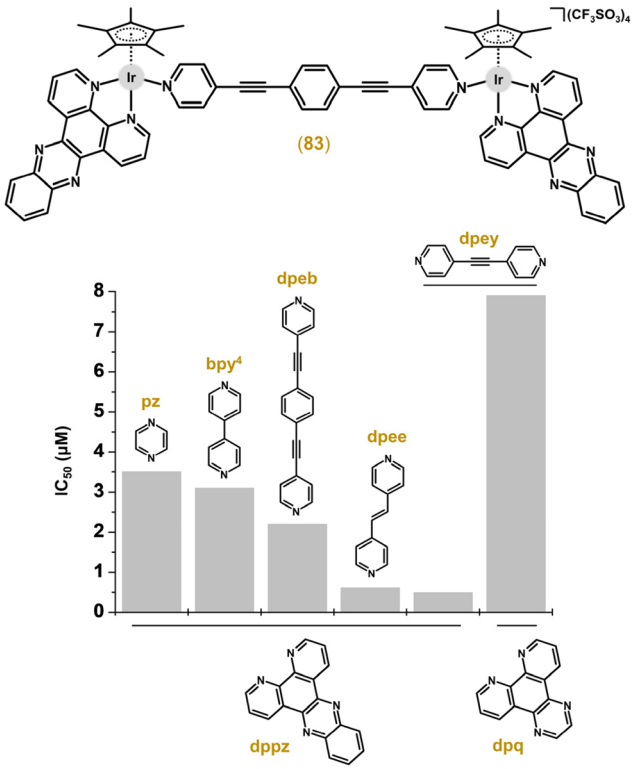


**Fig. 19** The structural formulas of the representative dinuclear complex $[Ir_2(\mu\text{-dpeb})(\eta^5\text{-Cp}^*)_2(dppz)_2](CF_3SO_3)_4$ (**83**; top) and its polypyridyl analogues, given with a comparison of their *in vitro* antiproliferative activity against MCF-7 breast carcinoma cells.

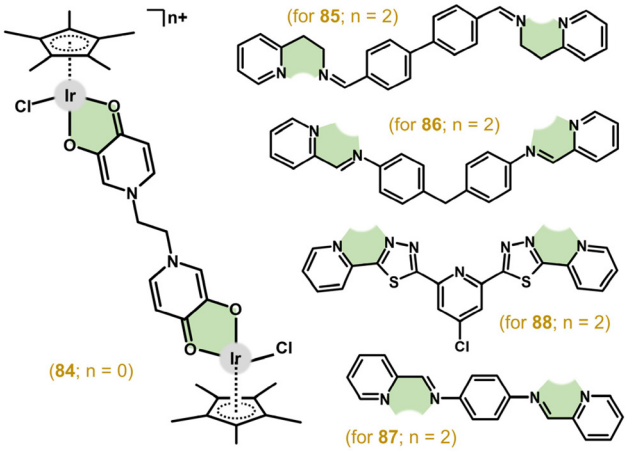


**Fig. 20** Structural formulas of dinuclear complex **84** and N-donor ligands involved in its analogues **85–88**.

containing larger dipyridinyl bridging ligands, specifically 4-[(*E*)-2-(4-pyridinyl)ethenyl]pyridine (dpee), 4-(2-pyridin-4-ylethynyl)pyridine (dpey) or 1,4-di(2-pyridin-4-ylethynyl) benzene (dpeb). Nevertheless, the type of polypyridyl chelating N,N-ligand seems to be more important for the resulting antiproliferative activity than a bridging ligand (Fig. 19). Interestingly, the bridging ligand used determined the type of nuclease activity, because dpee- and dpey-based complexes cleaved DNA in the dark, which was observed for the dpeb complex only when irradiated.

Hanif, Hartinger and co-workers prepared dinuclear Ir compounds containing various bitopical bispyridinone bridging ligands differing in the length of linkers between the two pyridinone units.[210] The linker length correlated with the lipophilicity and cytotoxic activity of the complexes, making $[Ir_2(\mu\text{-bpd})(\eta^5\text{-Cp}^*)_2Cl_2]$ (**84**; Fig. 20) with bis(3-hydroxy-2-methyl-4-pyridinon-1-yl)dodecane (Hbpd) the most potent complex with sub-micromolar activity ($IC_{50}$ = 0.2–0.9 μM) against HCT116, NCI-H460, SiHa and SW480 cell lines, markedly outperforming both the reference drugs used (mononuclear Ru complex IT-139, cisplatin). Importantly, **84** was less haemolytic towards red blood cells than its Rh analogue and cisplatin, with a negligible effect on vascular vessel formation in zebrafish embryos.

The $[Ir_2(\mu\text{-bphp})(\eta^5\text{-Cp}^*)_2Cl_2](PF_6)_2$ (**85**; Fig. 20) complex was derived from the tetradentate N-donor ligand *N*,*N*′-(biphenyl-4,4′-diyldimethylidyne)bis-2-(pyridin-2-yl)ethanamine (bphp).[211] This compound was highly cytotoxic, especially towards A2780 ($IC_{50}$ = 3.1 μM) and MCF-7 ($IC_{50}$ = 6.0 μM) cell lines, where it showed even higher activity than the Pt-based drugs. **85** was highly selective towards cancer cells (*e.g.*, the abovementioned A2780 and MCF-7 cells) over normal ones, studied in MRC-5 fibroblasts ($IC_{50}$ = 32.3 μM) and the primary culture of human hepatocytes ($IC_{50}$ = 61.3 μM). Recently, this work was followed by less cytotoxic analogues containing similar tetradentate N-donor ligands, this time derived from 4,4′–methylenedianiline (for **86** in Fig. 20)[225,226] and benzene-1,4-diamine (for **87** in Fig. 20).[226]

The $[Ir_2(\mu\text{-bphp})(\eta^5\text{-Cp}^*)_2Cl_2](PF_6)_2$ (**85**; Fig. 20) complex was derived from the tetradentate N-donor ligand *N*,*N*′-(biphenyl-4,4′-diyldimethylidyne)bis-2-(pyridin-2-yl)ethanamine (bphp).[211] This compound was highly cytotoxic, especially towards A2780 ($IC_{50}$ = 3.1 μM) and MCF-7 ($IC_{50}$ = 6.0 μM) cell lines, where it showed even higher activity than the Pt-based drugs. **85** was highly selective towards cancer cells (*e.g.*, the abovementioned A2780 and MCF-7 cells) over normal ones, studied in MRC-5 fibroblasts ($IC_{50}$ = 32.3 μM) and primary culture of human hepatocytes ($IC_{50}$ = 61.3 μM). Recently, this work was followed by less cytotoxic analogues containing similar tetradentate N-donor ligands, this time derived from 4,4′–methylenedianiline (for **86** in Fig. 20)[225,226] and benzene-1,4-diamine (for **87** in Fig. 20).[226]

Very recently, dinuclear complex **88** (Fig. 20) with a thiadiazole-based bitopic tetradentate N-donor ligand, showed low-micromolar antiproliferative activity in various human cancer cells (*e.g.*, $GI_{50}$ = 1.7 μM in MV4–11 cells).[227] Importantly, this highly effective complex outperformed its mononuclear analogue. The MoA and some related processes (*e.g.*, interaction with mixtures of small biomolecules) were studied in detail for **88** (see sections 4.5, 5.5 and 6.1.1).

The trinuclear complex derived from a quinolyl-benzimidazole-based polydentate ligand was inactive in MCF-7 and MDA-MB-231 cancer cells.[228] Highly cytotoxic octanuclear

complexes $[Ir_8(\mu\text{-dend}^1)(\eta^5\text{-Cp}^*)_8Cl_8]$ and $[Ir_8(\mu\text{-dend}^2)(\eta^5\text{-Cp}^*)_8Cl_8](PF_6)_8$ (**89**; Fig. 21) were developed from N,O-donor salicylaldimine ($Hdend^1$) and N,N-donor 2-iminopyridyl ($dend^2$) substituted poly(propyleneimine)diaminobutane-based dendrimers.[212] The best-performing complex **89** was more cytotoxic ($IC_{50}$ = 0.8 μM) than cisplatin ($IC_{50}$ = 1.5 μM) in A2780 cells, and retained high selectivity with $IC_{50}$ = 28.6 μM in normal HEK-293 cells.

Generally, metallacages contain two (tetranuclear metallarectangles), three (hexanuclear metallaprisms) or four (octanuclear metallacubes) conjugated dinuclear units (clips).[229] All three types have been reported for Ir–Cp$^x$ complexes, which in most cases showed high activity but low selectivity.[220–224] Higher and pharmacologically prospective selectivity towards cancer cells over normal ones was reached by tetranuclear complexes involving 3-undecyl-2,5-dihydroxy-1,4-benzoquinone (embelin, Hemb; Fig. 22).[222] For example, $[Ir_4(\mu\text{-emb})_2(\mu\text{-dpee})_2(\eta^5\text{-Cp}^*)_4](CF_3SO_3)_4$ (**90**; Fig. 21) exhibited markedly lower $IC_{50}$ values in cancer cells (*e.g.*, 0.6 μM in HeLa cells) compared with HEK-293 cells (70.8 μM).

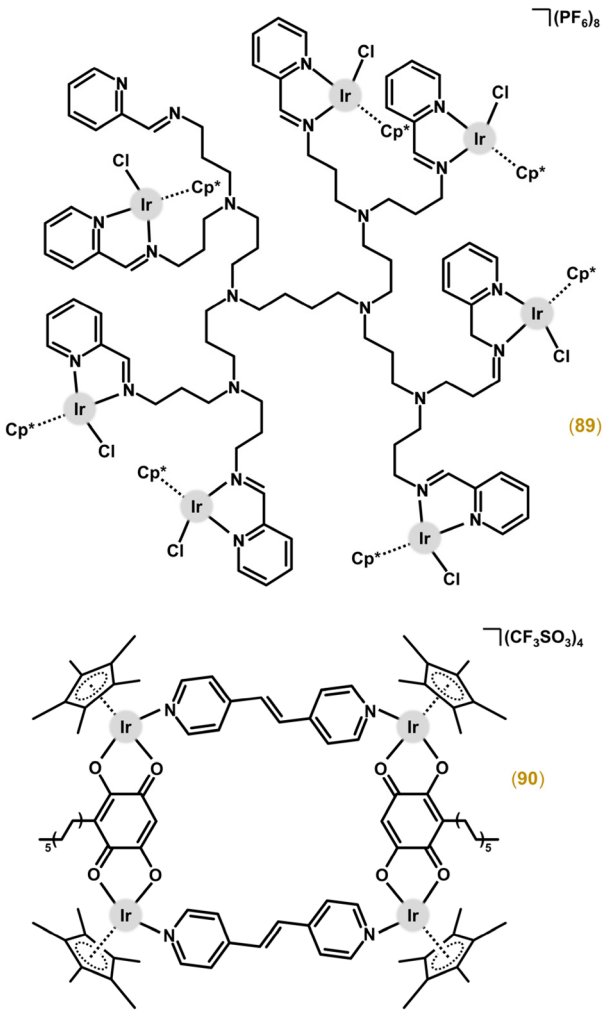


Fig. 21 Structural formulas of complexes **89** and **90**.

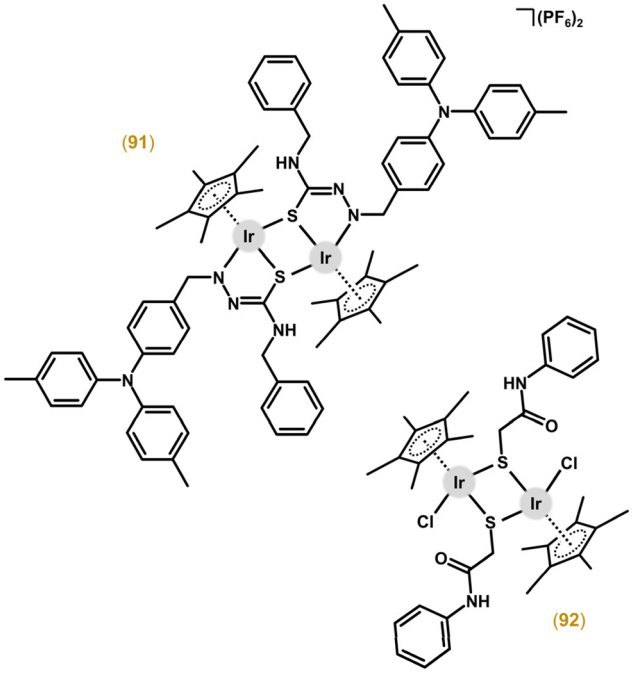


Fig. 22 Structural formulas of complexes **91** and **92**.

Thiolato and chalcogenato complexes showed nanomolar activity in human cancer and normal cells, implying their low selectivity, which excluded them from advanced pharmacological studies.[217–219] Similar dinuclear Ir complexes were prepared by two different research groups, with a sulfur atom being involved in the chelate ring and bridging both metal centres at the same time.[230–232] Complexes with pyrrole-2-thioamide ligands showed only low activity towards A549 cancer cells at a concentration of 100 μM.[230] Their analogues with triphenylamine-modified TSC (*e.g.*, **91**; Fig. 22)[231] or ferrocene-modified TSC[232] were effective against A549 and HeLa cancer cells, with low selectivity towards these cells over the BEAS-2B normal cells used. Complex **91** is discussed in more detail below (including *in vivo* anticancer activity).

The electroneutral $[Ir_2(\mu\text{-mpa})_2(\eta^5\text{-Cp}^*)_2Cl_2]$ (**92**; Fig. 22) complex involves 2-mercapto-*N*-phenylacetamide (Hmpa), which has a different coordination mode (an S-donor bridging ligand) than its Ru analogue $[Ru_2(\mu\text{-mpa})_2(\eta^6\text{-pcym})_2]$ with mpa coordinated as an N,S-chelating ligand bridging the two metal centres through the sulfur atom of mpa.[233] Both complexes exhibited comparable reductions of cancer cell viability expressed in mg $mL^{-1}$, implying a higher cytotoxicity of the Ir complex **92** (with respect to its higher $M_w$).

**3.3.2. Heterometallic complexes.** Similarly to the above-discussed multinuclear homometallic Ir–Cp$^x$ complexes, their heterometallic counterparts have recently been comprehensively reviewed.[31] The first combination of an Ir cyclopentadienyl motif with another metal was reported by Sheldrick and co-workers, who studied the DNA interaction of heterometallic conjugates of $\{Ir(\eta^5\text{-Cp}^*)(dppz)\}$ with various Pt(II) species (*e.g.*,

*trans*-{$Pt(NH_3)_2(DMF)$}) bridged by methionine-based peptides (see section 5.4 for more details).[234,235]

Other heterometallic Ir–$Cp^x$ complexes represent a family of ferrocene (Fc)-appended compounds.[153,174,215,236–240] Since Fc is involved in a well-known antimicrobial active agent, ferroquine, such compounds were often studied for their antimicrobial activity. Along with antimicrobial activity, these Fc-appended heterometallic complexes were also studied for their anticancer activity. Liu and co-workers suggested a positive effect from the introduction a ferrocene substituent into the structure of Ir–$Cp^x$ complexes,[78,239] because, for example, the heterometallic [$Ir(\eta^5$-Cp*)Cl($ppy^{Fc}$)] (**93**) complex exceeded the potency of its mononuclear analogue **43** (Fig. 23A).[239] Interestingly, a $Cp^x$ ring extension did not provide higher antiproliferative activity for the ferrocene-containing compounds (*e.g.*, **93**), which was in contrast with congeners involving unsubstituted ppy. Other strategies by the same research group to introduce the Fc entity into the structure of various Ir cyclopentadienyl complexes (see complexes **94** and **95** in Fig. 23B) did not lead to an improvement of the antiproliferative activity.[241,242]

A different design was applied for heterometallic Ir–Pt[243] and Ir–Ru[244] complexes (Fig. 24). Ir–Pt complex **96** was not

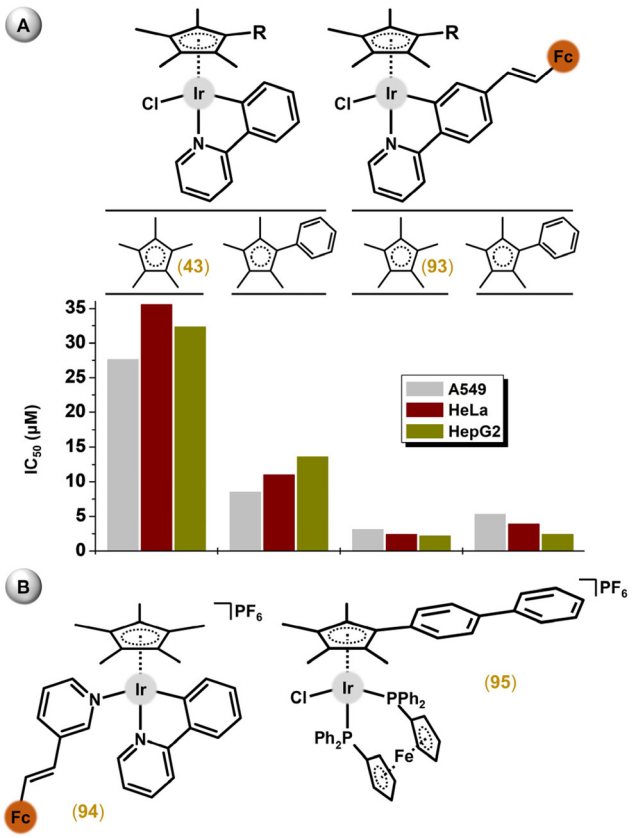


**Fig. 23** (A) Structural formulas and *in vitro* antiproliferative activity of [Ir($\eta^5$-$Cp^x$)Cl($ppy^n$)] complexes **43** and **93**, containing various $Cp^x$ derivatives (Cp* or $Cp^{ph}$) in combination with ppy or its ferrocene (Fc)-substituted derivative ($ppy^{Fc}$). (B) Structural formulas of ferrocene-containing complexes **94** and **95**.

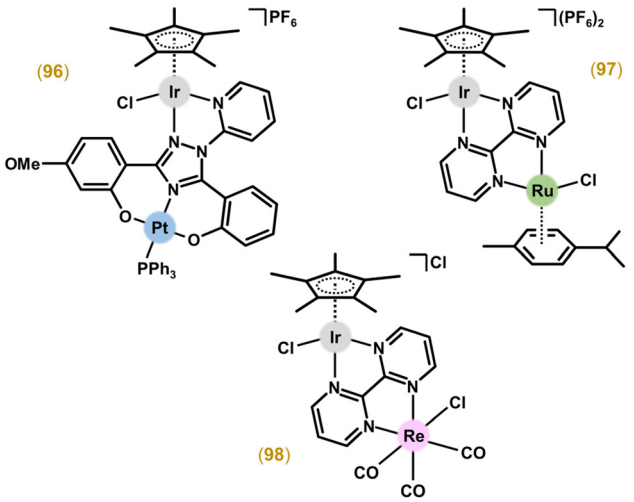


**Fig. 24** Structural formulas of heterometallic complexes **96–98**.

effective against MDA-MB-231 cells, which indicated its lower potency compared with the co-studied mononuclear Pt complex and dinuclear heterometallic Ru–Pt and Cu–Pt analogues.[243] The Ir–Ru complex [$Ir(\eta^5$-Cp*)Cl(μ-bpm)$Ru(\eta^6$-pcym)Cl]$(PF_6)_2$ (**97**), containing tetradentate 2,2′-bipyrimidine (bpm; Fig. 24), was studied, together with $Ir_2$ and $Ru_2$ analogues, in MDA-MB-468 (breast carcinoma) and Caco-2 (colon carcinoma) cells.[244] Although **97** was less effective ($IC_{50}$ = 1.9 μM) against MDA-MB-468 cells than $Ir_2$ ($IC_{50}$ = 1.8 μM) and $Ru_2$ ($IC_{50}$ = 0.9 μM) analogues, this heterometallic compound exceeded ($IC_{50}$ = 6.2 μM) both homometallic analogues ($IC_{50}$ = 32.4 and 46.0 μM for $Ir_2$ and $Ru_2$, respectively) in Caco-2 cells. Also of interest, **97** was more effective towards Caco-2 cells than both mononuclear parts, *i.e.*, [$Ir(\eta^5$-Cp*)(bpm)Cl]$PF_6$ ($IC_{50}$ = 50.4 μM) and [$Ru(\eta^6$-pcym)(bpm)Cl]$PF_6$ ($IC_{50}$ = 49.6 μM) (not studied in MDA-MB-468 cells).

The same research group also developed a new type of heterometallic complex, [$Ir(\eta^5$-Cp*)Cl(μ-bpm)$ReCl(CO)_3$]Cl (**98**; Fig. 24), using the conjugation of the Ir(III)–Cp* and Re(I)-tricarbonyl motif through the same bridging bpm ligand.[245] This complex showed approximately 5-fold higher antiproliferative activity against MDA-MB-468 cells ($IC_{50}$ = 24.1 μM) than its $Re_2$ homometallic and Ru–Re heterometallic analogues. **98** was highly selective towards MDA-MB-468 cells in comparison with non-cancerous HaCaT ones ($IC_{50}$ = 234.8 μM).

The combination of Ir and Cu was obtained with phosphanes (P-coordinated to Ir) derived from fluoroquinolones (O,O-coordinated to Cu).[246] These complexes, such as the best-performing complex, [$Ir(\eta^5$-Cp*)$Cl_2$(μ-pcfx)Cu(phen)$(H_2O)$]$NO_3$ (**99**; Fig. 25 and Fig. 4), were significantly more effective than cisplatin in various human cancer cell lines, whereas they were almost ineffective in non-cancerous HEK-293T cells. Especially the anticancer potency of **99** in DU145 cells is noteworthy not only because of the extremely low $IC_{50}$ value in the low-picomolar range ($IC_{50}$ = 1.3 × $10^{-6}$ μM; 24 h exposure time), but also because of the unusual recovery of treated cells ($IC_{50}$ =

 

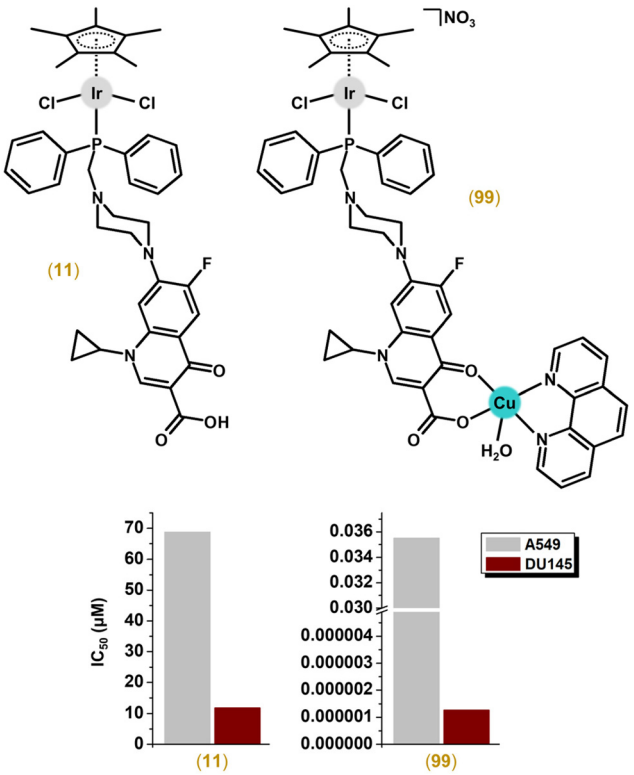


Fig. 25 Structural formulas and *in vitro* antiproliferative activity of mononuclear complex [Ir($\eta^5$-Cp*)$Cl_2$(pcfx)]$NO_3$ (**11**) and its heterometallic analogue [Ir($\eta^5$-Cp*)$Cl_2$(μ-pcfx)Cu(phen)($H_2O$)]$NO_3$ (**99**).

125.7 μM; 24 h exposure + 48 h recovery time in a drug-free environment). Similar results were obtained for **99** and analogues in, *e.g.*, MCF-7 cells, while the opposite effect was observed in A549 cells ($IC_{50}$ = 35.5 nM for 24 h exposure time, and $IC_{50}$ = 0.4 nM for 24 h exposure + 48 h recovery time). **99** was also loaded into liposomes (section 6.4). Importantly for future studies in the field of heterometallic anticancer Ir–$Cp^x$ complexes, **99** exhibited markedly higher antiproliferative activity in cancer cells (Fig. 25) than its mononuclear analogues (**11** and congeners; Fig. 4).[57,246]

### 3.3. Other structural types

Many researchers have tried to replace the chlorido ligand of widely studied chlorido Ir–$Cp^x$ complexes by a different monodentate ligand to improve biological activity. Obviously, when an electroneutral monodentate ligand is used to replace the chlorido ligand, the charge of the complex changes. The first investigation of this phenomenon involved [Ir($\eta^5$-Cp*)(dppz)(py)]$(CF_3SO_3)_2$ (**100**; Fig. 26).[207]

Contrasting results were reported for an electroneutral chlorido ppy complex and its ionic analogue with pyridine, [Ir($\eta^5$-$Cp^{bph}$)(ppy)(py)]$PF_6$ (**101**; Fig. 27).[44] In particular, **101** showed higher ($GI_{50}$ = 0.2 μM) activity in the NCI-60 human cancer cell screen and improved selectivity compared with the chlorido complex ($GI_{50}$ = 0.7 μM). Regarding similar $Cp^{ph}$ complexes, [Ir($\eta^5$-$Cp^{ph}$)(ppy)($py^{NMe2}$)]$PF_6$ (**102**; $py^{NMe2}$ = *N*,*N*-dimethylpyridin-4-amine) also outperformed cisplatin in the NCI-60 screening (Fig. 27; section 4.4).[162]

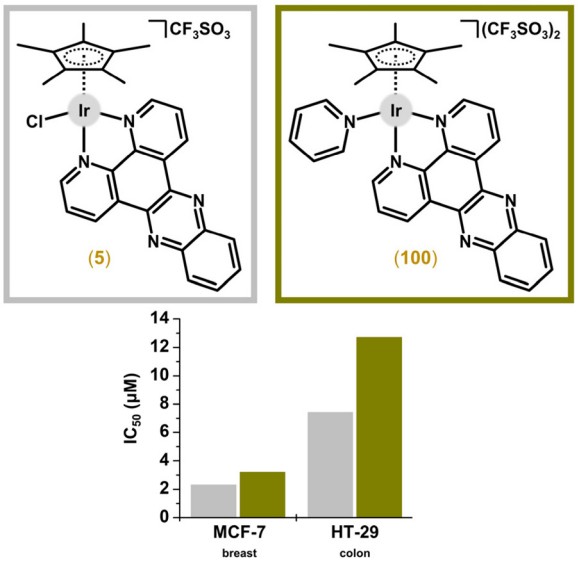


Fig. 26 Structural formulas and *in vitro* antiproliferative activity of [Ir($\eta^5$-Cp*)(dppz)X]$^{n+}$ complexes **5** and **100** containing various monodentate ligands.

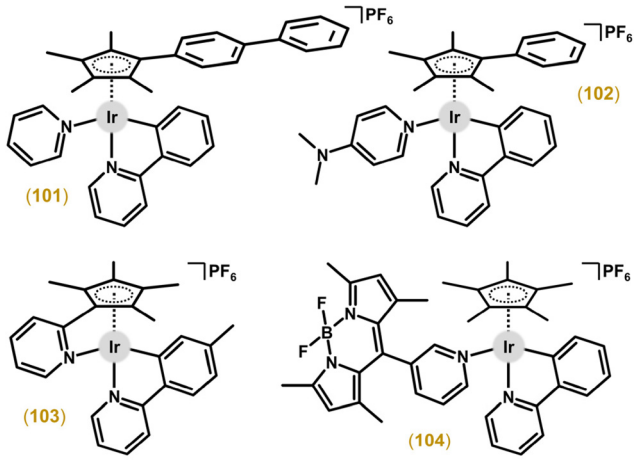


Fig. 27 Structural formulas of complexes **101**–**104**.

Other groups used pyridine for the introduction of other functionalities to Ir–$Cp^x$ complexes. However, mono- and trinuclear complexes with 4-ferrocenylpyridine were less effective than analogues with unsubstituted pyridine.[153] On the other hand, a similar complex with 3-pyridyl-BODIPY (**104**; Fig. 27) was more active than the chlorido complex in a small panel of human cancer cell lines (*e.g.*, $IC_{50}$ = 0.6 μM *vs.* 14.0 μM in A2780 cells).[163] Thanks to the fluorescent BODIPY substituent, this complex was also used for live cell imaging.

A different introduction of pyridine to Ir was reported by Pizarro and co-workers.[138,164,165] Specifically, they used 2-[(2,3,4,5-tetramethylcyclopenta-2,4-dien-1-yl)methyl]pyridine

($HCp^{mpy}$) as the $\eta^5$-bound arenyl ligand, the pendant pyridine of which coordinated to the central atom of the complexes.[164] The activity differed significantly according to the chelating C, N- or N,N-donor ligands used. $[Ir(\eta^5\text{-}Cp^{mpy})(ppy^1)]PF_6$ (**103**; $ppy^1$ = 2-(4-methylphenyl)pyridine) exhibited nanomolar activity towards the MCF-7 cell line ($IC_{50}$ = 0.05 μM) with promising selectivity towards this cancer cell line over the MRC-5 normal cells used (SI = 91.8).

A similar approach was reported for thiomaltol- and thiopyridone-based complexes with the chlorido ligand being replaced by 1-methyl-1*H*-imidazole (*e.g.*, complex **105** in Fig. 28).[193,195] Motivated by the clinically-studied Ru complex RAPTA-C, several Ir–$Cp^x$ complexes were prepared with pta as a monodentate P-donor ligand.[45,191,247] These pta complexes were in most cases of low-to-moderate antiproliferative activity. The representative Ir–pta complex $[Ir(\eta^5\text{-}Cp^*)(dpp)(pta)]CF_3SO_3$ (**106**; Fig. 28) was not stable under the mimicked extracellular conditions (100 mM NaCl solution), where it released its chelating dpp ligand and degraded to $[Ir(\eta^5\text{-}Cp^*)Cl_2(pta)]$; Hdpp = 1,3-diphenylpropane-1,3-dione.[191]

In some cases, the chlorido ligand was replaced by a different halogenido ligand.[43,46,248] For example, a pair of pyridylphosphinate complexes (*e.g.*, **107** in Fig. 28) differs markedly in their potency against the H460 cell line ($IC_{50}$ > 200 μM for the chlorido complex and $IC_{50}$ = 52 μM for its iodido analogue).[46] A similar approach was used for a series of hydrogensulfido Ir–$Cp^x$ complexes, including the highly cytotoxic $[Ir(\eta^5\text{-}Cp^{bph})(bpy)(SH)]PF_6$ complex (**108** in Fig. 28).[249]

Another design used bioactive carboxylato ligands (*e.g.*, histone deacetylase (HDAC) inhibitor 4-phenylbutyrate, pb) to replace the chlorido ligand, providing multi-component (multi-targeted) complexes releasing two bioactive species (*i.e.*, organic and Ir-based) under conditions that mimicked physiological conditions (section 6.2).[43,250] Another pair of complexes was derived from N,O-coordinated lidocaine and two different monodentate N-donor (bi)phenylcyanamide-based ligands.[251] These complexes were reported as one of only a few representatives of Ir cyclopentadienyl complexes studied for possible applications in PDT (section 6.3).

The $[Ir(\eta^5\text{-}Cp^*)(pyth\text{-}\kappa N,\kappa S)(pyth\text{-}\kappa S)]$ (**109**; Fig. 29) complex, with pyrimidine-2-thiol (Hpyth) coordinated as N,S-chelating (four-membered rings) and monodentate S-donor ligands, was markedly less cytotoxic than cisplatin and its Rh congener.[252] No relevant antiproliferative activity was detected either for a dinuclear Ir complex with $\{Ir(\eta^5\text{-}Cp^*)Cl\}$ and $\{Ir(\eta^5\text{-}Cp^*)Cl_2\}$ moieties bridged by a tridentate-coordinated azo ligand (2 + 1 fashion) bearing pyrazine and pyridine terminal substituents (**110**; Fig. 29).[135] The Ir(I) complex $[Ir(\eta^5\text{-}Cp^*)(\eta^4\text{-}L)]$, where L stands for *p*-benzoquinone ($IC_{50}$ = 93.0 μM in A2780 cells) and its dithio ($IC_{50}$ = 154.0 μM) and diseleno ($IC_{50}$ = 5.0 μM; **111**; Fig. 29) derivatives represent a unique design combining two hapto-coordinated ligands; $IC_{50}$ = 3.0 μM for cisplatin.[253]

Liu *et al.* obtained stable five-coordinated (16-electron) complexes *via* a solvent-involved rearrangement reaction with α-keto-β-diimine ligands (*e.g.*, **112** in Fig. 29)[254,255] or similar compounds derived from amine-imine ligands (*e.g.*, **113** in Fig. 29).[256] Among them, complexes involving isopropyl-substituted amino-imines structurally differed in the substitution on the $Cp^x$ ring (Me, Cy, ph, bph, Me-ph, F-ph; see section 4.2).[254] These complexes (*e.g.*, **112**), in most cases, exceeded the activity of cisplatin towards cancer cells; however, no selectivity over normal cells was found.

Other work on electron deficient five-coordinated complexes involves S,S-coordinated 1,2-dicarba-closododecarborane-1,2-dithiolato and benzene-1,2-dithiolato ligands. Unlike some Ru(II) or Os(II) congeners, Ir(III) complexes (*e.g.*, **114** in Fig. 29) were found to be inactive.[257] Lord and co-workers replaced the $\eta^5$-Cp* arenyl ligand with an $\eta^4$-cod arene within the structure of the electroneutral chlorido complex, $[Ir(\eta^4\text{-cod})$

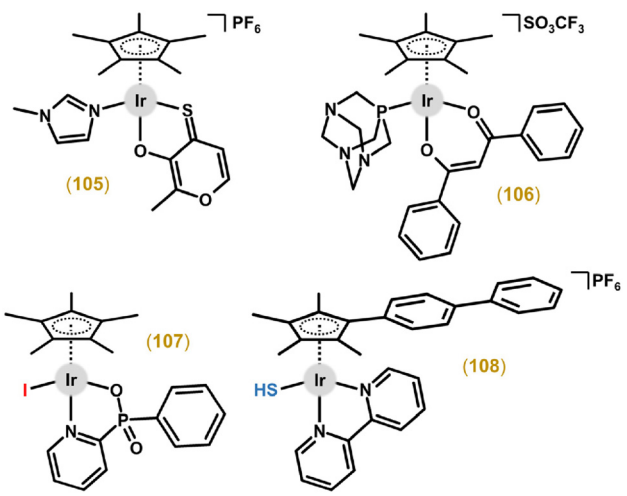


Fig. 28 Structural formulas of complexes **105**–**108**.

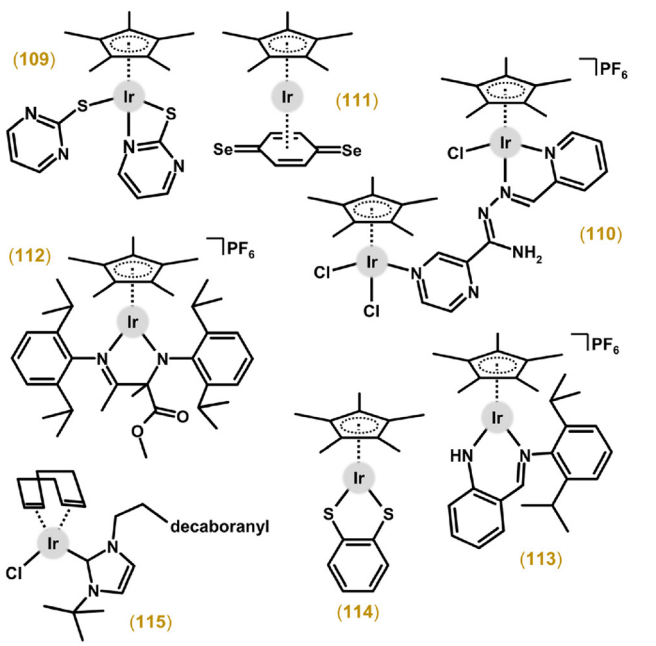


Fig. 29 Structural formulas of complexes **109**–**115**.

Cl(nhc$^1$)] (**115**; Fig. 29); nhc$^1$ = decaborane-appended NHC ligand.[71] Although **115** was less effective against cisplatin-sensitive cancer cell lines (*e.g.*, $IC_{50}$ = 2.2 μM in A2780 cells) than cisplatin ($IC_{50}$ = 1.3 μM), it exceeded the structurally similar cyclopentadienyl complex, [Ir(η$^5$-Cp*)Cl$_2$(nhc$^1$)] ($IC_{50}$ = 6.4 μM).

## 4. Structure–activity relationships

The anticancer Ir–Cp$^x$ complexes reviewed herein have often been studied with their Rh analogues and with structurally similar Ru and Os arene complexes, allowing the discussion of the central atom effect on antiproliferative activity (section 4.1). Furthermore, the [Ir(η$^5$-Cp$^x$)(L^L)X]$^{0/+}$ type anticancer Ir–Cp$^x$ compounds are discussed as they are more prominent than analogues containing three monodentate ligands (see section 2.1 and Fig. 3). Regarding [Ir(η$^5$-Cp$^x$)(L^L)X]$^{0/+}$ complexes, they consist of three ligands, namely, an η$^5$-coordinated Cp$^x$ ring, a bidentate (chelating) L^L ligand and a monodentate X ligand. Obviously, various SARs can be derived for the anticancer Ir–Cp$^x$ complexes reviewed with respect to their ligands. Thus, in this section, the effect of the composition of all three ligands on the resulting biological effect is also analysed (sections 4.2–4.4). Additionally, the effects of nuclearity (*i.e.*, the number of central atoms in multinuclear complexes) and counter-anions in ionic complexes are also discussed (sections 4.5 and 4.6).

### 4.1. Central atom effect

In one of the pioneering studies, Sheldrick and co-workers reported two pairs of analogous Ir and Ru complexes, which enabled a discussion of the central atom effect on biological activity.[22] In fact, although there were significant differences in the $IC_{50}$ values obtained, the trend did not direct future research. Specifically, Ir complex **5** was less potent ($IC_{50}$ = 2.3 and 7.4 μM) than its Ru analogue [Ru(η$^6$-hmb)Cl(dppz)]CF$_3$SO$_3$ ($IC_{50}$ = 2.1 and 2.5 μM) in MCF-7 and HT-29 cells, respectively (Fig. 30), but another co-studied Ir compound, **6** ($IC_{50}$ = 0.2 and 0.4 μM), exceeded its Ru congener, which showed $IC_{50}$ values of 2.1 and 1.4 μM in the same cancer cells.

Regarding the following works with Ru and Ir analogues being studied for their anticancer effect, some Ir compounds exceeded the potency of their Ru congeners.[46,59,60,111,114,146,157,192,197,245] In other cases, Ir complexes were comparably[46,59,60,111,114,192,197,256] or even less potent[53,59,64,92,104,110,116,142,148,157,167,201,203,241,244] than their Ru analogues (Fig. 30). The careful reader will have noticed that some papers belong to more than one category, which makes subsequent evaluation very difficult. The same then applies to the following discussion.

A similar conclusion can be drawn for the comparison of Ir–Cp$^x$ complexes and their direct Rh analogues. Specifically, several Ir complexes outperformed the anticancer activity of their Rh analogues,[43,64,67,83,89,112,141,145,184,190,191] while in other cases, Ir complexes exhibited only comparable[45,46,67,83,144,190,191,252] or even lower potency[43,45,67,79,83,86,144,168,184,190,191,252] than Rh compounds derived from the same ligands (Fig. 30). Only one paper was dedicated to Ir–Cp* and Os–pcym complexes.[175] For both pairs

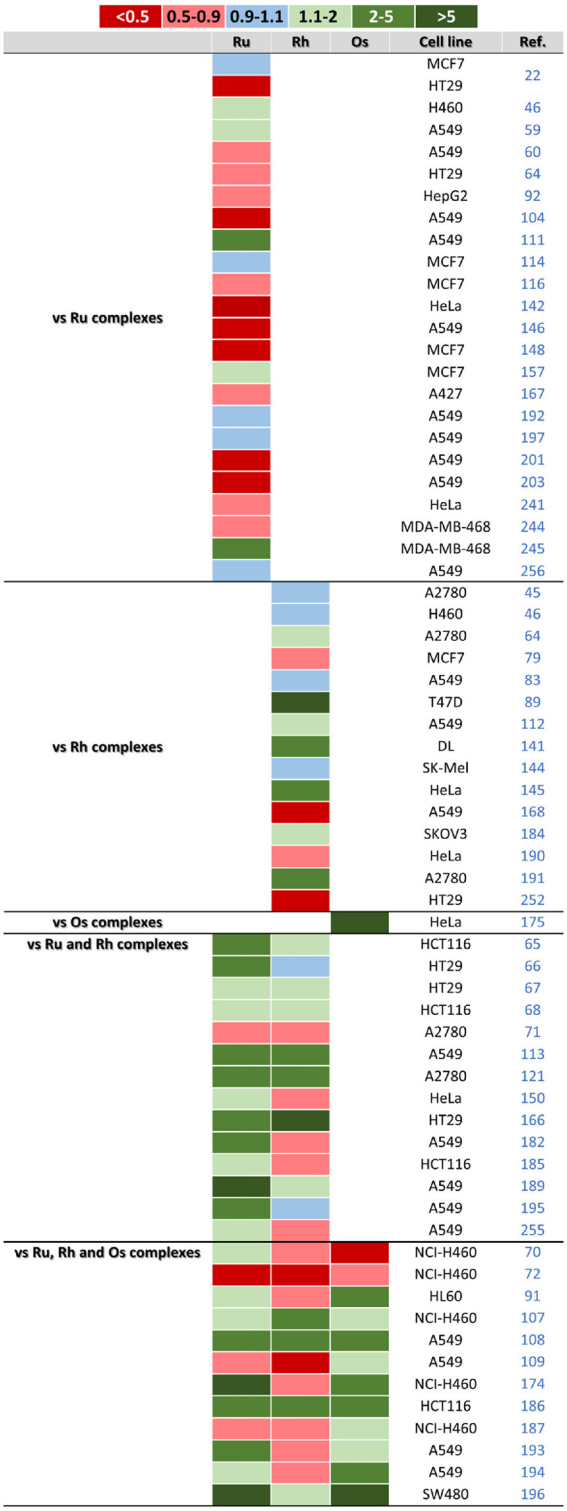


**Fig. 30** A comparison of the relative activity (RA) of Ir complexes with their Ru, Rh and/or Os analogues. RA = $IC_{50}$(Ru/Rh/Os complex)/$IC_{50}$(Ir complex). The best-performing Ir complexes and the data from lung cancer cells (where possible) were chosen for these comparisons.

of analogues derived from these metals, the Ir complex was more effective than its Os congener (Fig. 30).

Many papers have reported complexes derived from three (Ru/Rh/Ir or Ru/Os/Ir) of the four metals of interests. For these complexes, it can be concluded that Ir and Rh compounds are more effective than Ru ones (Fig. 30). This is because an equal number of papers reported the Ir[65,67,68,113,121,166,185,189,195] or Rh[65,66,71,121,150,182,185,255] complexes as the best-performing ones. Significantly fewer papers discuss Ru compounds as being more potent than structurally similar Ir and Rh compounds.[66,68] In some cases, Ir complexes exhibited the same biological effect as their Ru[68,166] or Rh[65–67,121,185,195] analogues, thus outperforming complexes of the third metal (*i.e.*, Rh or Ru, respectively). Several Ir compounds have shown the lowest potency.[71,121,150,182] The equal potency of the Ru, Rh and Ir complexes is exceptional in the literature.[185]

Regarding the second group of complexes derived from three different metals (Ru/Os/Ir in this case), 10 μM trinuclear Ir complex was comparably active to an equimolar dose of its Ru and Os analogues derived from the hexadentate quinolylbenzimidazole-based ligand ($IC_{50}$ were not reported for Ir complex).[228] The second paper reported on complexes containing various dithiolato ligands, but Ir complexes were inactive ($IC_{50}$ > 100 μM), and thus, less effective than their Ru and Os analogues.[257]

The last group of compounds is represented by co-studied complexes of all four metal (*i.e.*, Ru/Rh/Os/Ir). As in the case of the above-discussed Ru/Rh/Ir complexes, it was Ir[70,107,108,176,186,193,194,196] and Rh[70,91,107,174,193,194] complexes that were most often reported as the most active ones from Ru/Rh/Os/Ir analogues (Fig. 30). Other papers reported appropriate Ir complexes as having lower anticancer activity than Ru,[176] Ru and Rh,[91,109,187] Ru and Os,[107] and Rh and Os[70,193] analogues. Several Ir complexes were outperformed by all three Ru, Rh and Os analogues.[70,72,107,140,187]

The effect of the central atom type is discussed elsewhere[31] for multinuclear complexes.[121,152,153,209–224] Recently, a series of dinuclear Ru, Rh, Os and Ir complexes with two different bis(1-(pyridin-2-yl))(methanimine)-based bridging ligands was reported.[226] One Ir complex and its Ru and Os complexes were inactive ($IC_{50}$ > 100 μM) and outperformed by the Rh complex. The second Ir complex was moderately effective against the human cancer cell lines used, where it exceeded the potency of the Ru and Os analogues. Regarding its comparison with a similar Rh complex, it is ambiguous again, because the potency of the Ir complex is higher than (HCT116 cells), comparable to (SiHa cells) or lower than (SW480 cells) its Rh analogue.

### 4.2. Effect of a cyclopentadienyl ring

In pioneering work in 2011, Sadler and co-workers reported the dependence of antiproliferative activity (and other properties) on the $Cp^x$ ring size (Fig. 31).[41] In particular, inactive Cp* complexes were turned into active compounds when their Cp* ring was replaced by a more extended one, namely, 2,3,4,5-tetramethyl-1-phenylcyclopenta-2,4-dienyl ($Cp^{ph}$) or 1-(biphenyl-4-yl)-2,3,4,5-tetramethylcyclopenta-2,4-dienyl ($Cp^{bph}$). This was observed especially for phen and bpy complexes, the $Cp^{bph}$ complexes (**14** and **15**, Fig. 5) of which reached even sub-micromolar activity (Fig. 31). $Cp^{bph}$ complexes bearing en or pico were markedly less effective, but their $Cp^{bph}$ complexes still exceeded the potency of their Cp* analogues. The activity enhancement with increasing phenyl substitution on $Cp^x$ was confirmed by the same group for a series of electroneutral $[Ir(\eta^5\text{-}Cp^x)Cl(ppy)]$ complexes (Fig. 31).[154,158]

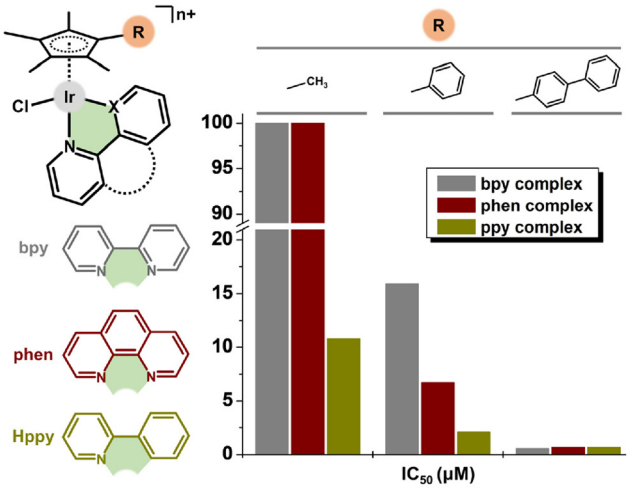


**Fig. 31** The dependence of the *in vitro* antiproliferative activity of $[Ir(\eta^5\text{-}Cp^x)Cl(L\text{^}L)]^{n+}$ complexes in A2780 ovarian carcinoma cells on the cyclopentadienyl ring size; $Cp^x$ = Cp*, $Cp^{ph}$ or $Cp^{bph}$, L^L = 2,2′-bipyridine (bpy; $n$ = 1), 1,10-phenanthroline (phen; $n$ = 1) or deprotonated 2-phenylpyridine (ppy; $n$ = 0).

In numerous subsequent studies, a $Cp^x$ ring extension was successfully applied for the enhancement of the antiproliferative activity of parent Cp* complexes. On the other hand, this dependence should not be accepted as being straightforward, because in numerous cases it was Cp* complexes that outperformed their $Cp^{ph}$ and $Cp^{bph}$ analogues. This is briefly summarized in Fig. 32.

Similarly to the majority of Ir–$Cp^{ph}$ and Ir–$Cp^{bph}$ complexes, ppy-based Ir–$Cp^x$ complexes involving the benzyl substituted $Cp^x$ ring exceeded the antiproliferative activity their Cp* analogues.[165] For a similar en-derived complex, the benzyl substituent of the $Cp^x$ ring did not induce any relevant antiproliferative activity of the previously mentioned inactive complex ($IC_{50}$ > 500 μM; MCF-7 cells).[138] Also of interest, it was reported that the effect of $Cp^x$ ring extension on the resulting antiproliferative activity could be different for chlorido complexes (positive effect) and their iodido counterparts (negligible or even negative effects).[248]

Although not studied for the final mononuclear complexes, substitution of the $Cp^x$ ring with a long-chain alcohol was found to be beneficial in terms of the antiproliferative activity of dinuclear $[Ir(\mu\text{-}Cl)(\eta^5\text{-}Cp^x)Cl]_2$ intermediates (see section 2.2), with $IC_{50}$ = 92.0 μM (Cp* complex), 30.0 μM (5-hydroxy-

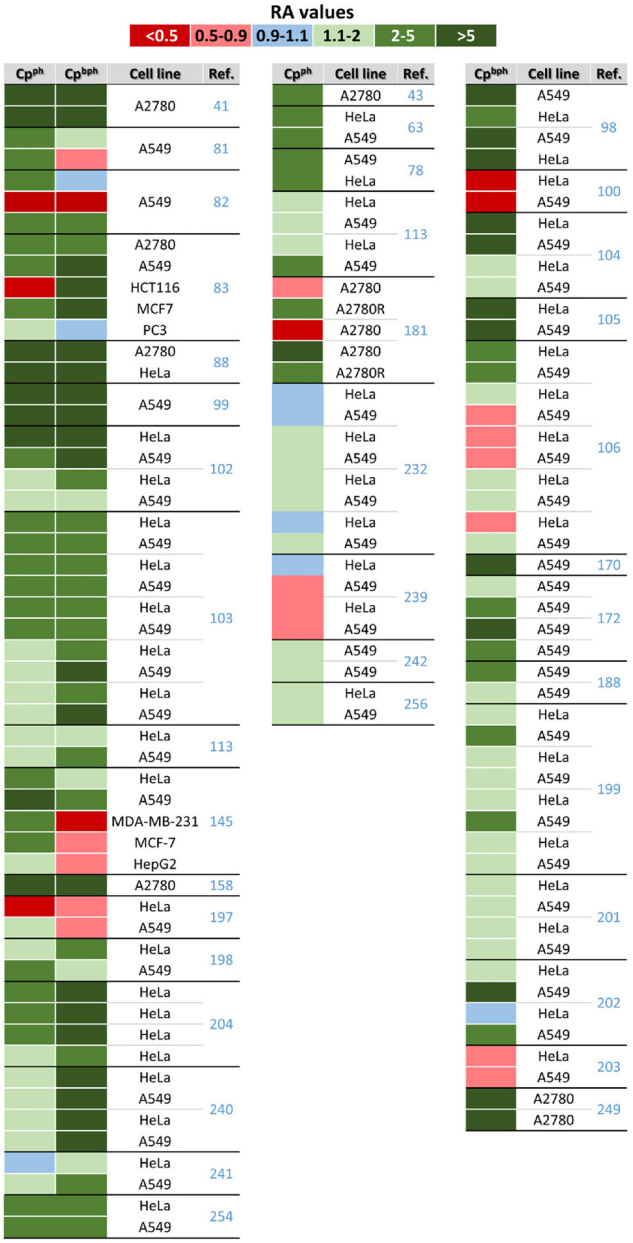


Fig. 32 A comparison of the relative activity (RA) of $Cp^{ph}$ and $Cp^{bph}$ complexes *versus* their Cp* analogue. RA = $IC_{50}$(Cp* complex)/$IC_{50}$($Cp^x$ complex); $Cp^x$ = $Cp^{ph}$ and $Cp^{bph}$.

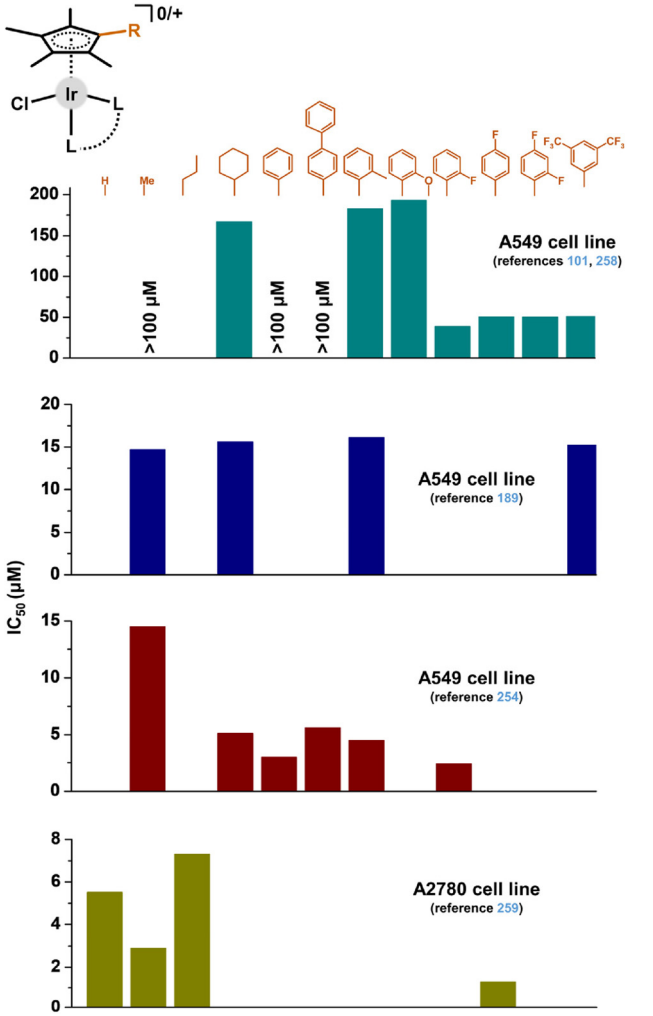


Fig. 33 A comparison of the *in vitro* antiproliferative activity ($IC_{50}$ values [μM]) of complexes containing different cyclopentadienyl derivatives. Dark cyan – zwitterionic iminopyridine complexes;[101,258] dark blue – complexes with phosphane-imines;[189] dark red – five-coordinated 16e⁻ complexes with amino-imines;[254] dark yellow – electroneutral [Ir($\eta^5$-$Cp^x$)Cl(ppy)] complex.[259]

pentyl derivative) and 10.2 μM (14-hydroxytetradecyl derivative) in the HT-29 cell line.[64]

Within their extended research on anticancer Ir–$Cp^x$ complexes, Liu and co-workers paid attention to different $Cp^x$ substituents,[189,254,258] than the notoriously used $Cp^{ph}$ and $Cp^{bph}$ ones. In particular, various $Cp^x$ rings were used within complexes derived from phosphane-imines,[189] amino-imines (in five-coordinated 16e⁻ complexes)[254] and iminopyridines (in zwitterionic complexes).[101,258] The data implied a positive effect of fluorine substitution on the $Cp^x$ ligand for the antiproliferative activity of such compounds (Fig. 33). Similar research was reported for electroneutral [Ir($\eta^5$-$Cp^x$)Cl(ppy)] complexes involving various $Cp^x$ ring substituents.[259] Their activity for a panel of cancer cells followed the order (of $Cp^x$ substituents) of 4-fluorophenyl > hydrogen > methyl > propyl, which again claimed that the fluoro-substituted $Cp^x$ ligand was beneficial for the resulting antiproliferative activity.

### 4.3. Effects of a chelating ligand

**4.3.1. Donor set effect.** In several works, complexes with a different donor set of coordinated chelating ligands have been prepared. The [Ir($\eta^5$-$Cp^{bph}$)Cl(pic)] (**37**; Fig. 9) complex involving N,O-coordinated pic was less potent than its congeners with the N,N-donor ligands phen and bpy (**14**, **15**; Fig. 34).[41] Despite the lower antiproliferative activity, **37** had higher affinity towards the model nucleobases 9-ethylguanine (EtG) and 9-ethyladenine. Although this result was encouraging for

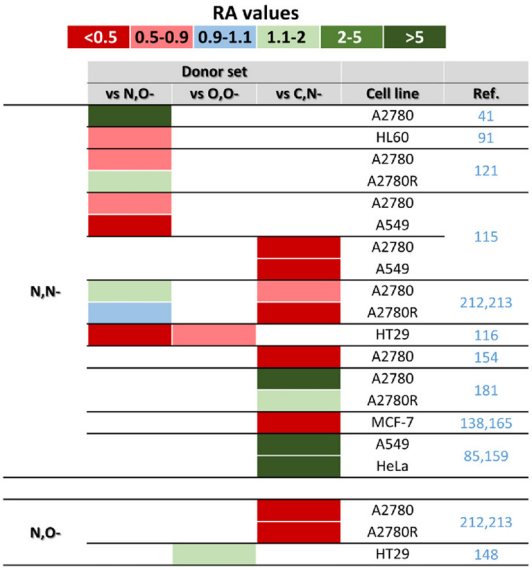


**Fig. 34** A comparison of the relative activity (RA) of complexes involving differently coordinated ligands. For the N,N- column: RA = $IC_{50}$ (complex with different donor set)/$IC_{50}$ (complex with an N,N-donor set); for the N,O- column: RA = $IC_{50}$ (complex with different donor set)/$IC_{50}$ (complex with an N,O-donor set).

future investigations with N,N-donor ligands instead of N,O-ones, most of the published results showed that complexes with an N,N-donor set were less anticancer effective than analogues with N,O-coordinated ligands (Fig. 34).[91,115,116,121]

Even in the case of the donor set effect, the resulting antiproliferative activity was cell-dependent, because an ionic complex containing the N,N-coordinated electroneutral *N*-[pyridin-2-ylmethylidene]aniline was less effective in A2780 cells but more potent in A2780Cis cells, in comparison with its electroneutral analogue involving deprotonated N,O-coordinated 2-[(*Z*)-(phenylimino)methyl]phenol (Fig. 34).[121]

Other studies report complexes with C,N-donor ligands, along with the N,N- and/or N,O-ones discussed above. Within a pair of isoelectronic complexes, it was the electroneutral complex **43** (with C,N-coordinated ppy) that showed a higher antiproliferative effect than its ionic bpy-based analogue (N,N-donor set).[41,154] In a similar manner, untypical doubly chelated Ir–$Cp^{mpy}$ complexes containing various C,N-donor ligands (*e.g.*, ppy[1] in **103**; Fig. 27) were several orders of magnitude more cytotoxic in various human cancer cells than congeners with N,N-donor ligands (Fig. 34).[138,164,165] For Ir–Cp* complexes with various benzimidazole derivatives, compounds with C,N-donor ligands were more effective than analogues involving N,O- and especially N,N-donor ligands (Fig. 34).[115] Similarly, the complex with the C,N-coordinated naphthaldimine outperformed its analogues with similar ligands derived from pyridine (N,N-donor set) or phenol (N,O-donor set) (Fig. 34).[212,213]

A different trend was observed for other pairs of complexes involving similar chelating C,N- and N,N-donor ligands. For complexes containing bidentate 7-azaindole derivatives with *N*1-phenyl (C,N-ligand in **59**; Fig. 12) or *N*1-pyridin-2-yl (N,N-ligand; section 6.4) substituents, it was electroneutral complex **59** that showed a lower activity ($IC_{50}$ > 50 μM in A2780 cells) than its more potent analogue with the N,N-donor ligand ($IC_{50}$ = 3.1 μM).[181] Similarly, the ppy-based complexes (C,N-donor set) were outperformed by their bpy analogues (N,N-donor set) bearing the rhodamine substituent for theranostic applications.[85,159]

McGowan and co-workers presented a series of complexes involving ligands with N,N-, N,O- and O,O-donor atoms.[116] Despite the ligands used being of a different chemical type (see **39** in Fig. 9 and **66** in Fig. 14), it can be concluded that the most active was the complex with an N,O-donor ligand (*i.e.*, **39**), while the complexes with N,N-donor ligands showed the lowest biological activity (Fig. 34). Later, the same research group used a similar N,O-donor ligand (3-amino-1-phenylbut-2-en-1-one) and its direct hydroxo analogue, which coordinated as an O,O-donor ligand.[148] This strategy allowed a relevant comparison of both complexes, which exhibited more or less similar biological effects ($IC_{50}$ = 83 and 93 μM in HT-29 cells, respectively). Both complexes were significantly less potent than the co-studied complex **39** ($IC_{50}$ = 5.1 μM). Finally, complex **72** with a unique O,Se-donor set (Fig. 15) was less active than its analogue involving analogous O,S-donor ligands (thiopyridone).[194,196]

**4.3.2. Chelate-ring size.** In the context of the effect of different donor sets of ligands used for the preparation of anticancer Ir–$Cp^x$ complexes, the effect of chelate ring size for several representatives containing ligands with the same donor set but forming chelate rings of different sizes can also be discussed. In the case of the abovementioned complexes with various benzimidazole derivatives, two types of N,N-donor ligands were used – one with pyridine (forming a five-membered chelate ring) and the second one with aniline (forming a six-membered chelate ring).[115] This variation led to different antiproliferative activities, showing that the aniline-derived complex with a six-membered chelate ring was more effective than its pyridine-based analogue with a smaller chelate.

Within the pair of dinuclear complexes involving the bridging 4,4-substituted biphenyl, complex **85**, the ligand of which formed two six-membered chelate rings (Fig. 20), was more cytotoxic ($IC_{50}$ in low-micromolar range) than its analogue containing a slightly different ligand forming five-membered chelate rings ($IC_{50}$ > 30 μM).[211]

### 4.4. Effect of a monodentate ligand

Sheldrick *et al.* reported [Ir(η[5]-Cp*)(dppz)(py)]$(CF_3SO_3)_2$ (**100**)[207] as being less cytotoxic in MCF-7 and HT-29 cells than its chlorido analogue **5** (Fig. 26).[22] This concept was revisited by Sadler and co-workers, and the significantly effective chlorido complex **47**[158] was a stepping stone for this cutting-edge research.[44] The derived ionic complex **101** (Fig. 27), involving monodentate pyridine instead of the chlorido ligand, aquates slowly yet is more active towards a wide range of cancer cells (*e.g.*, $IC_{50}$ = 0.1 μM in A2780 cells) compared with initial hydro-

 

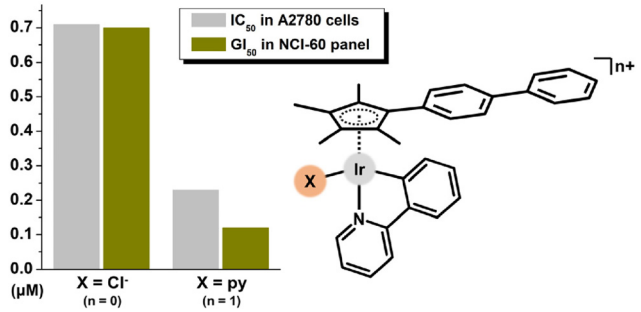


**Fig. 35** A comparison of the *in vitro* antiproliferative activity of $[Ir(\eta^5\text{-}Cp^{bph})(ppy)(X)]^{n+}$ complexes containing different monodentate ligands (X = Cl and $n$ = 0 for **47**; X = py and $n$ = 1 for **101**).

lytically unstable electroneutral chlorido complex **47** (Fig. 35). The mechanistic aspects of this highly promising complex (**101**) were investigated in detail relating them to redox balance in the cell.

A subsequent study showed that the introduction of an electron-donating group (*e.g.*, $NMe_2$) on the monodentate pyridine ring of similar Ir–$Cp^{ph}$ compounds generally increased the antiproliferative activity while electron-withdrawing groups decreased it, with **102** (Fig. 27) being the most effective in the series (with $IC_{50}$ = 0.2 μM in MCF-7 cells, *ca.* 36 times more active than cisplatin).[162] For these complexes (**101**, **102**), a benefit of replacing the chlorido ligand with a monodentate pyridine or its derivatives was unambiguously proved by the advanced NCI-60 screening.[44,162] A similar observation was reported for mono- and trinuclear Ir–Cp* complexes with *N*-alkyl substituted 2-methyliminophenol.[152,153]

Another structural modification involves the formation of a tethered ring, as shown above for structurally strained complex **103** (Fig. 27). **103** includes the cyclopentadienyl ligand with a tethered pyridine ($Cp^{mpy}$) that binds to the metal centre, resulting in a unique double chelated Ir–$Cp^x$ structure. **103** and its analogues were highly potent towards all human cancer cell lines tested, with $IC_{50}$ values in the sub-micromolar range. With the aim of thoroughly exploring the SAR, tethered complexes were investigated along with their non-tethered analogues, *e.g.*, with terminal monodentate pyridine for comparison. It was proved that the tethered complexes exhibited higher activity (nM range; Fig. 36) and selectivity.[165]

Regarding thiomaltol- and thiopyridone-based complexes (*e.g.*, **105** in Fig. 28) with the chlorido ligand replaced by N-donor 1-methyl-1*H*-imidazole,[193,195] or complexes bearing pta as the monodentate P-donor ligand (*e.g.*, **106**; Fig. 28),[45,191] the effect of such chemical modification was negligible or less positive than for pyridine-modified complexes.

Less work has been dedicated to different halogenido (bromido, iodido) complexes than the widely studied chlorido ones.[43,46,110,248] In this case it seems that the resulting antiproliferative activity is more dependent on the cell type than on the type of halogenido ligand used. In particular, the azopyridine-based iodido complex was more effective against A549

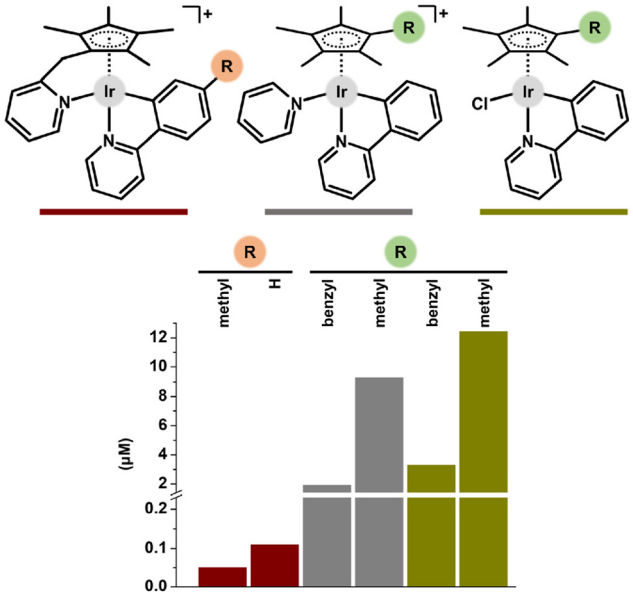


**Fig. 36** A comparison of the antiproliferative activity of tethered complexes (red) and their non-tethered pyridine (grey) and chlorido (dark yellow) analogues (studied in MCF-7 cells).

cells ($IC_{50}$ = 1.0 μM) than the chlorido analogue ($IC_{50}$ = 1.5 μM), while the opposite situation was observed in the A2780 cell line ($IC_{50}$ = 0.25 (for iodido) *vs.* 0.12 (for chlorido) μM).[248] Other works reported similarly equivocal results with a more cytotoxic iodido complex in H460 cells,[46] and the iodido complex was outperformed by the chlorido analogue in A2780 cells.[43]

The Ir–$Cp^{bph}$ hydrogensulfido complex **108** (Fig. 28) was comparably potent ($IC_{50}$ = 0.6 μM) to its chlorido analogue in A2780 cells, where **108** exceeded the antiproliferative activity of its Cp* analogue ($IC_{50}$ = 48.4 μM) and cisplatin ($IC_{50}$ = 1.2 μM).[249] In contrast to inactive Ir–Cp* chlorido complexes (with phen or bpy), their hydrogensulfido analogues were moderately effective in A2780 cells. The last type of monodentate ligand, which was used as a replacement of the chlorido ligand in Ir–$Cp^x$ complexes, is represented by a bioactive carboxylato ligand (valproato, 4-phenylbutyrato) discussed in section 6.2.[43,250]

### 4.5. Nuclearity

Some research teams have developed multinuclear complexes, which, in addition to mononuclear complexes, offer new chemotypes in the field of anticancer Ir cyclopentadienyl complexes. Multinuclear Ir–$Cp^x$ complexes were either derived from their mononuclear analogues (*e.g.*, **83**; Fig. 19)[207,208] or they were prepared with similar ligands of different denticities, which allowed the coordination of a different number of metal centres (*e.g.*, **89**; Fig. 21). Both synthetic strategies enable a comparison of the effect of the number of metal centres on the resulting anticancer activity.[212] For example, a series of dinuclear Ir complexes, $[Ir_2(\eta^5\text{-}Cp^*)_2(\mu\text{-}L)(pp)_2](CF_3SO_3)_4$ (*e.g.*, **83**; Fig. 19), with a chelating polypyridyl ligand (pp; *e.g.*, dppz)

and various bridging ligands (L), showed a greater ability to enter the cancer cells, consequently resulting in higher antiproliferative activity in MCF-7 and HT-29 cells,[207,208] compared to their formerly studied mononuclear chlorido analogue **5**.[22]

Some multinuclear complexes exhibited higher antiproliferative activity than their mononuclear analogues,[121,152,153,207,212,213,215,227] but other multinuclear Ir compounds were less effective in comparison with mononuclear complexes.[121,207,212–216] Obviously, it is difficult to compare complexes with different nuclearity, because not only the number of central atoms, but also the size and charge of the complex are different for mononuclear and multinuclear analogues.

An interesting comparison of the antiproliferative activity of mono- and multinuclear Ir complexes is obtained by calculating the activity per Ir atom. In this case, the strategy of using a higher number of expensive central atoms appears to be even more inefficient, since the multinuclear complexes in most cases had significantly lower activity per Ir atom than complexes with lower nuclearity (Fig. 37). In total, these results reported in the literature for Ir multinuclear complexes have not demonstrated their development as a suitable strategy.

Very recently, dinuclear complex **88** (Fig. 20), which exhibited low-micromolar antiproliferative activity in various human cancer cells, outperformed its inactive mononuclear analogue and also showed some important advantages within the MoA studies, as discussed in sections 5 and 6.[227] In contrast to the above-discussed results, this work clearly demonstrated that the development of multinuclear Ir–Cp$^x$ complexes was a viable strategy and a suitable research direction.

### 4.6. Effect of a counter-anion

The effect of a counter-anion of ionic complexes is usually overlooked. However, in the case of positively charged Ir–Cp$^x$ complex cations, anions should not be understood as innocent in terms of their effect on the resulting biological activity, as demonstrated in some papers dedicated to this topic.

The moderate antiproliferative activity of [Ir(η$^5$-Cp*)Cl(impy)]$PF_6$ (*e.g.*, $IC_{50}$ = 13.9 μM in HeLa cells) and [Ir(η$^5$-Cp*)Cl(qupy)]$PF_6$ (*e.g.*, $IC_{50}$ = 6.7 μM in HeLa cells) complexes was improved using a different counter-anion (Fig. 38); impy = 2,6-diisopropyl-*N*-(pyridin-2-ylmethylene)aniline, qupy = 2,6-diisopropyl-*N*-(quinolin-2-ylmethylene)aniline.[98,101] In particular, the [Ir(η$^5$-Cp*)Cl(impy)]OTs ($IC_{50}$ = 6.9 μM) and [Ir(η$^5$-Cp*)Cl(qupy)]OTs ($IC_{50}$ = 3.4 μM) complexes were more effective[101] than the $PF_6^-$ salts,[98] although the tosylate counter-anion used (OTs) was inactive itself.

The cation of the [Ir(η$^5$-Cp$^{bph}$)Cl(phen)]$PF_6$ (**14**; Fig. 5)[41] complex was used to investigate the effect of seven different counter-ions on the antiproliferative activity (studied in A549 cells).[260] Compounds involving smaller counter-anions ($Cl^-$, $PF_6^-$, $BF_4^-$, $SbF_6^-$, $CF_3SO_3^-$) exhibited higher antiproliferative activity than their analogues with bulkier anions ($BPh_4^-$, B(3,5-$(CF_3)_2Ph)_4$). These differences in antiproliferative activity were related to processes associated with the resulting biological effect (*e.g.*, hydrolysis rate, NADH oxidation, cell cycle modification or apoptosis induction), which appeared to follow the same trend as cancer cell cytotoxicity.

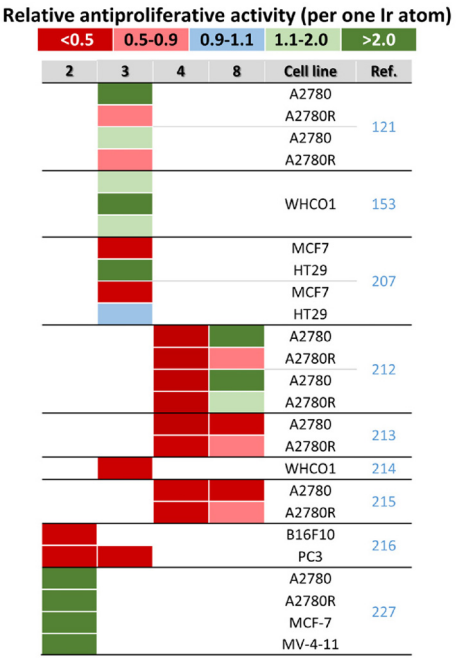


**Fig. 37** A comparison of the antiproliferative activity of multinuclear Ir complexes ($n$ = 3, 4 or 8) and their mononuclear analogues; $n$ stands for the number of Ir atoms. Relative activity (RA) = [$IC_{50}$(mononuclear complex)]/[$IC_{50}$(Ir multinuclear complex) × $n$].

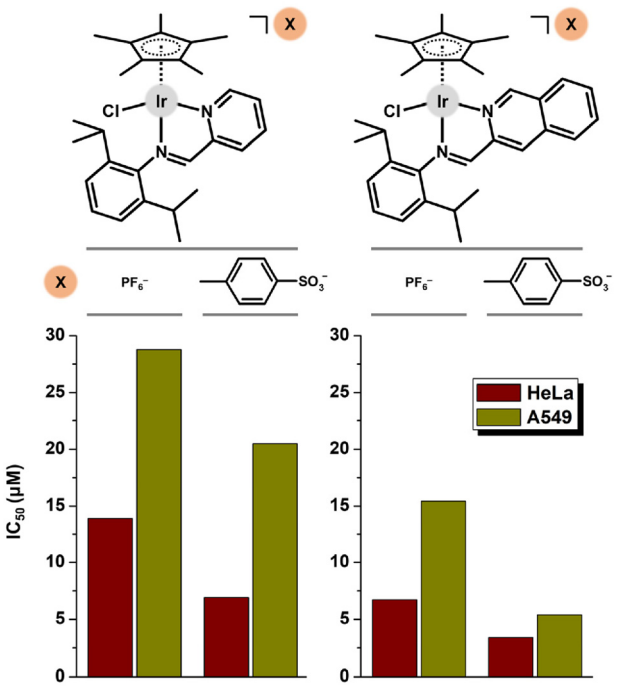


**Fig. 38** A comparison of the antiproliferative activity of Ir complexes with different counter-anions.

The same complex cation was used once again for the preparation of micellar systems.[261] In this work, the [Ir($\eta^5$-Cp$^{bph}$)Cl(phen)]Cl complex was used and studied in two ovarian cancer cell lines (OVCAR-3, SKOV-3 cells).[261] The obtained results are different for **14** ($PF_6^-$ salt; $IC_{50}$ = 0.7 μM, RA = 1.7 in A2780 cells) and [Ir($\eta^5$-Cp$^{bph}$)Cl(phen)]Cl ($Cl^-$ salt; $IC_{50}$ = 4.1 μM, RA = 3.7 in OVCAR-3 cells; $IC_{50}$ = 16.1 μM, RA = 2.3 in SKOV-3 cells). However, these results should not be accepted as evidence of the effect of the anion on the resulting activity because the results were obtained in different ovarian cancer cell lines under different experimental conditions (*e.g.*, exposure time).

Only slightly higher antiproliferative activity was reported for the $PF_6^-$ salts of 16-electron complex cations bearing various amine-imine ligands, compared with the co-studied chloride salts.[256] No effect was observed for inactive triazolyl-based complexes prepared as chloride and tetrafluoridoborate salts.[140]

# 5. Mechanisms of action

In general, anticancer non-platinum complexes represent chemotypes different from those of conventional platinum-based anticancer drugs; this is related to various biological and biochemical differences. Most importantly, anticancer non-platinum complexes (including Ir ones) have a different mechanism of action (MoA), which means that they target different intracellular targets and induce different processes in treated cancer cells, compared to conventional Pt-based drugs.[9,16–18] Some papers have been devoted solely to in-depth studies of MoAs, providing a comprehensive overview of the biological effect of these compounds and the mechanism through which cell death is induced.[76,77,262,263] Generally, Ir cyclopentadienyl complexes have a different cytotoxic profile than Pt-based drugs. They primarily target different intracellular targets than DNA (*e.g.*, mitochondria or lysosomes) and induce the generation of ROS and apoptosis in the treated cancer cells. Most papers pay attention to these processes in order to shed light on the MoA of newly developed complexes.

## 5.1. Hydrolysis and activation

The stability of the newly prepared bioactive compounds is a key parameter for them reaching the target cancer cells in their intact or pharmacokinetically acceptable forms. Similarly to cisplatin, which is hydrolysed from the *cis*-[$PtCl_2(NH_3)_2$] prodrug to the *cis*-[$Pt(H_2O)(OH)(NH_3)_2$] active form in the cell,[264] hydrolysis of Ir–Cp$^x$ complexes involves cleavage of the Ir–Cl bond and formation of the Ir–$OH_2$ species (or Ir–OH depending on p$K_a$)[265] under aqueous conditions. Such Ir–Cl bond hydrolysis was hypothesized as a necessary step (activation) involved in the MoA of anticancer Ir–Cp$^x$ complexes.[41] The studied complexes, [Ir($\eta^5$-Cp$^x$)Cl(L)]$PF_6$ (Cp$^x$ = Cp*, Cp$^{ph}$ or Cp$^{bph}$; L = en, bpy, phen, pico), underwent rapid hydrolysis under the aqueous conditions used ($^1$H NMR studies). The hydrolysis rate decreased, while the hydrolysis extent increased with the size of the Cp$^x$ ligand used. The equilibrium of the chlorido and aqua species was reversed by the addition of various concentrations of NaCl. In addition to Cp$^x$ ring extension, the extent and rate of hydrolysis can also be modified by the type of chelating ligand,[41] its substitution[204] or by the type of monodentate ligand.[43] The process of hydrolytic aquation was also investigated by DFT.[173,174,266]

The observed hydrolysis was also discussed as an activation step for interactions with model nucleobases. It was proved that Ir–Cp$^x$ complexes were readily coordinated by nucleobases when they were hydrolysed under aqueous conditions (*i.e.*, in the absence of chloride ions),[41,44] but no interaction was observed for similar complexes in the presence of chloride ions (*e.g.*, with PBS).[111] Nowadays, hydrolytic activation is not considered a necessary activation step for Ir–Cp$^x$ complexes, including chlorido complexes, as the most frequently studied ones. This was proved for the hydrolytically stable [Ir($\eta^5$-Cp$^{ph}$)(azpy)Cl]$PF_6$ (**116**; Fig. 39) complex, which outperformed its readily hydrolysable analogues (**14**, **15** and **47**) in terms of antiproliferative activity in the NCI-60 panel.[262] Similarly, other hydrolytically stable chlorido complexes also exhibited antiproliferative activity.[99,197]

Besides the chlorido complexes, analogues with different types of monodentate ligand are more stable, as reported for iodido[248] and pyridine complexes,[44,162] including the pyridine tethered ones,[138] but such compounds are still effective in various cancer cells. Complexes with monodentate pyridine are able to partially replace this pyridine with chlorides in the presence of physiological concentrations of $Cl^-$ ions.[44,163] Hydrolytically stable complexes can also covalently interact with various biomolecules, such as GSH,[248] EtG[99,138,162,164] or N,N-ligands,[165] even without hydrolytic activation. On the other hand, different reactivity of the chlorido (no reactivity) and aqua (reactive) complexes towards GSH was reported.[98] Also, complexes with monodentate N-donor ligands were shown to undergo the pH-dependent release of this ligand, leading to the activated Ir-aqua species.[138,193] Complex **71** (Fig. 15) was stable at biologically relevant pH values, as studied by HPLC at pH 5.8–7.9.[194]

Although the complexes described in this review were tested for their *in vitro* antiproliferative activity, and thus, dissolved in testing medium, stability studies in these media (such as DMEM) were rather exceptional.[57,107,109] For example, dichlorido complex **11** (Fig. 4) was stable in DMSO-$d_6$/$D_2O$ mix-

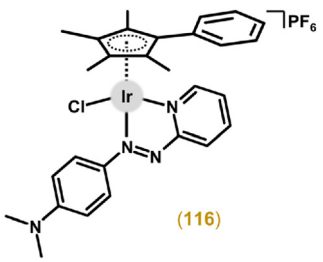


**Fig. 39** The structural formula of complex **116**.

tures of solvents, as well as in the mixture of DMSO with DMEM.[57] Its analogue (**12**) bearing different monodentate P-donor ligands (Fig. 4) was hydrolysed in the presence of water, but the diaqua species formed reacted with various concentrations of chlorides, implying that dichlorido complexes were most likely intact when accumulated in cells.[59]

Methodologically, $^1$H NMR or UV-Vis spectroscopy[41] are the most commonly chosen techniques; HPLC is used less frequently,[194–196,211] usually with similar results. In most cases, hydrolytic stability is investigated by $^1$H NMR in mixtures of $D_2O$ and some organic solvent (*e.g.*, MeOD-$d_4$, DMSO-$d_6$ or DMF-$d_7$) ensuring the solubility of Ir complexes, as their solubility in water is usually insufficient for $^1$H NMR experiments. In some cases, DMSO was considered unsuitable for chemical and biological studies of novel Ir–Cp$^x$ complexes because the complexes were unstable in this solvent due to its high coordination ability.[116,153,163,179,186] Both isomeric species with S- and O-coordinated DMSO were detected by $^1$H NMR.[176] On the other hand, unsaturated 16-electron Ir complexes (*e.g.*, **114**; Fig. 29) were stable in DMSO and its mixture with water,[254–257] although some evidence for the formation of 18-electron Ir–aqua species has also been reported.[112] Besides DMSO, instability in DCM and methanol was reported for Ir–Cp* complexes involving some ispinesib-derived ligands.[107,109]

Special in-solution behaviour was reported for tethered complex **103** and its analogues, which involved a pyridine-substituted Cp$^x$ ring (Cp$^{mpy}$) allowing double chelation of the Ir metal centre. It was observed that DMSO readily coordinated to Ir, which was associated with the tethered ring opening (not observed for DMF).[165] Intriguingly, the Ir–dmso adducts formed reformed the tether ring upon dissolution in water. Similar Ir–Cp$^{mpy}$ complexes interacted covalently with DMSO and methanol, but remained intact in water.[138] Activation of these complexes, which involve the release of pyridine of the Cp$^{mpy}$ ligand from Ir, was also observed at acidic pH (chlorido species formed) and in the presence of EtG (covalent adduct formed) or sodium formate (hydrido species formed).

The rapid formation of Ir–dmso adducts was also reported for **55** and **56** (Fig. 12),[177,178] and others.[174] The representative Ir–dmso adduct of **55** did not undergo the exchange reaction in the presence of methanol and water, suggesting that the dmso adduct was the active entity in biological experiments.

Regarding the mixture of solvents used, hydrolysis was observed to be dependent on the solvent composition.[80,211] For example, the [Ir($\eta^5$-Cp$^{bph}$)(bpy$^1$)Cl]PF$_6$ complex was hydrolysed in 10% MeOH (UV-Vis) but was stable in 50% MeOH (UV-Vis, $^1$H NMR).[80] The addition of NaCl or PBS often mimics the physiological concentration of chloride ions, in either extra- or intracellular environments.[41,59] This often leads to the suppression of hydrolysis observed in the absence of chloride ions. In contrast, the presence of chlorido ions can induce ligand exchange in complexes with a monodentate ligand other than chlorido, as observed for a hydrolytically stable iodido complex that was converted into the chlorido form in the presence of PBS.[110] Also of importance, hydrolysis was proved to be influenced by the counter-anion, with longer half-lives of hydrolysis observed for bulkier counter-anions (*e.g.*, $BPh_4$) than for smaller ones, including the most commonly used one, $PF_6^-$.[260]

Importantly, hydrolysis of the Ir–Cl bond of anticancer Ir–Cp$^x$ complexes should not be understood as a general feature of these compounds, because some works reported the Ir–Cp$^x$ chlorido complexes to be stable under aqueous conditions even in the absence of chloride ions.[121,124,166,172,202,215]

In the context of the activation of stable Ir–Cp$^x$ complexes, the possibility of redox activation has to be mentioned as well. This concept was first reported for [Ir($\eta^5$-Cp*)Cl(dppz)]PF$_6$ (*i.e.*, the $PF_6^-$ analogue of **5**),[22] which released its chlorido ligand through the metal–ligand two-electron dissociative reduction in DMF (*i.e.*, in the absence of water).[267] Another type of redox activation was reported for hydrolytically stable iodido complexes that were redox activated by the reaction of GSH with the azo bond of their azopyridine ligands.[248] Such activation resulted in the replacement of the iodido ligand with $GS^-$, which was associated with the GSH-to-GSSG oxidation and the formation of ROS.

### 5.2. Cellular take up, lipophilicity and intracellular localization

Cellular take up of anticancer Ir–Cp$^x$ metallodrugs is a crucial step for them to be effective. Several factors, such as size and charge (polarity), lipophilicity or targeting transport proteins, influence if and how a compound is taken up by cancer cells. Understanding if and how a new metallodrug is accumulated in cells is important for its development. Cellular take up (or cellular accumulation) studies are therefore very important and frequently performed. The most common techniques for these studies are ICP-MS (or its alternatives, ICP-OES or AAS) or fluorescence microscopy; OES = optical emission spectroscopy.

The first reported anticancer Ir–Cp$^x$ complexes **5** and **6** (Figs. 1 and 2)[22] were studied for their accumulation in HT-29 cells.[20] In this case, more effective complex **6** was taken up more by the cells (149.6 ng Ir per mg protein) than less potent **5** (70.4 ng Ir per mg protein). For the [Ir($\eta^5$-Cp$^x$)Cl(phen)]PF$_6$ (Cp$^x$ = Cp*, Cp$^{ph}$ or Cp$^{bph}$) complexes, log $P$ (−0.82, 0.48 and 1.11) and cellular accumulation (3.9, 23.5 and 88.8 ng Ir per $10^6$ cells) increased with the Cp$^x$ ring size, which correlated with the antiproliferative activity in A2780 cells (section 4.2).[41] In addition to the aforementioned extension of the Cp$^x$ ring, lipophilicity can also be enhanced by changing the charge of the compounds, as reported for a pair of hydrophilic ionic [Ir($\eta^5$-Cp*)Cl(phen)]PF$_6$ (log $P$ = −0.95) and lipophilic electroneutral [Ir($\eta^5$-Cp*)Cl(ppy)] (**43**; log $P$ = 1.57) complexes.[154] Electroneutral chlorido complex **47** was markedly less taken up in A2780 cancer cells than its ionic pyridine analogue **101** (Fig. 27).[44] The same effect of lipophilicity on the resulting antiproliferative activity was reported for complexes with various pic-based ligands, for which the most cytotoxic complex **38** was more lipophilic (log $P$ = 1.05) than less effective **37** (log $P$ = −0.15) and even an inactive analogue

 

bearing the hydrophilic carboxy group on the pic ligand (log $P$ = −2.73).[147]

Conjugation of the Ir–Cp$^x$ complex to a tumour-targeting cyclic nona-peptide c(CRWYDENAC) (**117**; Fig. 40) was reported, but the resulting antiproliferative activity was not studied.[268] Also for this targeting Ir complex and some others, HPLC analysis of relative hydrophobicity has been used to determine lipophilicity, in addition to the most commonly used log $P$ determination.[155,194,268]

The inactive [Ir(η$^5$-Cp*)Cl(phen)]PF$_6$ complex and its highly active analogue, [Ir(η$^5$-Cp*)(bq)Cl] (**118**; Fig. 40), were studied in more detail in terms of their mechanism of cellular accumulation; Hbq = 7,8-benzoquinoline.[76] The electroneutral complex **118** is more lipophilic, leading to higher cellular take up and higher in-cell DNA metalation. **118** entered the cancer cells by both energy-independent (passive diffusion) and -dependent transport processes, such as copper influx transporter CTR1. Endocytosis was not evidenced for **118**. Importantly, **118** was identified as a substrate of p-glycoprotein and multidrug resistance-associated protein 1 (MRP1) efflux pumps; this is different from cisplatin, which is not recognized by p-glycoprotein and MRP1. Similar results were obtained for complex **22**.[88]

Typically, electroneutral complexes are more lipophilic than their ionic analogues.[41,101,154] In some specific cases, rational modification of the lipophilic electroneutral complexes can lead to an increase in lipophilicity, despite the ionic character of the newly formed complex. This situation was reported for the chlorido complex **43** (log $P$ = 1.57),[154] which was modified by the monodentate-coordinated pyridyl-BODIPY ligand in the structure of the highly lipophilic complex **104** (log $P$ = 4.19), which could be attributed to the highly lipophilic pyridyl-BODIPY ligand.[163]

Within the series of highly potent Ru(II), Rh(III) and Ir(III) complexes, the Ir complex **48** was the most active in T47D cells, but its take up by cells was comparable to that of its Ru analogue, suggesting that the relationship between activity and cellular accumulation is not straightforward for these compounds.[166]

The first investigation into the intracellular organelle distribution was performed for the [Ir(η$^5$-Cp$^x$)Cl(phen)]PF$_6$ complexes (Cp$^x$ = Cp*, Cp$^{ph}$ or Cp$^{bph}$ (**14**)).[41] In A2780 cells, the results of ICP-MS intracellular distribution studies showed that the highest amount of Ir (>50%) accumulated in membranes, followed by cytosol/cytoskeleton and <10% of Ir was detected in the nucleus for all three Ir compounds. For electroneutral complexes involving various ppy derivatives (*e.g.*, **44**; Fig. 10), the highest Ir level was detected (ICP-MS) in cytosol, followed by membranes, the nucleus and cytoskeleton.[155] Similar dominant localization in cytosol was reported for tetranuclear Ir metallarectangles involving fluorescent BODIPY-based bridging ligands[269] and other compounds[93–95,163,173,186,244] Other complexes accumulated dominantly in mitochondria,[63,245,270,271] the nucleus,[57,100] the perinuclear region[272] or lysosomes (section 5.7).[82,85] A specific intracellular distribution was reported for BODIPY-bearing complex **56** (Fig. 12), which was detected in mitochondria and the endoplasmic reticulum (ER), from which the complex could be distributed to other organelles (*e.g.*, lysosomes) by lipid droplets.[178] A non-specific (pancellular) Ir distribution was also discussed for Ir cyclopentadienyl complexes.[179]

Besides the aforementioned BODIPY,[163,192,271–274] other intrinsically fluorescent moieties (*e.g.*, rhodamine B in **119**; Fig. 41)[85] or the luminescence of Ir complexes[170] were used in numerous studies on the intracellular localization of anticancer Ir–Cp$^x$ complexes. For example, Gupta and co-workers used a BODIPY-containing N,O-donor ligand for live cell imaging, which demonstrated targeted accumulation in the mitochondria.[271] For **56**, the presence of BODIPY allowed its fate in the cell to be tracked: it quickly permeates the plasma membrane and accumulates in the mitochondria and endoplasmic reticulum (see below).[178]

A unique study of the localization of the Ir–Cp$^x$ complex was carried out by a combination of cryo-soft X-ray tomography (cryo-SXT) and hard X-ray fluorescence tomography (cryo-XRF) in fully hydrated cancer cells at nanometric resolution.[164] This method overcomes the shortcomings of the aforementioned techniques, where ICP-MS (or AAS) has the disadvantage of

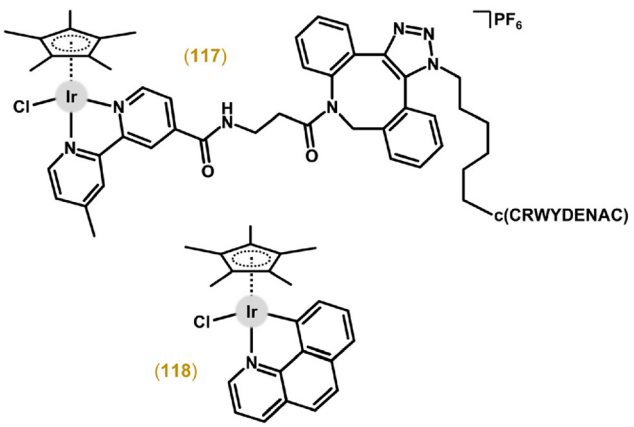


**Fig. 40** Structural formulas of complexes **117** and **118**.

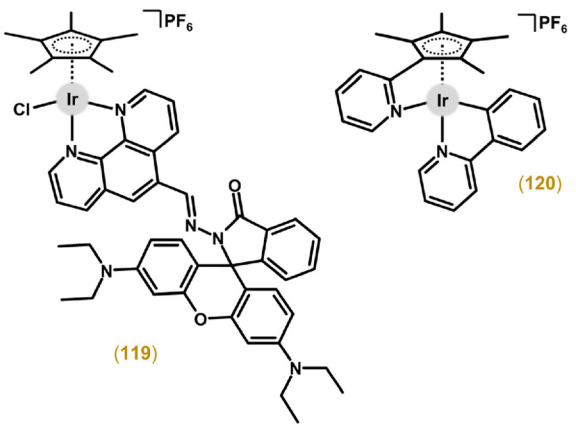


**Fig. 41** Structural formulas of complexes **119** and **120**.

mechanical manipulation of the cells, while microscopic techniques require the presence of a fluorophore in the tracked compound. In this case, **120** (analogue of **103** with ppy instead of ppy[1]; Fig. 41) was exclusively localized in mitochondria, as demonstrated by 3D cryo X-ray imaging.

### 5.3. Cell death type

The application of new compounds to cancer cells may lead to their death in the case of successful accumulation and sufficient anticancer activity. In general, cells can die through different types of cell death, but not all are equally beneficial. The most common cell death types are apoptosis (programmed cell death), necrosis (uncontrolled cell death), autophagy (self-eating) or less common cell death pathways (*e.g.*, ferroptosis, oncosis, paraptosis or pyroptosis).

**5.3.1. Apoptosis.** In 2010, complex **35** (Fig. 9) was, besides its interaction with DNA, studied for its ability to activate the known pro-apoptotic enzymes caspase-3/7.[145] In comparison with the reference apoptosis inducers (staurosporin, cisplatin) used, **35** did not induce apoptosis in the treated cancer cells, implying that the cell death mechanism was most likely different (*i.e.*, non-apoptotic) but remained unidentified. Still, it was concluded that **35** had a different MoA than the conventional Pt-based drug cisplatin.

In 2012, various intracellular processes (induction of ROS formation, induction of apoptosis or cell respiration) associated with the MoA of the Ir–Cp$^x$ compounds were investigated, laying the basis for future studies of their MoAs.[208] In particular, both dinuclear dppz-based complexes $[Ir_2(\mu\text{-L})(\eta^5\text{-Cp}^*)_2(dppz)_2](CF_3SO_3)_4$ (L = 4,4′-ethyne-1,2-diyldipyridine or 4,4′-(benzene-1,4-diyldiethyne-2,1-diyl)dipyridine for **83** in Fig. 19) induced lower cell impedance and a respiration rate decrease connected with acidification alternation of adherent MCF-7 cells. More importantly, this work provided the first detection of apoptosis induced by anticancer Ir–Cp$^x$ complexes in non-adhesive Jurkat leukaemia cells. Flow cytometry of annexin V/propidium iodide (PrI)-stained cells was used and remains one of the most commonly used techniques to study apoptosis with novel anticancer Ir–Cp$^x$ complexes.

Complex **14** (Fig. 5) was studied in great detail for its MoA.[77] Flow cytometry experiments showed faster induction of apoptosis for **14** than for cisplatin. At longer exposure times, populations of late apoptotic/necrotic cells were detected for both compounds. The induced apoptosis was associated with DNA fragmentation (as proved by an ELISA colorimetric experiment and agarose gel electrophoresis) and mitochondria disruption (tetramethylrhodamine ethyl ester (TMRE) staining). Interestingly, the latter phenomenon was not observed for cisplatin.

To prove that apoptosis induced by anticancer Ir–Cp$^x$ compounds is connected to a redox-mediated MoA and the formation of ROS in the treated cells, various ROS scavengers, such as *N*-acetyl-L-cysteine (NAC), are applied in non-toxic concentrations to cancer cells together with the Ir complex. For example, **49** (Fig. 10) induced early apoptosis in a higher K562 cell population than in an analogous experiment with co-applied NAC.[169]

Apoptosis was also studied by fluorescence microscopy[117] or TEM[262] through the induction of cancer cell morphology changes (membrane blebbing, chromatin condensation, nucleus pyknosis, DNA fragmentation). Microscopy imaging (high content screening, HCS) was also used for studies on caspase 3 positive apoptotic cancer cells.[263] Western-blot experiments (*e.g.*, anti-apoptotic factor Bcl-2, pro-apoptotic factor Bax or caspases) are often used to provide evidence of apoptosis and its type.[63,169,233,241]

When apoptosis is identified as an induced type of cell death, supporting experiments are usually performed to demonstrate that apoptosis-related processes, such as DNA fragmentation, cell cycle modification or expression of caspases, are occurring in the treated cells.[54,59,61,77,119,148,177] Cell senescence was detected together with apoptosis in A2780 cells treated with ppy-based Ir complexes with different Cp$^x$ derivatives.[259]

**5.3.2. Necrosis.** Since apoptosis is usually studied by flow cytometry with dual staining of cancer cells with annexin V/PrI, necrotic cells can be detected together with normal (live) and apoptotic (early and late) cells. However, although there are quite a few such studies, only a limited number of Ir–Cp$^x$ complexes (*e.g.*, **121** in Fig. 42) induced a higher proportion of necrotic cells.[180,188] Other complexes (*e.g.*, **53**; Fig. 11) did not induce necrosis, as sometimes proved by experiments with specific necrosis inhibitors (*e.g.*, necrostatin-1).[96,175,202]

**5.3.3. Ferroptosis.** The phototoxic complex **27** (Fig. 7) was studied for its ability to induce ferroptosis in 4T1 cells, where several ferroptosis-related hallmarks were examined.[96] The GSH concentration in solution and in cancer cells decreased in the presence of **27** and laser irradiation, as a result of GSH oxidation to GSSG. Since GSH is important for the subsequent inhibition of glutathione peroxidase 4 (GPX4)-mediated lipid peroxidation (LPO) degradation, GPX4 expression in cancer cells was also studied and proved to be significantly reduced in the presence of **27** and laser irradiation. Similarly, higher intracellular LPO levels were detected by confocal microscopy and markedly reduced by the specific ferroptosis inhibitor ferrostatin-1 (Fer-1). In association with the detection of ferroptosis, other cell death pathways were also examined utilizing

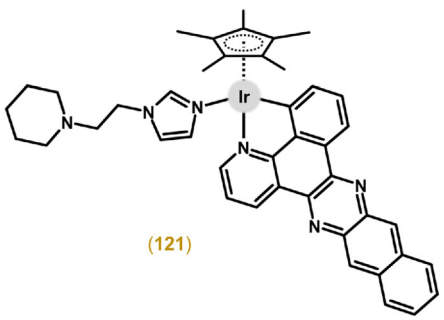


(121)

**Fig. 42** The structural formula of complex **121**.

 

their specific inhibitors (necrostatin-1, 3-methyladenine), but neither necrosis nor autophagy were induced by **27** in cancer cells. On the other hand, the cancer cell viability was markedly increased when the apoptosis inhibitor z-VAD-FMK was used, proving that **27** triggered cell death through the combined effects of apoptosis and ferroptosis.

**5.3.4. Autophagy.** Complex **8** was studied in 8505C cells, where, in addition to evidence of apoptosis and necrosis (flow cytometry, Annexin/PrI staining), autophagic vesicles were detected by flow cytometry.[54] The ongoing process of autophagy was demonstrated by an experiment with the specific autophagy inhibitor 3-methyladenine, the application of which led to an increase in the viability of 8505C cells. Similar results were reported for analogical complex **9** (Fig. 4).[55] Nevertheless, in both cases, apoptosis was identified as the main cell death mechanism, whereas autophagy was only noted as an irrelevant process in connection with the MoAs of **8** and **9**.[54,55] A similar conclusion that apoptosis predominates over autophagy has been reached for other Ir complexes.[175,189]

Although complex **79** (Fig. 17) induced apoptosis and various associated processes (*e.g.*, mitochondria disruption, ROS production or caspase-3 activity), it also induced autophagy in A549 cells.[202] This was proved by co-treatment with the autophagy inhibitor 3-methyladenine, causing a significant decrease in the cytotoxicity of **79**. In contrast, inhibitors of necroptosis, protein synthesis or proteases did not show the same effect.

### 5.4. DNA as a target

The pioneering works considered, analogically to Pt-based drugs, DNA as an intracellular target molecule for Ir–Cp$^x$ anticancer complexes.[22,34–36,79,207,208,234,275] Obviously, it was proved for $[Ir(\eta^5\text{-Cp}^*)(dppz)(L)]^{n+}$ complexes, involving an amino acid or simple peptide (L), that these agents effectively intercalated ctDNA and the strength of such interactions increased with the charge of the complex cation ($n$).[34] Importantly, Ir-dppz complexes also cleaved supercoiled plasmid DNA (after a short irradiation time). Covalent adducts of the studied Ir–Cp$^x$ complexes and model nucleobases (*e.g.*, EtG or adenosine monophosphate) were successfully prepared and characterized by NMR or crystallographically (Fig. 43).[34,35]

Later it was proved that the type of DNA interaction of $[Ir(\eta^5\text{-Cp}^*)(dppz)(L)]^{n+}$ complexes (*e.g.*, **5**) was driven by L (covalent for L = Cl, intercalative for L = tu and tmtu) and its size (stronger interaction of the complex containing bulkier tmtu than for its analogue with unsubstituted tu); tu = thiourea.[36] It was proved that the size of the bridging ligand was decisive for the type of DNA interaction for dinuclear complexes.[207,208,275] For example, the dinuclear complex bridged by pyrazine mono-intercalated DNA, while its analogue with 4,4′-bipyridine induced double-intercalation.[207] Similar dinuclear complexes showed nuclease activity towards DNA either in the dark (shorter linkers) or photoinduced (longer ones).[208]

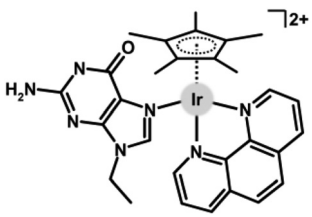


**Fig. 43** The structural formula of the adduct of $[Ir(\eta^5\text{-Cp}^*)(EtG)(phen)]^{2+}$ with 9-ethylguanine (EtG).

Another early reported complex **35** (Fig. 9) was also studied for its interaction with DNA.[145] However, **35** (as well as its Rh analogue) interacted with DNA (altered recognition of the drug-modified DNA by BamHI restriction nuclease), most likely non-covalently (*i.e.*, differently than cisplatin), since the thermodynamic stability of the DNA used was not changed by **35** (circular dichroism experiments).

The $[Ir(\eta^5\text{-Cp}^x)Cl(phen)]PF_6$ (Cp$^x$ = Cp*, Cp$^{ph}$ or Cp$^{bph}$ (**14**)) complexes bound effectively to the DNA of A2780 cells, to an even higher extent (5.5–7.7%) than the DNA-targeting anticancer metallodrug cisplatin (*ca.* 1%).[41] A binding mechanism is most likely combinative for the formation of guanine-N7 covalent adducts (DFT, EtG interaction studies) and intercalation (quenching of the EtBr-DNA fluorescence). The ability to interact with DNA (Cp$^{bph}$ > Cp$^{ph}$ > Cp*) correlated with the antiproliferative activity and cellular take up results (see above). Interestingly, although these complexes derived from an N,N-donor ligand (phen) interacted exclusively with EtG (a model molecule for studying interactions with DNA), their analogues with N,O-[41] and C,N-donor[154,155] ligands were also coordinated by 9-methyladenine. EtG was also used in other studies as a model nucleobase for DNA interaction studies.[168] In some works, guanosine monophosphate (GMP) was used for the same purpose.[88,111,121,176,214] Other complexes interacted with unsubstituted guanine and adenosine 3′-phosphate 5′-phosphosulfate salt.[93]

Notably, **14** was, together with **15**, **47** and **116**, studied in detail for its MoA and it was proved that DNA was one of several targets for these compounds.[262] Specifically, COMPARE analysis (quantitative comparison with >40 000 conventional drugs) provided positive correlations with drugs that were DNA interactors, DNA antimetabolites, topoisomerase inhibitors, protein synthesis inhibitors, mitosis inhibitors and redox mediators, according their MoAs. Especially the identification of a possible link between the MoA of Ir–Cp$^x$ complexes and cellular redox homeostasis was essential for further studies in this field (section 5.5). The same research group reported a similar MoA of electroneutral chlorido complex **47** to that of its ionic analogue **101** (Fig. 27), involving the monodentate pyridine ligand (based on the NCI-60 screening and COMPARE analysis).[44]

Reverse phase protein microarrays (RPPA) were used for the detailed description of the MoA of **116**.[263] As a response to the induced DNA damage, the levels of various proteins (or phosphorylated variants labelled with asterisks) increased (*e.g.*, CHK2*, CDC25A and p53*). Levels of other proteins (*e.g.*, tubulin, CDK1, Rb*) correlated with the results of cell cycle

analysis. Furthermore, the levels of some apoptotic proteins were also determined. Specifically, high levels of inhibitors of apoptosis proteins, survivin and XIAP were detected by RPPA, while the mitochondrial pro-survival protein BCL-X was down-regulated. Similarly, BCL-2 and BAK initiator proteins, and PARP* (cleaved by caspase-3) were found to be up-regulated, as also reported elsewhere.[175,200,205]

Interestingly, although DNA is nowadays not considered to be the main target for Ir–Cp$^x$ complexes, their ability to reach the cancer cell nucleus and interact with nuclear DNA is surprisingly high, as reported for **14**, which showed *ca.* 13-fold higher level of DNA metalation than cisplatin in A2780 cells.[77] In contrast, antiproliferative activity experiments performed in the Chinese hamster ovary (CHO-K1; NER-proficient wild-type) cell line and its mutant (MMC-2; NER deficient) indicated a lower degree of DNA damage than that with cisplatin.[84]

Besides the quenching of the EtBr-DNA fluorescence,[41] similar competitive DNA binding experiments have also been performed with different dyes. For example, **45** (Fig. 10) effectively displaced the DNA minor-groove binder Hoechst 33258 from ctDNA, suggesting that **45** was capable of binding to the DNA minor groove.[156] A similar observation was reported for **48**.[166] Exceptionally, no DNA interaction was observed for cytotoxic Ir complexes (*e.g.*, **33**; Fig. 8) in cell-free DNA experiments.[115] On the other hand, **33** induced DNA damage through the production of ROS, as proved by the detection of phosphorylated histone marker (γH2AX), as also reported for the heterometallic Ir–Re complex **97** (Fig. 24).[245]

Heterometallic dppz-derived Ir–Pt complexes (*e.g.*, **122** in Fig. 44) showed specific simultaneous covalent (Pt moiety) and intercalative (Ir-dppz moiety) DNA binding.[234,235] In addition to the widely published covalent and non-covalent (*i.e.*, intercalative) interactions of Ir–Cp$^x$ complexes with DNA, their ability to cleave DNA[34,208] has also been described in some papers,[98,204] while some compounds did not show this biological effect.[80,198,199]

### 5.5. Redox-mediated MoA

The redox-mediated MoA refers to how a substance (metallodrug) exerts its effect through disruption to cellular redox homeostasis. It is directly connected to the transfer of electrons between such drugs and biomolecules and it plays a critical role in many cellular processes (antioxidant defense, signalling pathways, enzyme activity, gene expressions *etc.*). It is a fundamental concept in pharmacology and cell biology and its understanding is crucial for drug development. Various transition metal complexes, including Ir–Cp$^x$ ones, act through the redox-mediated MoA.[276] They disrupt cellular redox homeostasis either directly through metal or ligand redox centres or indirectly through binding to redox biomolecules. Given that redox-modulating reactions are often catalytic,[44,277] such redox-modulating compounds (including anticancer Ir–Cp$^x$ complexes) can be classified under the concept of catalytic metallodrugs.[278,279] Either way, the primary process is the induction of ROS formation.

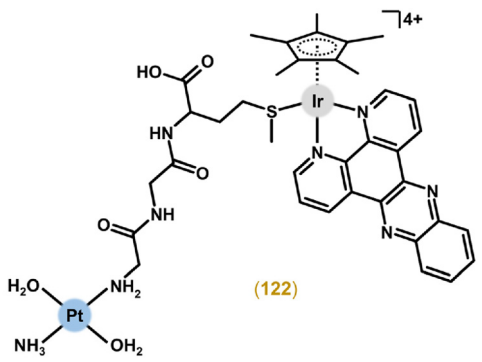


Fig. 44 The structural formula of complex **122**.

The first mention of a possible link between ROS and the anticancer activity of Ir–Cp$^x$ complexes was published for dinuclear dppz-based Ir complexes inducing apoptosis and other biochemical changes in Jurkat cells.[208] Later, COMPARE analysis revealed a correlation between the biological effects of **14**, **15** and **116** and redox mediators, which led to further biochemical experiments (mitochondrial membrane polarization, TEM visualization of organelle structure) demonstrating the redox-mediated MoA of Ir–Cp$^x$ complexes.[262] Also for **15**, **47** and **116**, a synergy with the redox modulator L-buthionine sulfoximine (L-BSO) was observed in A2780 cells.[262,276] L-BSO is an inhibitor of γ-glutamylcysteine synthetase involved in GSH synthesis, the application of which decreases GSH levels and increases the level of ROS in cells. Co-administration of the complexes with a non-toxic concentration of L-BSO led to >5-fold improvement of potency in A2780 cells. This was later proved to be associated with an increase of cellular take up of similar complex **118** (Fig. 40), most likely as a result of inhibition of the MRP1/GS-X efflux pump, which eliminates the GS adducts of xenobiotics (*e.g.*, Pt drugs or Ir–Cp$^x$ complexes in this study) from cancer cells.[76] Similarly, the pre-treatment of HeLa cells with L-BSO improved the cytotoxic potency of **53** (Fig. 11).[175]

Compound **14** was proved, in contrast to cisplatin, to induce mitochondrial membrane disruption (TMRE staining of cells). This disruption is directly connected to the production of ROS in treated cells.[77] Indeed, ROS production was proved by increased fluorescence in A2780 cells treated with **14** using 2′,7′-dichlorodihydrofluorescein diacetate (DCFH-DA) dye (not observed for cisplatin). Similar results were also reported for other Ir complexes.[167,168] In connection with mitochondria disruption, it was also demonstrated by the release of various intra-mitochondrial compounds (cytochrome c) into the cytosol[169,232] or by changes to the oxygen consumption rate (OCR) or ATP synthesis.[115]

A significant increase in the ROS level was detected by flow cytometry in A2780 cells treated with pyridine complex **101** (Fig. 27), and this increase was markedly higher than that with the chlorido analogue **47**.[44] Related to this detection of ROS in cells, model cell-free experiments with NADH demonstrated hydrogen peroxide production in the presence of **101** and oxygen (not observed when performed under an inert atmo-

 

sphere or in the presence of catalase). High ROS levels were also detected in A2780 cells treated with similar complexes with monodentate-coordinated pyridine derivatives (*e.g.*, **102**; Fig. 27).[162] The dichlorido complexes (*e.g.*, **11**)[57] were also reported to induce the production of high ROS populations. The presence of a second metal in heterometallic complexes did not lead either to higher ROS levels in the treated cells or to a higher extent of NADH oxidation.[78]

The mentioned production of $H_2O_2$ by **101** (detected by peroxide test sticks)[44] was also reported for **55** and its analogues (Fig. 12), for which peroxide production was clearly demonstrated by the Amplex Red® assay.[177] Interestingly, only some of the tested complexes induced detectable $H_2O_2$ formation, which the authors attributed to differences in hydride donor strength (hydricity) given by the type of electron donating/withdrawing substituent on the oxazoline-based ligands used. The same trend of $H_2O_2$ production was observed for these complexes in HeLa cells by advanced flow cytometry experiments with an $H_2O_2$-selective redox sensor.

Usually, a type of ROS/RNS is not specified, because non-selective ROS probes (*e.g.*, DCFH-DA or $H_2$DCFDA) are used.[77,204] Only some reports discussed more specific flow cytometry 2D experiments indicating the production of superoxide radicals.[211,248] A special experiment was conducted by Salmain, Sobczak-Thépot and co-workers, who treated HeLa cells with a fluorescent protein-based $H_2O_2$-selective redox sensor for flow cytometry (discussed above in this section).[177,179]

In some cases, only a slight increase in intracellular ROS levels was induced by anticancer Ir–Cp*x* complexes;[101,104,108,109,147,160,161,170,174,193,206,251,258] this was also reported to be comparable with cisplatin.[169] A decrease in ROS (or RNS) was even observed in cells treated with some anticancer complexes (*e.g.*, **8** and **9**),[54,55] suggesting that the induction of RO(N)S formation should not be viewed as a simple Fenton-like reaction triggered by the presence of metal (Ir) ions. Similar ROS levels were detected in SW620 and HepG2 cells, differing in sensitivity toward Ir–Cp* complexes containing ispinesib-derived ligands.[107] It was also reported that ROS production in treated cancer cells did not disturb the mitochondrial membrane potential as it remained almost unchanged.[159,198]

Sometimes the redox-mediated MoA and involvement of ROS are proved by experiments with ROS scavengers, such as NAC or tempol, which are usually co-applied at non-toxic concentrations to cells treated with anticancer Ir–Cp$^x$ complexes.[100,169,175,200] Pre-treatment with NAC also indicated a link between ROS formation and lysosomal damage (section 5.7), and reduced the number of apoptotic cancer cells.[200] ROS production by the Ir complex (*e.g.*, **119** in Fig. 41) also activated the NF-κB channel, which is related to ROS overproduction in cells.[258] Specific scavengers (DMSO for $^{\bullet}OH$, SOD for $^{\bullet}O_2^-$ and $NaN_3$ for $^1O_2$) were used for Ir dichlorido complexes (*e.g.*, **11**), which showed that the complexes induced the production of all three types of ROS in treated cancer cells.[59,60]

ROS production in cells is often linked to NADH oxidation induced by Ir–Cp$^x$ anticancer compounds. In most cases where both phenomena have been studied, a correlation has been observed because NADH oxidizing Ir–Cp$^x$ complexes also induced ROS production in treated cells.[44] Similarly, some complexes (*e.g.*, **123** in Fig. 45) did not exhibit an oxidative effect towards NADH and did not induce ROS formation in cells.[85] Exceptionally, ROS were produced in cancer cells by complexes that did not interact with NADH.[105,106,159,231] Some recent works discuss the redox-mediated MoA in the context of the levels of specific proteins, the expression of which is regulated by oxidative stress defense pathways (section 5.8).[227,263]

### 5.6. Cell cycle analysis

Although the cell cycle is directly related to cell division and DNA (section 5.4), it is discussed after section 5.5, which discusses ROS and the redox-mediated MoA, because ROS can also damage DNA and induce cell cycle changes. In general, cell cycle analysis is used to determine the distribution of cells in different cell cycle phases, namely G1 (gap 1; also reported as G0/G1), S (synthesis), G2 (gap 2) and M (mitosis), which are closely connected to the effects of new drugs (*e.g.*, anticancer Ir compounds) on cell proliferation. It is most commonly performed using flow cytometry with a specific DNA staining dye (*e.g.*, PrI).

Probably the first investigation of the effect of Ir–Cp$^x$ compounds on the cell cycle was performed for dichlorido complex **8**, the biological effect of which was associated with apoptosis, necrosis and autophagy (in 8505C cells).[54] Cell cycle analysis showed that **8** induced an increase of apoptosis-related sub-G1 cells with fragmented DNA at the expense of the G1, S and G2/M cell cycle phases, suggesting that apoptosis was the dominant type of cell death for **8**. However, another investigation from the same year reported that **48**, which induced early apoptosis in HT29 cells, did not induce similar DNA fragmentation, as no sub-G1 cells were detected.[166] Application of **48** led to an increase in the population of both the S and G2/M phases of the cell cycle.

For highly effective complex **14** (Fig. 5), a different type and dynamics of cell cycle modification was determined in comparison with cisplatin.[77] In particular, **14** only blocked A2780 and HL-60 cells in the G0/G1 phase after 48 h, while cisplatin induced an increase in S-phase cell populations after 24 h. This observation was supported by impedance-based real-time monitoring of the effects on cancer cell growth, the results of

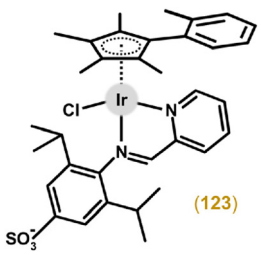


**Fig. 45** The structural formula of complex **123**.

which for **14** correlated with DNA interfering drugs inhibiting protein translation and inducing G1 (or S) cell cycle arrest. Similar cell cycle modification results (G1 arrest) were reported for more anticancer Ir–Cp$^x$ complexes.[168] Other compounds induced an increase in the number of cells in the S phase of the cell cycle (*e.g.*, **70** and **105**).[193] In some cases, the cell cycle remains more or less unmodified.[104]

The often ambiguous connection between cell cycle alterations, as induced by anticancer Ir–Cp$^x$ complexes, and other biological mechanisms can be clarified by additional research findings.[260] Specifically, the cytotoxic [Ir($\eta^5$-Cp$^{bph}$)(bpy)Cl]$CF_3SO_3$ complex induced S and G2/M arrest, whereas the cell cycle phase distribution of cells treated with the inactive [Ir($\eta^5$-Cp$^{bph}$)(bpy)Cl]$BPh_4$ complex remained more or less unchanged. On the other hand, the very severe changes to cancer cells treated with dinuclear complex **88** did not lead to relevant cell cycle changes, which remained largely unchanged compared to non-treated cells.[227]

Thus, the main importance of studies on cell cycle modification lies in distinguishing the MoA from that of cisplatin, which induces characteristic cell cycle changes.

### 5.7. Specific organelle damage

The effects of compounds on DNA (cell nucleus; section 5.4) and mitochondria (related to ROS induction; section 5.5) have been discussed, but more cellular targets are available. Lysosomes are single-membrane organelles containing various digestive enzymes (*e.g.*, proteases, nucleases or lipases) and having an acidic environment inside. They are essential for maintaining cellular function. Liu and co-workers reported that Ir complexes (*e.g.*, **73** in Fig. 16) disrupted the lysosomal integrity in HeLa cells, which was studied using the acridine orange fluorescent probe (red fluorescence in lysosomes, green fluorescence in cytosol and the nucleus).[197] Other Ir–Cp$^x$ compounds were shown to accumulate in lysosomes (*e.g.*, **18**)[82] or even specifically target these organelles and induce permeabilization of the lysosomal membrane in cancer cells, leading to lysosomal rupture and cancer cell death.[85,103,104,147,170–172,198,199,201,202,206] Lysosome damage was also proved by the concentration-dependent release of cathepsin B into the cytosol.[102]

Interestingly, although disruption of the lysosomal membrane has been reported for a number of complexes, further studies with the protease inhibitor leupeptin did not alter the antiproliferative activity of **79**.[202] This suggests that cell death is not due to lysosomal damage but rather may result from another type of cell death (mitochondrial apoptotic pathway).

Complex **56** (Fig. 12), which partially accumulated in the endoplasmic reticulum (ER), induced ER stress.[178] ER stress, in general, is connected with a complex unfolded protein response (UPR), the key signal activators (*e.g.*, protein kinase RNA-like ER kinase, PERK) of which were upregulated in the treated cancer cells. Along with ER stress, **56** disrupted the integrity of the Golgi apparatus. An effect on the ER was also detected in cells treated with **33**, which triggered the integrated stress response (ISR) as a consequence of induced mitochondrial dysfunction.[115]

Complex **57** bearing the terminal bioorthogonal azido group effectively targeted proteins involved in protein folding and actin cytoskeleton regulation.[179] This resulted in the inhibition of the folding activity of heat shock protein HSP90 and disorganization of the cytoskeleton.

### 5.8. Gene expression analysis

Complexes **47** and **116** (Fig. 39), which were studied in the NCI-60 panel,[262] were also screened in a panel of 916 cell lines from 28 tissue types (Sanger Cancer Genome), where **116** was 78- and 36-fold times more potent than **47** and cisplatin, respectively.[263] Furthermore, **116**, in contrast to **47**, was highly potent in primary patient-derived ovarian cancer cell lines isolated from patients prior to treatment and after taxane/cisplatin application. Compound **116** had a different pattern of activity towards the cancer cell lines used than other screened anticancer drugs, indicating its unique MoA. For **116**, gene expression was studied in A2780 cells by RNA sequencing at different time points (up to 48 h exposure). The highest number (746) of differentially expressed genes was detected at $t$ = 12 h, of which *ca.* twice as many genes were down-regulated. A detailed analysis of the results showed that the **117**-treated cancer cells activated stress (general) and oxidative stress response pathways (*e.g.*, Nrf2 and the two AP-1 transcription factors); Nrf2 = nuclear factor erythroid 2-related factor 2. This was linked by flow cytometry to the formation of high ROS levels in A2780 cells. In connection with the induction of apoptosis (flow cytometry), genes for inhibitors of apoptosis, which inhibit the activation of caspase proteins (*e.g.*, BIRC3), were up-regulated. Similarly, dinuclear complex **88** up-regulated HO-1 and NQO1 proteins, the expression of which is regulated by the Keap1/Nrf2 pathway involved in oxidative stress defense and the induction of ROS production in cancer cells.[227]

Complex **26** (Fig. 7) was studied by RT-PCR (reverse transcription polymerase chain reaction) in 3D spheroids of SCC070 cells, where the expression of stemness regulators, the drug efflux transporter and differentiation markers were investigated.[92] However, **26** showed a lower ability to reduce the expression of the tested regulatory genes than its Ru analogues. Gene expression studies (microarray data, supported by RT-qPCR) performed on apoptotic cells treated with **33** (Fig. 8) showed, for example, a significant decrease in histone gene expression, which was consistent with other results (*e.g.*, cell cycle arrest) obtained for this complex.[115]

### 5.9. *In vivo* studies

In contrast with the above-discussed results obtained on cell cultures in a controlled laboratory environment (*in vitro* testing), *in vivo* studies of anticancer activity are performed on whole, living organisms. Obviously, *in vivo* studies provide scientists with a more accurate and comprehensive picture of how a substance will act on the treated organism. As no Ir cyclopentadienyl complexes have entered clinical trials on

 

human patients, only results obtained in animals are discussed in this section.

Although the *in vitro* activity of the [Ir(η$^5$-Cp*)Cl(pbt)]PF$_6$ (**124**; Fig. 46) complex did not reach 50% cell viability reduction even at 20 mg mL$^{-1}$ concentration, it was tested for its *in vivo* activity in mice bearing Dalton's lymphoma ascites tumour cells; pbt = 2-(1*H*-pyrazol-3-yl)benzothiazole.[118] **124** increased the life span of tumour bearing mice (T/C = 152% at 15 mg kg$^{-1}$ dose), but it was toxic at 30 mg kg$^{-1}$ dose, resulting in premature death of the treated animals.

The *in vivo* anticancer activity of **76** (Fig. 16) was studied in the CT26 colon cancer mouse xenograft model (3 or 5 mg kg$^{-1}$ doses for 7 days).[200] After 24 days, there was a significant dose-dependent inhibition of tumour volume and weight (62.3 and 56.4%, respectively, for 5 mg kg$^{-1}$ dose), without body weight loss.

The hexanuclear Ir metallaprism was less effective than its Rh analogue in tumour-induced C57L6/J mice.[221] For the Ir complex, treated animals died after three days with no reduction in tumour volume.

The Ir iodido complex was reported to be less toxic *in vivo* than its chlorido analogue towards zebrafish (*Danio rerio*) embryos, but both these Ir–Cp$^x$ complexes were more toxic than cisplatin.[248]

Dinuclear complex **91** involving a triphenylamine-modified TSC (Fig. 22) was studied using the A549 mouse xenograft model (lung cancer).[231] The complex was not toxic (no mortality and weight change) and showed promising tumour growth inhibition. The induced tumour volume and weight changes were lower compared to control groups of animals (vehicle and cisplatin-treated mice). The tumour inhibition rate was *ca.* 57% for **91**, which significantly outperformed cisplatin with *ca.* 12%. Histological analysis of the isolated tumours showed evidence for the paraptosis-like cell death induced by **91**. Importantly, the biochemical blood indicators of myelosuppression and hepatotoxicity (decrease in the white blood cell count, absolute value of monocytes, blood urea nitrogen, aspartate aminotransferase, creatinine, alkaline phosphatase, alanine aminotransferase) were, in most cases, less pronounced for **91** than for cisplatin. On the other hand, metastatic infiltrating foci of cancer cells were detected in the lungs and liver, indicating a high possibility of infiltration and metastasis in animals treated with **91**. Similar heterometallic complex **125** (Fig. 47) with a ferrocene-modified TSC ligand was also highly anticancer active *in vivo* in the same mouse model.[232]

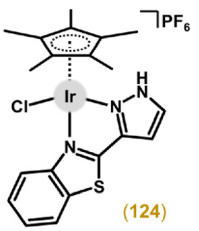


**Fig. 46** The structural formula of complex **124**.

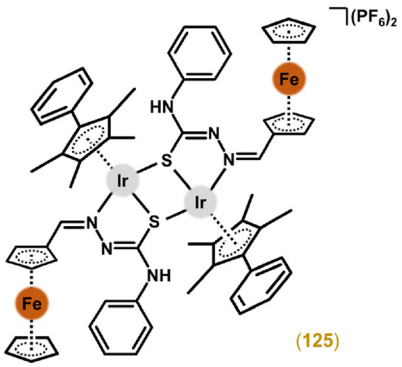


**Fig. 47** The structural formula of complex **125**.

Complex **33** had a maximum tolerated dose of 1.3 mg kg$^{-1}$ in healthy BALB/c mice, with predominant accumulation in the liver, kidneys and lungs.[115] In an orthotopic model of lung cancer (A549 cells marked with luciferase) in nude mice, **33** was administered at 0.9 mg kg$^{-1}$ doses, inducing no signs of toxicity and reducing the primary tumour but not in the neighbouring invaded lymphatic nodes.

Complex **13** (3 mg kg$^{-1}$ doses) reduced the tumour size (volume, weight) markedly more effectively (1.20 g) than cisplatin (1.45 g) in the A549 lung cancer transplanted mice.[63] No negative side effects or metastasis in the lungs or other organs were observed for **13**, representing another advantage over cisplatin.

Drug delivery systems loaded with anticancer Ir–Cp$^x$ complexes seem to be a very promising approach (see section 6.4). For example, complex **22**, administered to mice bearing the A549 human lung xenograft at 1.25 mg kg$^{-1}$ dose (higher doses were toxic) exhibited greater tumour growth inhibition (TGI = 78%) than cisplatin (54%).[88] Other improvements to the *in vivo* anticancer activity were obtained by the formation of liposomes loaded with **22**.

The phototoxic ferroptosis-inducing complex **27** (Fig. 7) was studied for its *in vivo* anticancer activity in 4T1 tumour-bearing Balb/c mice.[96] A dose of 5 mg kg$^{-1}$ (i.p.) was followed by 635 nm laser irradiation for 10 min. **27** itself (*i.e.*, without irradiation) inhibited tumour growth (TGI = 43%) to a lesser extent than that detected in irradiated animals (TGI = 89%), indicating the synergistic effects of chemo- and phototherapy. No relevant toxicity was observed in major organs, which proved the promising biocompatibility of **27**.

## 6. Anticancer activity-related aspects

In general, the anticancer activity of newly developed (metallo) drugs is often evaluated with respect to the composition of the new compounds (SAR; section 4) and the manner in which they induce cancer cell death (MoA; section 5). In addition, there are other aspects and processes that either influence the resulting biological effect (*e.g.*, interactions with biomolecules)

or represent a specialised research/application area (*e.g.*, targeting or PDT), as discussed in detail in this section.

### 6.1. Interaction with biomolecules

#### 6.1.1. Small biomolecules

*6.1.1.1. NAD(H).* The interaction of new Ir–Cp$^x$ anticancer complexes with NAD(H) coenzymes is often studied for its close connection to the redox-mediated MoA.[276–278] From a chemical point of view, the reduction of $NAD^+$ to NADH (usually with formate as a hydride source) was studied[280,281] before the first mention of the reduction of NADH by the Ir–Cp$^x$ complex as a catalyst for such a transfer hydrogenation reaction and the discussion of possible biochemical consequences.[282] For various metallodrugs, including Ir–Cp$^x$ compounds, the oxidation of NADH is accepted as a source of ROS within a redox-mediated MoA. Similarly, the use of hydrogenation reactions with NADH as a hydride source for the reduction of biologically relevant compounds (quinones) has been described for Ir–Cp$^x$ complexes.[283]

The first reported $[Ir(\eta^5\text{-}Cp^{ph})(H_2O)(phen)]^{2+}$ (**126**; Fig. 48) complex effectively and repeatedly oxidized NADH to $NAD^+$.[282] This process was studied by $^1$H NMR and UV-Vis spectroscopy, which remain the most widely used techniques for studies of NAD(H) conversions. The oxidation of NADH was associated with hydride transfer to the metal centre and with the formation of the Ir–H hydrido species detectable by $^1$H NMR in very strong fields (*ca.* −10 ppm). Such hydride subtraction led to the formation of $H_2$, which is an antioxidant by itself. The formation of $H_2$ was indirectly demonstrated by an increase in pH. Importantly for future research, the oxidation of NADH has been also demonstrated as a proton source for the reduction of physiologically relevant biomolecules – in this case, pyruvate was used, which was partially reduced to lactate in the presence of **126** and NADH. For analogous complex **101** (Fig. 27) it was observed that hydride transfer from NADH could be linked to ROS production, as hydrogen peroxide was detected in cell-free experiments in the presence of oxygen.[44]

Some Ir–Cp$^x$ complexes retained their integrity and the formation of the Ir–H species was not discussed despite high NADH-to-$NAD^+$ oxidation.[163] Other complexes readily oxidized NADH, but the Ir–H $^1$H NMR signal was not detected.[110] Negligible or even no NADH oxidation was observed for anticancer Ir–Cp$^x$ complexes.[85,104] On the other hand, another Ir complex was inactive in cancer cells and outperformed by its direct Rh analogue, while their NADH-oxidizing abilities were comparable.[86] The ability to oxidize NADH was also reported for mononuclear dichlorido complexes[59] and dinuclear Ir–Cp* complexes.[225,227] Detailed kinetic studies were reported for the model compound $[Ir(\eta^5\text{-}Cp^*)(H_2O)(phen)]^{2+}$.[284]

The ability of some Ir–Cp$^x$ complexes to reduce $NAD^+$ to NADH in the presence of formate as a hydride source and the positive effects of formate concentration on antimicrobial (antiplasmodial) activity were also observed (anticancer activity was not studied).[285] Other antimicrobial-active Ir–Cp$^x$ complexes did not reduce $NAD^+$ to NADH.[286]

*6.1.1.2. GSH.* Reduced glutathione (GSH) is a tripeptide (γ-Glu-Cys-Gly) that has several important functions in most cells, including cancer cells.[287] GSH performs various functions in cells, for example, it is a key antioxidant, plays an essential role in detoxification (of toxins or xenobiotics) and also supports the proper functioning of immune cells (and the immune system as such), as well as maintaining the proper structure and function of proteins.

Probably the first consideration of a possible interaction between mononuclear Ir–Cp$^x$ complexes and GSH was reported for **47** and **101**.[44] Both complexes formed a covalent Ir–SG adduct, as proved by $^1$H NMR and mass spectrometry. This process was faster for the more hydrolytically labile chlorido complex **47**. Interaction with GSH has also been described for other Ir complexes, either to form similar Ir–SG adducts[133,136,170] or the product has not been specified.[86,99] Some anticancer Ir–Cp$^x$ complexes did not interact with GSH.[93,100,102]

A specific case was reported for a series of Ir iodido complexes, which formed the abovementioned Ir–SG adduct, which subsequently catalysed GSH oxidation to glutathione disulfide (GSSG).[248] The process of GSH-to-GSSG oxidation was linked to the reversible attack of glutathione on the azo bond of the azopyridine ligand. As a consequence, the studied iodido complexes decomposed, releasing the azopyridine ligand and forming the dinuclear trithiolato species, $[Ir_2(\eta^5\text{-}Cp^*)_2(\mu\text{-}SG)_3]^+$, with three bridging –SG ligands (Fig. 49). This decomposition mechanism has also been reported elsewhere.[111]

Importantly, some works have also reported the oxidation of GSH to GSSG in DMSO-containing mixtures of solvents as an effect of Ir compounds,[95,217,244,249] but this should be attributed to DMSO and its known oxidative effect towards GSH.[111,288]

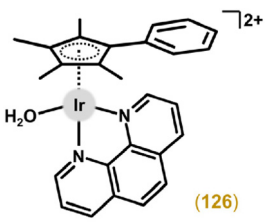


Fig. 48 The structural formula of complex **126**.

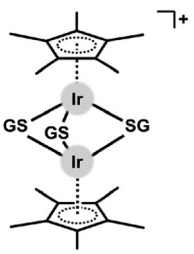


Fig. 49 The structural formula of the $[Ir_2(\eta^5\text{-}Cp^*)_2(\mu\text{-}SG)_3]^+$ dimer; GSH = reduced glutathione.

*6.1.1.3. Amino acids.* In the context of studying the interactions of Ir–Cp$^x$ complexes with GSH, a higher affinity for sulfur-containing amino acids (*N*-acetyl-L-methionine or *N*-acetyl-L-cysteine) over nitrogen-containing ones (*N*-acetyl-L-histidine) was observed in HPLC/ESI-MS experiments under biologically relevant conditions for **71** (Fig. 15).[194] Complexes **51** and **52** interacted with Cys and other biomolecules (His, methionine, EtG).[173,174] Similarly, the [Ir($\eta^5$-Cp*)Cl(bphen)]$PF_6$ complex interacted rapidly with NAC, but did not show any affinity towards tyrosine and serine.[88] In contrast, an affinity towards unsubstituted Cys was observed for another Ir complex,[187] while other complexes did not interact with Cys.[107] DFT calculations were also used for studies of the reactivity of a model Ir–Cp$^x$ complex with Cys and selenocysteine.[289]

*6.1.1.4. Ascorbic acid.* Ascorbic acid (ASA) is an abundant intracellular antioxidant that is frequently used in the field of multi-component platinum(IV) anticancer complexes, where ASA facilitates the reductive release of their axial ligands.[290] In contrast, only a few investigations on anticancer Ir–Cp$^x$ complexes have involved ASA in any of its possible chemical or biochemical roles.

Complex **30**, which contains the aza bond outside the chelate ring (Fig. 8), making it accessible for various reactions, was shown to interact not only with NADH and GSH, but it also oxidized ASA to dehydroascorbate, as proved by $^1$H NMR studies.[111] Other Ir–Cp$^x$ mononuclear (**54**; Fig. 12)[176] and dinuclear (**88**)[227] complexes without similar reactive bonds were stable in the presence of ASA and did not induce any changes to this biomolecule.

*6.1.1.5. Mixture of biomolecules.* It is apparent that single biomolecule experiments mimic the intracellular environment only imperfectly and should be considered only as a chemical model system for studying reactivity rather than biochemical evidence of the MoA. Aware of this shortcoming, some authors have used a mixture of multiple biomolecules to increase the relevance of such model studies.

In the first article that discussed the oxidation of NADH in the presence of **126**, GSH was used as a possible scavenger of the NADH oxidation.[282] However, no effect was observed and NADH was oxidized to $NAD^+$ even in the presence of excess GSH.

Complex **30** (Fig. 8) oxidized NADH (to $NAD^+$) and ASA (to dehydroascorbate), which was associated with the reduction of the *exo*-chelate azo bond.[111] In the presence of GSH, the release of the chelating ligand and the formation of the above-mentioned $[Ir_2(\eta^5\text{-Cp}^*)_2(\mu\text{-SG})_3]^+$ species were observed together with GSH-to-GSSG oxidation. The results of $^1$H NMR studies of **30** in various mixtures of NADH, ASA and GSH showed different magnitudes of individual processes – for example, NADH was oxidized to a lesser extent in the presence of GSH, ASA or their mixture. Interestingly, the pro-oxidant effect of ASA on GSH oxidation was related to the recovery of ASA from dehydroascorbate. While the presence of the azo bond on the chelating ligand used was essential for the observed biochemical phenomena, the individual events (*e.g.*, NADH or ASA oxidation) did not occur with the free ligand. Thus, **30** should therefore be understood as an example of complexes with a metal-activated ligand.

Highly effective (low-micromolar $GI_{50}$ values) dinuclear complex **88** oxidized NADH to $NAD^+$ when mixed with NADH or with NADH and GSH.[227] When mixed with both NADH and GSH, **88** formed a covalent adduct with –SG, which was not observed for **88** when mixed with GSH alone. In contrast to GSH, the presence of ASA caused a decrease in the extent of NADH oxidation, which was completely suppressed in the mixture of **88** with all three biomolecules (NADH, GSH, ASA). Even with these in-solution results, **88** induced cancer cell death *via* a redox-mediated MoA, and the levels of both NAD(H) coenzymes were significantly reduced in treated cancer cells.

### 6.1.2. Proteins

*6.1.2.1. Albumins.* Bovine serum albumin (BSA) is a frequently used model transport protein for pre-pharmacokinetic studies of the behaviour of novel Ir complexes in blood.[119] In most cases, fluorescence spectroscopy is used to study the interaction of Ir–Cp$^x$ compounds and naturally fluorescent albumins. Such experiments have usually provided a positive response interpreted as the ability of the new compounds to interact with albumins. Since albumins are blood transport proteins, release from the Ir-albumin adducts formed is also important, but has been studied relatively rarely.[168] Some papers have also reported $^1$H NMR studies on Ir complexes with albumins, to investigate their stability in the presence of transport proteins.[111,176]

Less frequently, human serum albumin (HSA) or apo-transferrin has been used for analogous fluorescence spectroscopy studies of the interactions of Ir–Cp$^x$ complexes and blood transport proteins.[59,62,114,133,166,167] Glucose was also studied for its possible binding to **32** in blood, but no interaction was detected using UV-Vis experiments.[114] Complex **22** was studied for its stability in blood plasma, where it showed a lower ability to bind plasma proteins ($t_{\frac{1}{2}}$ = 6.1 h) than cisplatin ($t_{\frac{1}{2}}$ = 1.8 h).[88]

*6.1.2.2. Other proteins.* In 2010, when DNA was considered the only target for Ir–Cp$^x$ complexes, experiments were carried out on new Ir complexes and ubiquitin (Ub)[74] and cathepsin B (catB)[53] were employed as model proteins. Although the Ir compounds used, in contrast to Ru analogues, did not interact with Ub and catB, these works paved the way for further research that considered proteins as possible targets for Ir–Cp$^x$ compounds.[53,74] DFT analysis of *N*-acetyl-L-cysteine-*N*′-methylamide, a model for the Cys residue of, *e.g.*, catB, revealed that Ir (and Rh) complexes had less affinity towards Cys (*i.e.*, formed weaker M–S bonds) than Ru and Os analogues.[53] Low micromolar inhibition activity towards catB was also reported for **43** and **45**.[156]

Complexes **43** and **47** were studied for their interaction with the methionine (Met)-rich protein calmodulin by electron-capture dissociation (ECD) tandem mass spectrometry (MS).[291] The results indicated weak Met binding by the Ir–Cp$^x$ compounds used, without loss of the chelating ppy ligand, which

was different from cisplatin, which lost its ligands and cross-linked the protein. Similar Ir–Cp$^x$ complexes bearing an aldehyde group on their ppy ligand were also studied by ECD-MS for their interaction with different model peptides (substance P, bombesin).[292] The complexes bind covalently to peptides *via* histidine (Ir–His bond) and lysine (imine formation of Lys with an aldehyde group).

Enzyme thioredoxin reductase (Trx-R) plays a key role in various intracellular processes, such as protecting from oxidative stress or DNA synthesis and repair. Trx-R was studied as a possible mechanistic target for complexes bearing various picolinamides, where Ir–Cp$^x$ compounds showed nanomolar $IC_{50}$ values of Trx-R-inhibition and outperformed their Ru analogues.[120] Within another series of anticancer complexes reported by the same research team, both Ir (**39**; Fig. 9) and Ru compounds showed inhibition effects towards Trx-R in the nanomolar range.[148]

Tether complex **102**, although the best-performing of the reported series of complexes, did not show any inhibitory effect on the enzymatic activity of Trx-R, while some of its less cytotoxic congeners (both tethered and nontethered) inhibited it.[165] The $[Ir(\mu\text{-}Cl)(\eta^5\text{-}Cp^x)Cl]_2$ dimers with differently substituted Cp$^x$ rings showed no correlation between antiproliferative activity and Trx-R inhibition, since the more anticancer active complex inhibited Trx-R less effectively.[64] Other complexes did not inhibit Trx-R.[149]

Topoisomerase IIa (TOP2A) is a nuclear enzyme that plays a critical role in controlling DNA function. It is also the target of anticancer drugs that generate enzyme-mediated DNA damage. Chlorido complex **70** (Fig. 15) and its 1-methylimidazole analogue **105** (Fig. 28) effectively inhibited TOP2A, although their effects were less pronounced than that of the Ru analogues.[193]

A pair of Ir–Cp* complexes was derived from ispinesib-based ligands.[107] Ipsinesib is a kinesin spindle protein (KSP) inhibitor and this effect was also studied for the Ir complexes, which reduced the KSP activity to <20% even at 1 nM concentration. Lower KSP inhibitory activity was reported by the same research group for more stable analogues with different binding of ipsinesib on a carrier ligand (*e.g.*, **29**; Fig. 8).[109]

Complex **56** (Fig. 12), which induced various effects in cancer cells, including ER stress and Golgi apparatus dispersion, also altered the gel electrophoretic mobility studied in HeLa cell extract (*in vitro*) and in live HeLa cells (*in vivo*).[178] This observation implied covalent interactions with protein(s) that were not further specified. Studies with *N*-acetyl histidine, NAC methyl ester, phenylbutylamine (mimicking lysine) and butyramide (mimicking glutamine and asparagine) were performed for **56** as model experiments for such protein interactions. Analogous complex **57** is functionalized by a bioorthogonal azido probe allowing the identification of intracellular protein targets by bioorthogonal click reactions.[179]

### 6.2. Complexes with bioactive ligands

**6.2.1. Pharmacological context.** Regarding the design of these complexes, the use of bidentate bioactive ligands does not appear to be a viable strategy. Either such bidentate ligands are not released from the complex, which suppresses their own activity, or they are released from the complex, but this leads to the formation of inactive metal-based metabolites. More preferable is the use of complexes bearing bioactive monodentate ligands (multi-component complexes), which release an aqua/hydroxido complex species that has its own biological activity. The use of carrier ligands to bind releasable bioactive substituents also appears promising for the development of multi-component complexes.

**6.2.2. Complexes with bidentate bioactive ligands.** In some works, ligands with their own biological activity were used for the preparation of anticancer Ir–Cp$^x$ complexes. Since the release of such ligands from the complexes has not been demonstrated, these ligands cannot be assumed to have an independent biological effect. For example, the $[Ir(\eta^5\text{-}Cp^*)Cl(cur^1)]$ complex involves a bioactive curcumin derivative, cur$^1$, which, based on UV-Vis studies, remains in the complex under aqueous conditions; Hcur$^1$ = (1*E*,6*E*)-1,7-bis(phenyl)-1,6-heptadiene-3,5-dione.[190] The opposite situation, where the bioactive ligand used is released immediately, is also not pharmacologically viable. For example, complex **127** (Fig. 50), a pta analogue of **68** (Fig. 14), was studied for its stability under the simulated physiological conditions at different NaCl concentrations (5 mM, 100 mM), where this complex was immediately decomposed and hydrolysed, which was connected with the release of bidentate-coordinated curcumin.[45] Similar results were reported for the pta analogue **106** (Fig. 28) containing β-diketone dibenzoylmethane.[191] The released organic ligand usually accumulates less in cancer cells and the Ir-containing metabolites (*i.e.*, $[Ir(\eta^5\text{-}Cp^*)Cl_2(pta)]$ and $[Ir(\eta^5\text{-}Cp^*)(H_2O)_2(pta)]^{2+}$ for **106** and **127**; Fig. 50) usually have very little biological effect.[53]

Dinuclear complexes containing highly cytotoxic avobenzone also showed cytotoxic potency in the low-micromolar range as did the free avobenzone.[192] Highly active C,N-coordinated ppy ligands containing androsterone were used to prepare a series of Ir complexes, but their activity was not higher than that of the free organic derivatives.[157] These complexes, however, were not studied for their in-solution stability.

Other Ir complexes, derived from bidentate-coordinated moderately cytotoxic ispinesib-derived ligands, were unstable in the DMEM testing medium.[107] Based on this observation, the authors also studied stability in the presence of Cys and His, which represent highly-concentrated components of DMEM. The results showed extensive release of bidentate ligands in the presence of His, which coordinated to the Ir centre. A similar synthetic strategy was used with the pyridine-2-ylmethanimine bidentate ligand bearing ispinesib or 7-chloroquinazolin-4(3*H*)-one as bioactive functionalities.[108,109]

**6.2.3. Multi-component complexes.** Two different approaches can be used to obtain multi-component Ir–Cp$^x$ complexes. First, the $[Ir(\eta^5\text{-}Cp^x)(L\text{^}L)Cl]^{0/+}$ complexes contain carrier ligands (*i.e.*, a chelating L^L ligand or Cp$^x$) substituted (biofunctionalized) by a bioactive substituent *via* a cleavable bond allowing its release under physiological (preferably intracellular) conditions. Or second, complexes of the general

 

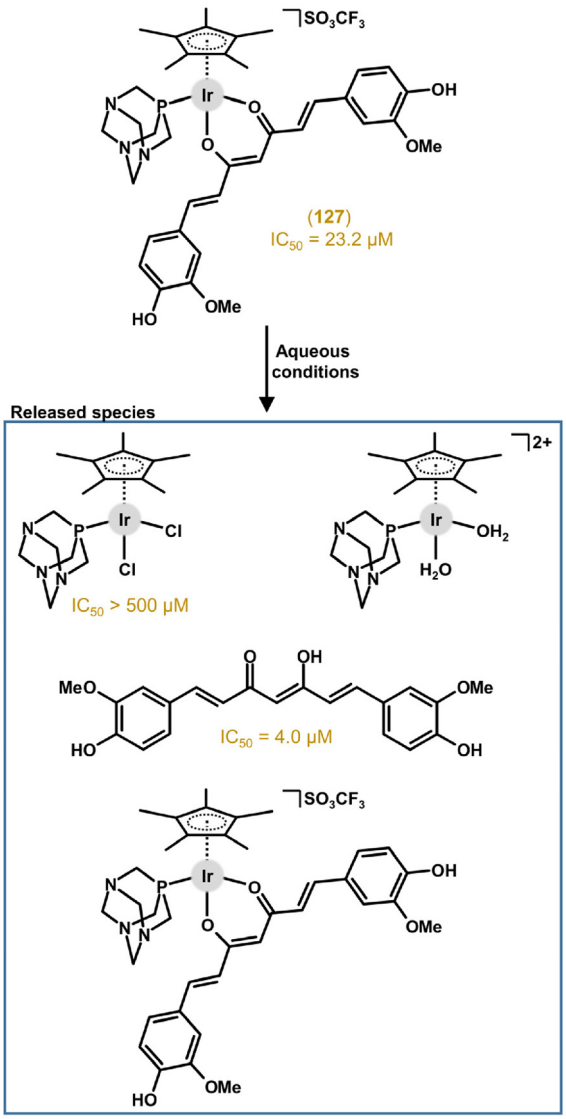


**Fig. 50** The structural formula of complex **127** and the route to its decomposition in the presence of water (water : DMSO mixture; $^{1}H$,$^{31}P$ NMR studies), given together with the $IC_{50}$ values determined in A2780 cells.

formula $[Ir(\eta^5\text{-}Cp^x)(L\text{^}L)(X)]^{0/+}$ involve a releasable monodentate bioactive ligand X.

The strategy with releasable substituents on a carrier ligand was used for the first time for the complex involving bpy conjugated to lipoic acid (LA) through the peptide bond.[136] This inactive complex ($IC_{50}$ > 200 μM in various cancer cells) was stable in the presence of water, thus LA was not released from the complex. The antimalarial drug artemisinin was used for the biofunctionalization of a series of Ir–$Cp^x$ complexes (*e.g.*, **20**; Fig. 6) through the ester bond of their chelating bpy-based ligands.[83] Compounds were studied for their anticancer and antimicrobial activity, but stability studies were not conducted.

Another series of Ir–Cp* complexes is based on double-substituted bpy diesters bearing two different bioactive substituents *via* the ethyl linker (*e.g.*, GST inhibitor ethacrynate and COX inhibitor flurbiprofen for the most effective Ir complex **128** (Fig. 51)); GST = glutathione S-transferase, COX = cyclooxygenase.[84] These Ir complexes (and their Ru analogues) underwent a transesterification process in methanol and in a mixture of 1% DMSO/99% RPMI, leading to the release of bioactive substituents as carboxylates or hydroxyethyl esters. With respect to the biological type of substituent used, the inhibition of GST and COX was studied and shown to be induced by the complexes. Since these complexes also metalated DNA, they could be considered as representatives of multi-modal (multi-targeted) anticancer complexes that induced cell death in treated cancer cells through multiple independent processes.

Complexes involving a bpy derivative biofunctionalized with sulfonamide or dichloroacetate (dca) bioactive substituents were inactive in the human cancer cells used.[52,86] Complexes with two substituents (*e.g.*, dca) conjugated to bpy *via* ester bonds were examined by mass spectrometry in the presence of porcine liver esterase (PLE).[52] The results showed that although the free bpy derivative readily released its carboxy substituents in the presence of PLE due to enzymatic cleavage, the same ligand was stable after its coordination to the Ir complex, which was not cleaved by PLE to yield independent bioactive species.

Regarding the second design of multi-component $[Ir(\eta^5\text{-}Cp^x)(L\text{^}L)(X)]^{0/+}$ complexes, the first complexes with releasable monodentate bioactive ligands (X) were derived from the moderately effective $[Ir(\eta^5\text{-}Cp^*)Cl(dpa)]PF_6$ complex; dpa = *N*-(pyridin-2-yl)pyridin-2-amine (dipyridylamine).[43] However, its analogues with O-coordinated HDAC inhibitors valproate (vp) or 4-phenylbutyrate (pb) were comparably (for pb) or even less (for vp) effective in A2780 cells.

Another $[Ir(\eta^5\text{-}Cp^{ph})(pb)(phen)]PF_6$ (**129**; Fig. 52) complex also contains pb.[250] This complex readily released pb in the presence of water, providing two bioactive species (*i.e.*, pb and an Ir-based entity, $[Ir(\eta^5\text{-}Cp^{ph})(H_2O)(phen)]^{2+}$) under simulated physiological conditions. A specific effect of both biologically independent species was detected in cancer cells. In particular, **129** inhibited the HDAC activity (released pb ligand) and

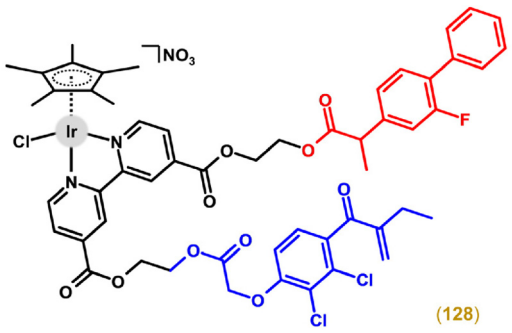


**Fig. 51** The structural formula of multi-component complex **128** involving GST inhibitor ethacrynate (blue) and COX inhibitor flurbiprofen (red).

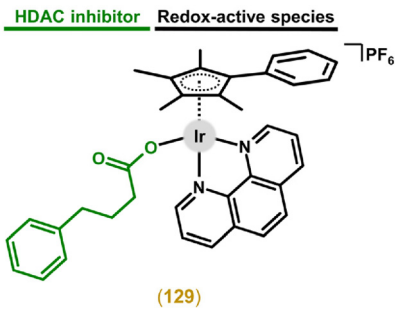


Fig. 52 The structural formula of complex **129**.

induced a high ROS population (released $[Ir(\eta^5\text{-}Cp^{ph})(H_2O)(phen)]^{2+}$ species). **129** also exhibited the ability to overcome acquired resistance against cisplatin and showed higher selectivity towards cancer cells over normal ones, both to a greater extent than that of its chlorido analogue $[Ir(\eta^5\text{-}Cp^{ph})Cl(phen)]PF_6$.

### 6.3. Complexes for photodynamic therapy

Photodynamic therapy (PDT) is a pharmacological concept that utilizes light-sensitive drugs to treat various diseases, including cancer. In principle, PDT consists of the application of a drug, its accumulation in the diseased tissue (cells) and irradiation with a specific wavelength of light, which leads to the production of highly toxic species (ROS, singlet oxygen) that damage cells and cause their death. In the field of Ir complexes, PDT is more often studied for octahedral polypyridyl or cyclometalated complexes,[293] while studies on half-sandwich Ir–$Cp^x$ compounds are relatively rare.

The possible potential of Ir–$Cp^x$ complexes for PDT was described in 2013 for the dinuclear trithiolato Ir complex, which was (similarly to its Ru and Rh congeners) able to generate ROS upon irradiation with UV light, as proved by the cleavage of DNA.[218] The observed DNA cleavage was significantly inhibited by sodium azide ($NaN_3$), which was used as a known ROS quencher.

The $[Ir(\eta^5\text{-}Cp^*)Cl(PBI)]PF_6$ (**130**; Fig. 53) complex was derived from a perylene bisimide (PBI) derivative, which is known to have a high fluorescence quantum yield and be a suitable ligand for complexes with accelerated intersystem crossing (ISC) from the singlet to triplet excited state, greatly promoting singlet oxygen ($^1O_2$) production.[270] Indeed, **130**, which is photostable in aqueous solution, produced $^1O_2$ upon irradiation at 420 nm. Importantly, this feature translated into high phototoxicity in various cancer cells (nanomolar $IC_{50}$ values, PI = 7.8–23.0).

For other complexes (*e.g.*, **131**; Fig. 53) derived from N,O-coordinated lidocaine and involving (pyren-1-yl)ethynyl derivatives of phenylcyanamide, their photodynamic properties have also been described.[251] Both complexes were highly photostable in solution and induced $^1O_2$ formation. Their phototoxicity in HeLa cells was excellent with PI = 278 and 417 (450 nm light irradiation). The complexes accumulated in the nucleus

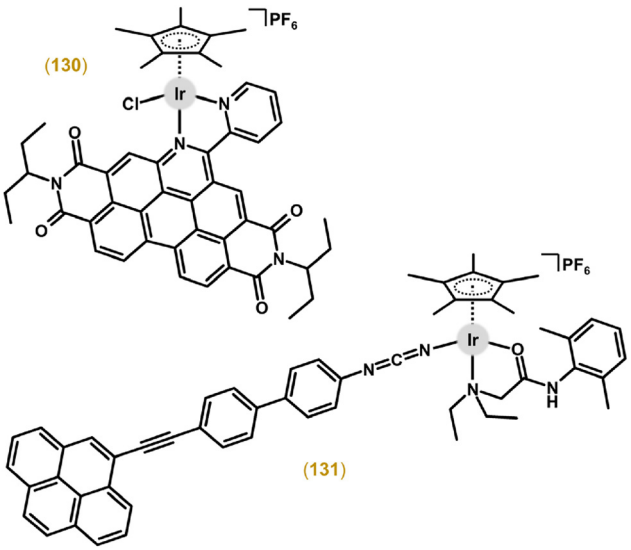


Fig. 53 Structural formulas of complexes **130** and **131**.

and effectively induced ROS formation (in-cell experiment) and DNA photocleavage (cell-free experiment). Interestingly, the observed DNA photocleavage was inhibited by hydroxyl (DMSO, KI, catalase) and superoxide (superoxide dismutase) radical scavengers, while the $^1O_2$ quenchers (TEMP, DABCO, $NaN_3$) did not inhibit it. The number of early apoptotic HeLa cells was higher in the irradiated population than in the dark.

Su *et al.* developed iridium-thiosemicarbazone complexes (*e.g.*, **62** in Fig. 13) for dual chemo- and photodynamic therapy by introducing a photosensitizer moiety into the TSC ligand. **62** showed remarkable phototoxic behaviour against SKOV3 cells ($IC_{50}$ = 2.3 μM, $\lambda_{irr}$ > 400 nm), as well as up to 7.4-fold lower toxicity in the dark.[184] Photostable complex **27** (Fig. 7) produced $^1O_2$, superoxide and hydroxyl radicals, and extensively oxidized NADH upon irradiation by 635 nm light.[96] In connection, high NADH photooxidation was also detected in cancer cells, leading to a decrease of ATP production and disruption to mitochondria. The irradiation of **27**-treated 4T1 cancer cells improved its moderate dark cytotoxicity ($IC_{50}$ = 38.4 μM) to low-micromolar values ($IC_{50}$ = 2.0 μM), resulting in PI = 18.8. Approximately 2-fold higher cytotoxicity and a lower PI of 10.2 were detected for non-cancerous LO2 cells. Apoptosis and ferroptosis were detected in irradiated cancer cells.

The strategy of using π-expansive ligands was applied to prolong the excited state lifetimes; this is known to be beneficial for the photobiochemical properties including photocytotoxicity.[180] Complexes were photostable and induced the production of $^1O_2$. Chlorido complexes, especially their analogues bearing a monodentate heterocyclic N-donor ligand (*e.g.*, imidazole), exhibited a higher antiproliferative activity when irradiated than in the dark. Thus, complexes with the most extended pbpn ligand showed higher activity, as exemplified by the chlorido complex **58** (Fig. 12) with $IC_{50,dark}$ = 2.2 μM and $IC_{50,blue\ light}$ = 6.9 nM in A549 cells (PI = 323). An analogue

of **58** with *N*-(ethylpiperidyl)imidazole (Imepip; **121** in Fig. 42) instead of the chlorido ligand exhibited PI values of 1317 (2D culture of A549 cells) and 240 in the advanced model of 3D spheroids. **121** was highly selective towards cancer cells, even when irradiated, and showed no haemolytic activity against red blood cells (RBCs). Relevant differences were also discussed for other processes (ROS production, NADH oxidation, mitochondria disruption) studied under dark and light conditions.

An extensive series of Ir–Cp* chlorido complexes involving various 2,2′-(phenylmethanediyl)bis(1*H*-pyrrole) derivatives as chelating N-donor ligands showed, in some cases, higher antiproliferative activity upon white light irradiation than in the dark.[294] Complex **32** induced the formation of $^1O_2$ when irradiated by visible light (400–700 nm).[114] Its antiproliferative activity in HeLa and MCF-7 cells was higher after irradiation with yellow light than in the dark (PI = 2.2 and 2.4, respectively).

### 6.4. Other aspects

**6.4.1. Hypoxia.** Complex **39** (Fig. 9) was studied at three different $O_2$ concentrations.[148] In contrast to some co-studied Ru complexes, the potency of **39** decreased with a decrease of $O_2$ concentration ($IC_{50}$ = 5.1 μM for 21% $O_2$ and 20.0 μM for 0.1% $O_2$), implying only low potential for the treatment of hypoxic tumours. Ir complex **23** (Fig. 7) was comparably potent in MDA-MB-231 cells under normoxia and hypoxia conditions, but its activity in T47D cells was lower under hypoxia conditions compared to that under a normal oxygen concentration.[89] Similar results, indicating comparable anticancer potency under both $O_2$ concentrations used, were also reported elsewhere for other Ir complexes studied in HeLa and CaCo-2 cells.[95] Interestingly, the Ir complexes (*e.g.*, **132**; Fig. 54) were effective under hypoxia conditions even when 1 mM GSH was co-administered to the treated cancer cells, and showed high antiproliferative activity in HCT-116 cancer stem cells (CSCs).

Phototoxic complex **27** was highly effective under normoxia (see above) and hypoxia conditions, where its light $IC_{50}$ values equalled 5.2 μM (PI = 11.2), indicating that $^1O_2$ production played only a partial role in the MoA.[96] This proved to be connected to other ROS (superoxide and hydroxyl radical) detected in additional experiments with species-specific ROS probes.

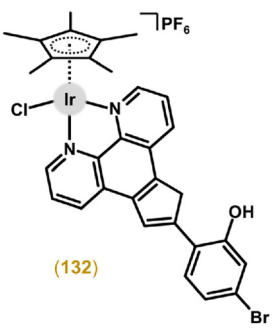

(132)

Fig. 54 The structural formula of complex **132**.

**6.4.2. Antimetastatic activity.** Antimetastatic activity studies are used to investigate the ability of new compounds to prevent the formation of metastasis. The representative complex **76** (Fig. 16) showed promising antimetastatic activity *in vitro* (wound healing and transwell migration assays, and colony and spheroid formation – studied in A549 cells),[200] as also reported for some other complexes.[63,105,113,151,159–161,189,232,239–241,256]

**6.4.3. Angiogenesis.** Angiogenesis is the process by which new blood vessels are formed from old ones. Regarding its connection to cancer, it plays a key role in cancer progression, as tumours need a high and constant supply of oxygen and nutrients (tumour angiogenesis). Tumour angiogenesis is essential for growth and metastasizing to distant organs.

Complex **133** (see section 7.3 for the structural formula), which is the phenyl-substituted derivative of **48**, was studied *in vitro* for its ability to inhibit tube formation in EA.hy926 normal endothelial cells (studied on matrigel matrix from Engelbreth–Holm–Swarm (EHS) mouse sarcoma cells).[167] **133** exhibited higher antiangiogenic activity than cisplatin, but it was less antiangiogenic than the co-studied Ru analogues, based on three evaluated parameters – total vessel length, number of meshes, and total mesh area.

As an *in vitro* model experiment, Liu and co-workers studied the level of matrix metalloproteinase 9 (MMP-9) in A549 cells by flow cytometry, because MMPs are known to be related to angiogenesis and tumour invasion in general.[159]

Treatment of zebrafish embryos with **22** strongly inhibited their subintestinal venous plexus (SIVP) (studied by confocal microscopy), which indicated a high and dose-dependent antiangiogenic effect.[88] Importantly, an effective antiangiogenic dose of **22** did not induce lethality and morphological changes in the treated embryos. The antiangiogenic effect of **22** is related to its inhibitory activity towards VEGFA and BMP signalling, which are found to be downregulated in zebrafish embryos (VEGFA is a key proangiogenic factor in neovascularization, BMPs promote angiogenesis by inducing cell proliferation and migration).

**6.4.4. Immunotherapy.** Anticancer immunotherapy involves various related phenomena such as programmed death-ligand 1 (PD-L1). This is a protein on the surface of cancer cells that helps them evade the immune system. Upregulation of PD-L1 expression is involved in chemotherapy resistance. Higher PD-L1 expression was detected for cisplatin-treated A549 cancer cells than for **76** (Fig. 16) after 48 h as well as after 7 days.[200] This observation suggests that **76** has a lower ability to induce immunosuppression and resistance to chemotherapy than cisplatin. Interestingly, the treatment of A549 cells with a combination of **76** and cisplatin resulted in a slight decrease in PD-L1 expression.

**6.4.5. Chemosensitizers.** It was reported for some inactive Ir–Cp$^x$ complexes that they acted as selective chemosensitizers for cancer cells treated with other drugs. For example, the $IC_{50}$ values of carboplatin decreased by 30–50% after pre-treatment with [Ir($\eta^5$-Cp*)(bpy)Cl]Cl.[143] In cancer cells, the application of non-toxic concentrations of Ir complexes led to an increase of

the ROS populations and $NAD^+$/NADH ratios. Importantly, chemosensitizing effects were not observed in non-cancerous cells. The highly cytotoxic complex **76** was tested in combination with cisplatin in A549 cells, but only mild synergistic cytotoxicity was observed with a combination index of 0.88.[200]

**6.4.6. Theranostics.** The pharmacological concept of theranostics is a rapidly developing field that is based on molecular imaging and therapy using a single substance (or technique). The first Ir–$Cp^x$ complexes, which were discussed as theranostic agents, involve monodentate-coordinate isomeric 3- or 4-pyridyl-BODIPY ligands (*e.g.*, **104**; Fig. 27).[163] As mentioned above (section 3.4), **104** outperformed its chlorido analogue in various cancer cell lines. While the photostable complex retained high activity, the presence of BODIPY, which is a fluorescence imaging reporter, enabled observation of the dynamics of cellular take up, accumulation and distribution of the metallodrug (**104**) directly in living cancer cells, where the complexes showed extremely fast accumulation ($t$ < 90 s).

As mentioned above, some Ir–$Cp^x$ anticancer complexes are fluorescent or luminescent by themselves (*i.e.*, without a fluorophore); this has been exploited, *e.g.*, for intracellular localization of such complexes, and in principle these compounds can be viewed as theranostics.[63,85,93,159,163,170,192,198,272]

**6.4.7. Drug delivery.** The Ir-phen complex [Ir($\eta^5$-$Cp^{bph}$)Cl(phen)]Cl and its Ir-dppn (**134**) and Ru-dppn analogues were used for the preparation of polymeric micelles through coordination between the dechlorinated aqua species and poly(ethylene glycol)-*b*-poly(glutamic acid) (Fig. 55).[261] The formation of micelles led to higher cellular accumulation of complexes, higher antiproliferative activity and DNA metalation. Micelles involving the Ir-dppn species were readily accumulated and retained in tumours in A2780Cis subcutaneous xenografts (5 mg $kg^{-1}$ dose administered by intravenous injection). Importantly, micelles loaded with Ir-dppn species displayed higher anticancer activity (tumour volume was reduced by 70.2%) than the complex itself (tumour volume was reduced by 56.9%), thus showing great promise for future studies.

Complex **22**, which was highly effective *in vitro* and *in vivo*, was encapsulated in liposomes (*ca.* 80 nm) formed from FDA-approved DSPE-PEG2000-biotin.[88] Loaded liposomes had higher antiproliferative activity *in vitro* in HeLa cells ($IC_{50}$ = 16 nM) than **22** itself ($IC_{50}$ = 150 nM). Encouragingly, the loaded liposomes also showed higher anticancer activity *in vivo* (TGI = 85%) even though they were applied at lower doses (0.2 mg Ir per kg) than **22**. Despite the lower doses, **22**-loaded liposomes induced a gradual loss of body weight of treated mice and signs of systemic toxicity and poor biocompatibility. This is associated with markedly higher accumulation of **22** in important organs when loaded into liposomes – for example, 145-fold higher Ir accumulation in the brain was found for **22**-loaded liposomes compared to **22** itself.

Encapsulation of dichlorido complex **11** (Fig. 4) into Pluronic P-123 micelles was reported to be beneficial for the resulting antiproliferative activity, which was several times higher ($IC_{50}$ = 4.1 μM in DU-145 cells) than that for the free complex in the same cells ($IC_{50}$ = 11.8 μM).[57] The same research group loaded heterometallic Ir–Cu complex **99** (Fig. 25) into cholesterol/phosphatidylcholine liposomes of >100 nm in size.[246] These loaded liposomes, however, were less effective in cancer cells than **99** itself.

Complex **47** was readily loaded into amphiphilic hyaluronan-based delivery formulations, which were pH- and reduction-responsive (dissociation in the presence of 20 mM GSH).[295] The **47**-loaded formulations were even more potent *in vitro* than free **47** in A549 cells. *In vivo*, micelles efficiently accumulated in the tumour, where they enhanced tumour inhibition without body weight loss in A549 tumour-bearing female Balb/c nude mice, indicating negligible systemic toxicity of the hyaluronan-based formulations used.

Another delivery system developed for anticancer Ir–$Cp^x$ compounds was based on biocompatible anisotropic polymeric materials, which are known for their long circulation times under physiological conditions.[296] Specifically, poly(2-hydroxypropyl-methacrylamide)-based polymer was loaded with [Ir($\eta^5$-$Cp^{ph}$)Cl(ppy)] (**135**), a $Cp^{ph}$ analogue of **43**, and such formulations (Fig. 56) exhibited higher potency in human cancer cells than the free Ir complex, although the intracellular Ir level was more or less comparable for cells treated with the formulations and the complex.

**6.4.8. 3D cancer cell spheroids.** In the context of *in vivo* studies of the anticancer activity of Ir–$Cp^x$ complexes (section 5.9), experiments performed on 3D cancer cell spheroids should also be mentioned. In contrast to two-dimensional (2D) cell cultures, which are usually used for *in vitro* studies, spheroids are three-dimensional (3D) cell cultures that mimic some aspects (*e.g.*, cell–cell interaction, hypoxia, drug penetration or effects of extracellular matrix) of real tissues or tumours (in the case of cancer cell spheroids). Spheroids thus represent a valuable *in vitro* tool for basic insights into *in vivo* anticancer activity.

The [Ir($\eta^5$-$Cp^{ph}$)Cl(paza)]$PF_6$ complex, containing *N*1-pyridin-2-yl-7-azaindole (paza) as a chelating N,N-donor ligand (**136**; Fig. 57), exhibited *ca.* 1.5-fold higher anticancer potency in MCF-7 spheroids than cisplatin; this correlated with the results obtained on 2D cultures of MCF-7 cells.[181] Importantly, the potency of this complex was only slightly lower in 3D ($IC_{50}$

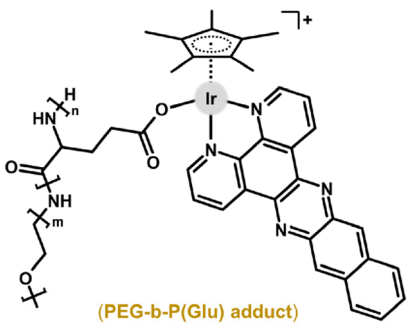


Fig. 55 The structural formula of the adduct of **134** with poly(ethylene glycol)-*b*-poly(glutamic acid).

 

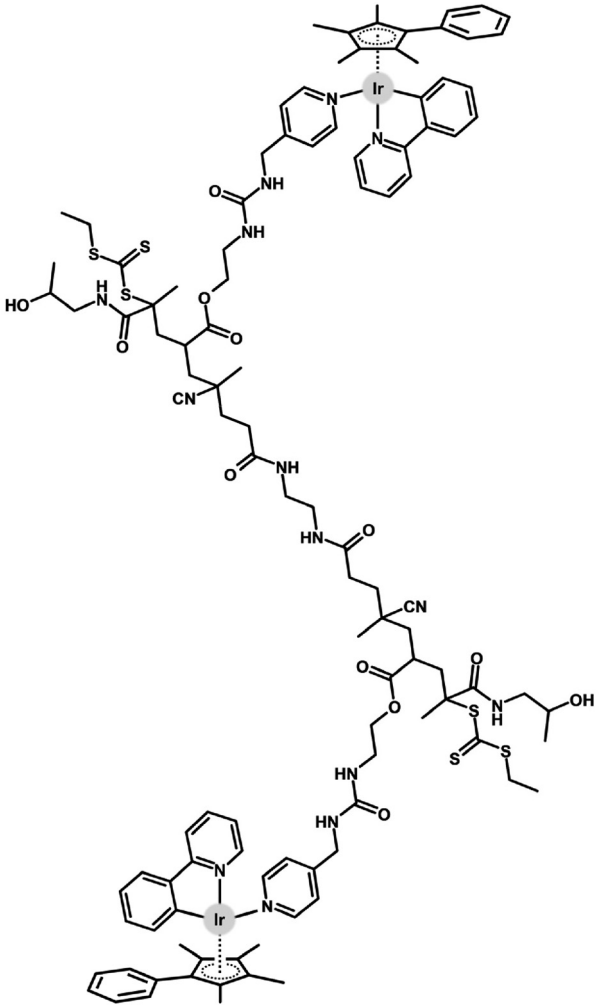

Fig. 56 A conjugate of complex **135** with poly(2-hydroxypropyl-methacrylamide)-based polymer.

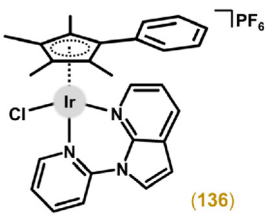


Fig. 57 The structural formula of complex **136**.

= 22.9 μM) than in 2D ($IC_{50}$ = 6.9 μM) cultures, which was not the case for other Ir complexes, such as **71**, which was markedly less effective in A549 and CH1/PA-1 spheroids ($IC_{50}$ = 136 and 114 μM, respectively) than in 2D cultures ($IC_{50}$ = 1.1 and 0.6 μM, respectively).[194] The authors also reported that benzyl-substituted complex **71** was distributed differently (metabolising cells on the surface of the spheroid) than its methyl analogue (necrotic cells in the spheroid core), based on laser ablation-ICP-MS studies.

Complex **26** (Fig. 7) was less effective against 3D spheroids of SCC070 cells, representing a stemness pathway-activated oral squamous cell carcinoma (OSCC), than co-studied Ru complexes.[92] The lower activity of **26** than that observed for the best-performing Ru compounds is discussed as being connected to the lower potency for inhibiting stemness gene expression (miRNA studies).

Dichlorido complexes with various monodentate diphenylphospane derivatives (*e.g.*, **11**; Fig. 4), as well as heterometallic analogue **98**, were effective in 3D spheroids of A549 and DU-145 cancer cells ($IC_{50}$ not specified).[57,60,246]

# 7. Other types of biological activity

Besides widely studied anticancer Ir(III) cyclopentadienyl complexes, fewer studies have been dealing with the antimicrobial activity of such compounds, and only a few investigations have been dedicated to research on different types of biological activity (antioxidant activity, treatment of Alzheimer's disease) exhibited by Ir–$Cp^x$ complexes.

## 7.1. Antimicrobial activity

Many microbial (bacterial, fungal) infections are connected with problems of resistance towards the drugs used (*e.g.*, bacteria against antibiotics). Microbial resistance to conventional and many newly developed drugs has raised considerable interest in research on new classes of antimicrobial agents. The application of transition metal complexes derived from various d-block elements seems to be a reasonable research and development strategy.[297–299] In contrast to organic antimicrobial compounds, metal complexes offer a variety of structural types thanks to various oxidation states and coordination numbers of the studied complexes.

The first report on the antimicrobial activity of Ir–$Cp^x$ complexes dates back to 2010, but the [Ir($\eta^5$-Cp*)Cl(qui)] (**34**; Fig. 9) complex was insufficiently active against Gram positive (+ve) strains, *Staphylococcus aureus*, *Micrococcus luteus*, *Enterococcus faecalis* and *Staphylococcus epidermidis*, and even inactive against Gram negative (–ve) strains, *Escherichia coli*, *Klebsiella pneumoniae* and *Pseudomonas aeruginosa*.[144]

Later, most of the structural types of Ir–$Cp^x$ complexes that were discussed in Section 3 for anticancer activity were also investigated for antimicrobial activity. Specifically, mononuclear dichlorido complexes (**137**),[300] mononuclear chlorido complexes with bidentate N,N- (**138**),[301] N,O- (**34**),[144] N,S- (**139**),[302] C,N- (**140**)[303] or O,O- (**141**)[304] donor chelating ligands, and homometallic (**142**)[305] and heterometallic (**143**)[236] multinuclear complexes were tested for their antimicrobial activity (Fig. 58).

Similar to the anticancer Ir–$Cp^x$ complexes, in some cases, their antimicrobial analogues have been described with a basic description of their MoA and a discussion of the SAR. For example, various processes known to be related to the MoA of biologically (anticancer and antimicrobial) active Ir–$Cp^x$ complexes have been studied. Examples include stability studies and hydrolysis,[131,306] DNA interaction and

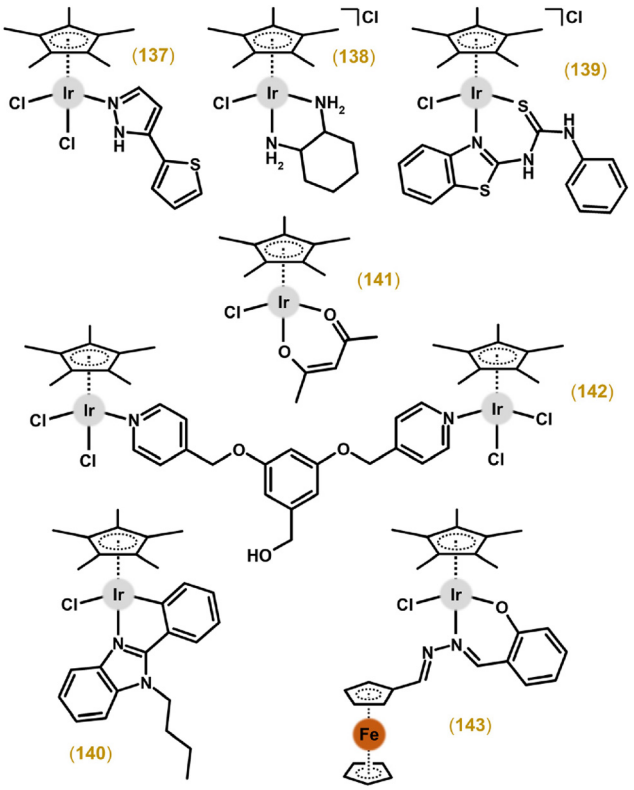


Fig. 58 Structural formulas of complexes **137–143** studied for their antimicrobial activity.

cleavage,[128,129,252,300] or NAD(H) transfer hydrogenations.[285,286] Regarding SARs, the influence of the cyclopentadienyl ring (Cp*, $Cp^{ph}$, $Cp^{bph}$),[131,301,306] the monodentate ligand (chlorido *vs.* bromido and iodido),[306] the central atom (Ir *vs.* Ru, Rh, Os or other d-block metals)[301,307] and the donor set effect[286,308,309] has been studied in the context of antimicrobial Ir–$Cp^x$ complexes. In some works, the authors also paid appropriate attention to safety and toxicity, usually studied as the potency towards normal (healthy) cells,[83,131,286,306,310] or by using advanced models.[128,129,301,306,311,312] A detailed overview and relevant discussion of this field are beyond the scope of this text.

### 7.2. Antioxidant activity

Antioxidant activity refers to the ability of a compound to neutralize free radicals by the transfer of electrons. In the body (cells), antioxidants help to protect cells from oxidative stress, which is known to be associated with various diseases, including cancer or neurodegenerative disorders.

The $[Ir(\eta^5\text{-}Cp^*)Cl_2(pct^1)]$ (**144**; Fig. 59) complex, which involves monodentate S-donor *O*-methyl phenylcarbamothioate ($pct^1$) and has higher antimicrobial activity than the reference drug kanamycin, was also studied for its antioxidant activity by the DPPH free radical scavenging method (DPPH = 1,1-diphenyl-2-picryl-hydrazyl).[313] Its DPPH radical scavenging activity (DRSA) was 90% (tested at 1 mg $mL^{-1}$ concentration),

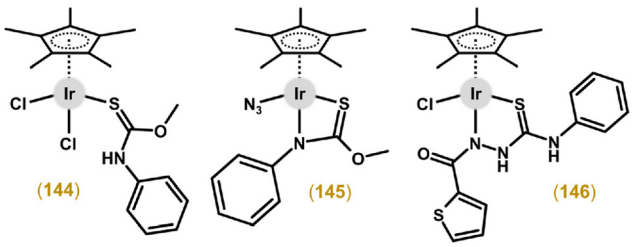


Fig. 59 Structural formulas of complexes **144–146** studied for their antioxidant activity.

which was comparable with the reference compound used (ASA). Similar antioxidant potency (92%) was reached by the electroneutral azido $[Ir(\eta^5\text{-}Cp^*)(pct^1)(N_3)]$ (**145**; Fig. 59) complex with a bidentate N,S-coordinated $pct^1$ ligand. Also of interest, within both series of these dichlorido and azido complexes, the extent of antioxidant activity followed the order of Ir ≫ Ru > Rh.

The same order of antioxidant activity was observed for Ir, Rh and Ru chlorido complexes containing a coumarin-*N*-acylhydrazone hybrid ligand.[314] A similar Ir–Cp* complex containing 3-methoxy-benzhydrazide showed the highest DPPH-scavenging ability, which was almost of the same level as that for the positive control (ASA) and higher than those of the Ru and Rh analogues and the co-studied Ir complex containing a different chelating N,O-ligand (*i.e.*, 4-hydroxy-benzhydrazide).[315]

The next study by the same research group reported on a similar series of dichlorido and diazido complexes and showed that the dichlorido complexes were inactive in the antioxidant activity screening, while diazido complexes showed some DPPH scavenging activity.[316] Remarkably, the Ir diazido complex containing a benzothiazole-based ligand was markedly less effective than its Rh analogue, but in the case of Ir and Rh complexes with a benzimidazole-based ligand, their antioxidant effect was comparable.

Within extensive series of Ru, Rh and Ir complexes with various thiourea-based N,S-donor ligands, it was the Ir complexes (*e.g.*, **146** in Fig. 59) that outperformed their analogues, since they showed remarkable antioxidant activity almost as high as the positive control (ASA).[317] Similar results were reported for complexes involving 3-acetyl-coumarin-substituted TSC.[318] Within dinuclear Ir and Rh complexes containing a salicylaldehyde based TSC bridging ligand, Rh complexes exhibited slightly higher antioxidant activity.[319]

In some cases, the antioxidant activity was negligible, as reported for a series of antimicrobial active Ir complexes with various monodentate N-donor pyridine-4-carbothioamides[320] or other ligands.[141,321]

### 7.3. Alzheimer's disease

Alzheimer's disease (AD) is an incurable neurodegenerative brain disorder and one of the most common causes of dementia. The lack of effective drugs motivates medicinal chemists to develop and investigate potential drugs for the treatment of

 

AD. Among them, various types of transition metal complexes have been reported.[322] It is known that the aggregation of amyloid-β (Aβ) peptides is directly connected to AD pathogenesis, which is why Aβ aggregates represent an important target for newly developed AD drugs.

Regarding Ir cyclopentadienyl complexes, probably the only report on these complexes and their inhibition of Aβ aggregation was published by Barnham, Ruiz and co-workers in 2015.[323] In this study, the $[Ir(\eta^5\text{-}Cp^*)(bzim^1)Cl]PF_6$ (**48**; Fig. 60) complex was studied together with the Ru analogue, $[Ru(\eta^6\text{-}pcym)(bzim^1)Cl]PF_6$, and Pt complex, $[Pt(bzim^1)Cl_2]$. Although all three complexes inhibited Aβ aggregation effectively, it was only the Ir complex **48** that protected the primary cortical neurons from the neurotoxic effects of Aβ. Earlier, **48** was also reported to be highly effective against various cancer cells (section 3.2.3).[166]

### 7.4. Platelets

Platelets (thrombocytes) are small fragments of cells in the blood that play a critical role in preventing bleeding by forming clots. They also play a role in arterial thrombosis and cancer metastasis. The $[Ir(\eta^5\text{-}Cp^*)Cl(pip)]BF_4$ (**147**; Fig. 61) complex, derived from 1-(pyridin-2-yl)imidazo[1,5-*a*]pyridine derivative (pip), was studied as a potential antiplatelet drug.[324] **147** efficiently inhibited the collagen-stimulated aggregation of the patient-derived platelets, even in the presence of known inhibitors of this process. The complex also interfered with other associated processes, such as ATP release, intracellular $Ca^{2+}$ mobilization or the phosphorylation of various regulatory proteins (*e.g.*, Akt, p38, MAPK or JNK1). **147** influenced the bleeding time in the tail transection model of mice. Specifically, the bleeding time was prolonged to 323 s (2 mg $kg^{-1}$ dose of **147**; no rebleeding observed) from 151 s observed for the control group. The observed results are promising in terms of possible prevention or treatment of thromboembolic disorders or disruption of tumorigenic or pro-metastatic interactions between platelets and tumour cells.

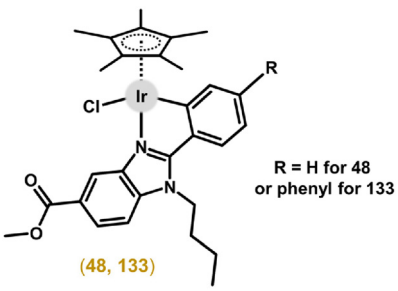


**Fig. 60** Structural formulas of complexes **48** and **133**.

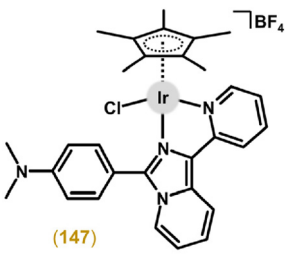


**Fig. 61** The structural formula of complex **147**.

## 8. Conclusion

This work provides the reader with an overview of the current knowledge on anticancer iridium(III) cyclopentadienyl (Ir–$Cp^x$) complexes. Although the structure of Ir–$Cp^x$ complexes is rather strict (*i.e.*, a $Cp^x$ ligand and three additional positions), various synthetic approaches can be used to modify their (bio) chemical and biological properties, including reactivity and anticancer activity. Over the years, various structural types of Ir–$Cp^x$ complexes have been developed and studied for their anticancer activity, which are categorized in the text according to their nuclearity, number of coordinated ligands, and type of donor atom, allowing for a detailed discussion of the SARs. In this regard, the development of Ir–$Cp^x$ complexes involving an extended cyclopentadienyl ligand (*e.g.*, $Cp^{bph}$), a C,N-donor chelating ligand, and a kinetically stable monodentate ligand (*e.g.*, pyridine or its derivatives) appears to be a suitable strategy for the development of novel bioactive Ir–$Cp^x$ complexes. The MoA of anticancer Ir–$Cp^x$ complexes, although still not fully understood, differs not only from that of Pt drugs but also from those of the structurally similar half-sandwich Ru(II), Rh(III) and Os(II) analogues; this highlights their potential for novel therapeutic approaches. Importantly, several representatives have also been shown to be highly active *in vivo*, either alone or advantageously as a cargo in various drug delivery systems. The reviewed results and findings clearly indicate that the research and development of novel Ir–$Cp^x$ complexes is a viable strategy in the field of bioinorganic, bioorganometallic and medicinal chemistry, as many of the reviewed Ir–$Cp^x$ complexes meet the basic criteria for new alternatives to conventional anticancer platinum-based drugs.

## Data availability

No primary research results, software or code have been included and no new data were generated or analysed as part of this review.

## Conflicts of interest

There are no conflicts to declare.

## Acknowledgements

This work was supported by the Czech Health Research Council of the Ministry of Health of the Czech Republic (AZV Project NU22-08-00236).

## References


1 C. Housecroft and A. Sharpe, *Inorganic Chemistry*, 4th edn, Pearson, London, Great Britain, 2012.

2 G. J. Sunley and D. J. Watson, High productivity methanol carbonylation catalysis using iridium – The Cativa process for the manufacture of acetic acid, *Catal. Today*, 2000, **58**, 293–307, DOI: 10.1016/S0920-5861(00)00263-7.

3 J.-Y. Cho, M. K. Tse, D. Holmes and R. E. Maleczka Jr., and M. R. Smith III, Remarkably selective iridium catalysts for the elaboration of aromatic C-H bonds, *Science*, 2002, **295**, 305–308, DOI: 10.1126/science.1067074.

4 K. Murata, T. Ikariya and R. Noyori, New chiral rhodium and iridium complexes with chiral diamine ligands for asymmetric transfer hydrogenation of aromatic ketones, *J. Org. Chem.*, 1999, **64**, 2186–2187, DOI: 10.1021/jo990213a.

5 J. F. Hull, D. Balcells, J. D. Blakemore, C. D. Incarvito, O. Eisenstein, G. W. Brudvig and R. H. Crabtree, Highly active and robust Cp* iridium complexes for catalytic water oxidation, *J. Am. Chem. Soc.*, 2009, **131**, 8730–8731, DOI: 10.1021/ja901270f.

6 B. Rosenberg, L. Van Camp and T. Krigas, Inhibition of cell division in *Escherichia coli* by electrolysis products from a platinum electrode, *Nature*, 1965, **205**, 698–699, DOI: 10.1038/205698a0.

7 L. Kelland, The resurgence of platinum-based cancer chemotherapy, *Nat. Rev. Cancer*, 2007, **7**, 573–584, DOI: 10.1038/nrc2167.

8 *Metallo-Drugs: Development and Action of Anticancer Agents. Metal Ions in Life Sciences Book 18*, ed. A. Sigel, H. Sigel, E. Freisinger and R. K. O. Sigel, De Gruyter, 1nd edn, 2018.

9 S. M. Meier-Menches, C. Gerner, W. Berger, C. G. Hartinger and B. K. Keppler, Structureactivity relationships for ruthenium and osmium anticancer agents - towards clinical development, *Chem. Soc. Rev.*, 2018, **47**, 909–928, DOI: 10.1039/C7CS00332C.

10 M. R. Berger, F. T. Garzon, B. K. Keppler and D. Schmahl, Efficacy of new ruthenium complexes against chemically induced autochthonous colorectal carcinoma in rats, *Anticancer Res.*, 1989, **9**, 761–765. PMID: 2764521.

11 G. Sava, S. Pacor, G. Mestroni and E. Alessio, Effects of the Ru(III) complexes [*mer*-$RuCl_3(DMSO)_2Im$] and Na[*trans*-$RuCl_4(DMSO)Im$] on solid mouse tumors, *Anti-Cancer Drugs*, 1992, **3**, 25–31, DOI: 10.1097/00001813-199202000-00005.

12 S. Monro, K. L. Colón, H. Yin, J. Roque III, P. Konda, S. Gujar, R. P. Thummel, L. Lilge, C. G. Cameron and S. A. McFarland, Transition metal complexes and photodynamic therapy from a tumor-centered approach: Challenges, opportunities, and highlights from the development of TLD1433, *Chem. Rev.*, 2019, **119**, 797–828, DOI: 10.1021/acs.chemrev.8b00211.

13 D. G. Craciunescu, Molecular interactions between the complex anions of transition metals and nitrogenous organic bases of biological importance, *An. R. Acad. Farm.*, 1977, **43**, 265–292. Link.

14 T. Giraldi, G. Sava, G. Mestroni, G. Zassinovich and D. Stolfa, Antitumour action of rhodium(I) and iridium(I) complexes, *Chem.-Biol. Interact.*, 1978, **22**, 231–238, DOI: 10.1016/0009-2797(78)90128-X.

15 G. R. Gale, E. M. Walker Jr., A. B. Smith and A. E. Stone, Antitumor and antimitogenic properties of the photochemical reaction product of ammonium hexachloroiridate (IV), *Proc. Soc. Exp. Biol. Med.*, 1971, **136**, 1197–1202, DOI: 10.3181/00379727-136-35457.

16 C. H. Leung, H. J. Zhong, D. S. H. Chan and D. L. Ma, Bioactive iridium and rhodium complexes as therapeutic agents, *Coord. Chem. Rev.*, 2013, **257**, 1764–1776, DOI: 10.1016/j.ccr.2013.01.034.

17 K. Máliková, L. Masaryk and P. Štarha, Anticancer half-sandwich rhodium(III) complexes, *Inorganics*, 2021, **9**, 26, DOI: 10.3390/inorganics9040026.

18 E. J. Anthony, E. M. Bolitho, H. E. Bridgewater, O. W. L. Carter, J. M. Donnelly, C. Imberti, E. C. Lant, F. Lermyte, R. J. Needham, M. Palau, P. J. Sadler, H. Shi, F.-X. Wang, W.-Y. Zhang and Z. Zhang, *Chem. Sci.*, 2020, **11**, 12888–12917, DOI: 10.1039/D0SC04082G.

19 G. Sava, S. Zorzet, L. Perissin, G. Mestroni, G. Zassinovich and A. Bontempi, Coordination metal complexes of Rh(I), Ir(I) and Ru(II): Recent advances on antimetastatic activity on solid mouse tumors, *Inorg. Chim. Acta*, 1987, **137**, 69–71, DOI: 10.1016/S0020-1693(00)87119-4.

20 M. A. Scharwitz, I. Ott, R. Gust, A. Kromm and W. S. Sheldrick, Synthesis, cellular uptake and structure-activity relationships for potent cytotoxic trichloridoiridium(III) polypyridyl complexes, *J. Inorg. Biochem.*, 2008, **102**, 1623–1630, DOI: 10.1016/j.jinorgbio.2008.03.001.

21 C.-H. Leung, H.-J. Zhong, H. Yang, Z. Cheng, D. S.-H. Chan, V. P.-Y. Ma, R. Abagyan, C.-Y. Wong and D.-L. Ma, A metal-based inhibitor of tumor necrosis factor-α, *Angew. Chem., Int. Ed.*, 2012, **51**, 9010–9014, DOI: 10.1002/anie.201202937.

22 S. Schafer, I. Ott, R. Gust and W. S. Sheldrick, Influence of the polypyridyl (pp) ligand size on the DNA binding properties, cytotoxicity and cellular uptake of organoruthenium(II) complexes of the type $[(\eta^6\text{-}C_6Me_6)Ru(L)(pp)]^{n+}$ [L = Cl, n = 1; L = $(NH_2)_2CS$, n = 2], *Eur. J. Inorg. Chem.*, 2007, 3034–3046, DOI: 10.1002/ejic.200700206.

23 A. Kastl, A. Wilbuer, A. L. Merkel, L. Feng, P. Di Fazio, M. Ocker and E. Meggers, Dual anticancer activity in a single compound: visible light-induced apoptosis by an antiangiogenic iridium complex, *Chem. Commun.*, 2012, **48**, 1863–1865, DOI: 10.1039/C1CC15378A.

24 J.-P. Tranchier, J. Dubarle-Offner, L. Peyroux, G. Gontard, T. Riedel, P. J. Dyson and H. Amouri, Iridium-stabilized p-selenocyclohexadienyls: Synthesis, molecular structure, and cytotoxicity, *Synlett*, 2015, 1563–1566, DOI: 10.1055/s-0034-1378838.

25 S. L. Croft, R. A. Neal, D. G. Craciunescu and G. Certad-Fombona, The activity of platinum, iridium and rhodium


 

drug complexes against *Leishmania donovani*, *Trop. Med. Parasitol.*, 1991, **42**, 48–51. PMID: 1598504.

26 P. Štarha and Z. Trávníček, Non-platinum complexes containing releasable biologically active ligands, *Coord. Chem. Rev.*, 2019, **395**, 130–145, DOI: **10.1016/j.ccr.2019.06.001**.

27 Y. Geldmacher, M. Oleszak and W. S. Sheldrick, Rhodium(III) and iridium(III) complexes as anticancer agents, *Inorg. Chim. Acta*, 2012, **393**, 84–102, DOI: **10.1016/j.ica.2012.06.046**.

28 Z. Liu and P. J. Sadler, Organoiridium complexes: Anticancer agents and catalysts, *Acc. Chem. Res.*, 2014, **47**, 1174–1185, DOI: **10.1021/ar400266c**.

29 D. L. Ma, C. Wu, K. J. Wu and C. H. Leung, Iridium(III) complexes targeting apoptotic cell death in cancer cells, *Molecules*, 2019, **24**, 2739, DOI: **10.3390/molecules24152739**.

30 R. M. Lord and P. C. McGowan, Organometallic iridium arene compounds: the effects of C-donor ligands on anticancer activity, *Chem. Lett.*, 2019, **48**, 916–924, DOI: **10.1246/cl.190179**.

31 P. Štarha, Multinuclear biologically active Ru, Rh, Os and Ir arene complexes, *Coord. Chem. Rev.*, 2021, **431**, 213690, DOI: **10.1016/j.ccr.2020.213690**.

32 M. Scharwitz, T. van Almsick and W. S. Sheldrick, Chloro(ethylenediamine-$\kappa^2$N)($\eta^5$-pentamethylcyclopentadienyl)iridium(III) trifluoromethanesulfonate, *Acta Crystallogr., Sect. E:Struct. Rep. Online*, 2007, **63**, m1469–m1470, DOI: **10.1107/S1600536807019575**.

33 R. Ziessel, Efficient homogeneous photochemical water gas shift reaction catalyzed under extremely mild conditions by novel iridium(III) complexes: [($\eta^5$-$Me_5C_5$)Ir(bpy)Cl]$^+$, [($\eta^5$-$Me_5C_5$)Ir(bpy)H]$^+$, and [($\eta^5$-$Me_5C_5$)Ir(phen)Cl]$^+$ (bpy = 2,2′-bipyridine; phen = 1,10-phenanthroline), *J. Chem. Soc., Chem. Commun.*, 1988, 16–17, DOI: **10.1039/C39880000016**.

34 D. Herebian and W. S. Sheldrick, Synthesis and DNA binding properties of bioorganometallic ($\eta^5$-pentamethylcyclopentadienyl)iridium(III) complexes of the type [($\eta^5$-$C_5Me_5$)Ir(Aa)(dppz)]$^{n+}$ (dppz = dipyrido[3,2-a:2′,3′-c]phenazine, n = 1–3), with S-coordinated amino acids (Aa) or peptides, *J. Chem. Soc., Dalton Trans.*, 2002, 966–974, DOI: **10.1039/B107656F**.

35 P. Annen, S. Schildberg and W. S. Sheldrick, ($\eta^5$-Pentamethylcyclopentadienyl)iridium(III) complexes of purine nucleobases and nucleotides: a comparison with ($\eta^6$-arene)ruthenium(II) and ($\eta^5$-pentamethylcyclopentadienyl)rhodium(III) species, *Inorg. Chim. Acta*, 2000, **307**, 115–124, DOI: **10.1016/S0020-1693(00)00212-7**.

36 S. Schafer and W. S. Sheldrick, Coligand tuning of the DNA binding properties of half-sandwich organometallic intercalators: Influence of polypyridyl (pp) and monodentate ligands (L = Cl, $(NH_2)_2CS$, $(NMe_2)_2CS$) on the intercalation of ($\eta^5$-pentamethylcyclopentadienyl)-iridium(III)-dipyridoquinoxaline and -dipyridophenazine complexes, *J. Organomet. Chem.*, 2007, **692**, 1300–1309, DOI: **10.1016/j.jorganchem.2006.10.033**.

37 J. W. Kang, K. Moseley and P. M. Maitlis, Pentamethylcyclopentadienylrhodium and -iridium halides. I. Synthesis and properties, *J. Am. Chem. Soc.*, 1969, **91**, 5970–5977, DOI: **10.1021/ja01050a008**.

38 C. White, A. Yates and P. M. Maitlis, ($\eta^5$-Pentamethylcyclopentadienyl)rhodium and -iridium compounds, *Inorg. Synth.*, 1992, **29**, 228–234, DOI: **10.1002/9780470132609.ch53**.

39 J. Tönnemann, J. Risse, Z. Grote, R. Scopelliti and K. Severin, Efficient and rapid synthesis of chlorido–bridged half–sandwich complexes of ruthenium, rhodium, and iridium by microwave heating, *Eur. J. Inorg. Chem.*, 2013, 4558–4562, DOI: **10.1002/ejic.201300600**.

40 D. M. Morris, M. McGeagh, D. De Peña and J. S. Merol, Extending the range of pentasubstituted cyclopentadienyl compounds: The synthesis of a series of tetramethyl(alkyl or aryl)cyclopentadienes (Cp*$R$), their iridium complexes and their catalytic activity for asymmetric transfer hydrogenation, *Polyhedron*, 2014, **84**, 120–135, DOI: **10.1016/j.poly.2014.06.053**.

41 Z. Liu, A. Habtemariam, A. M. Pizarro, S. A. Fletcher, A. Kisova, O. Vrana, L. Salassa, P. C. A. Bruijnincx, G. J. Clarkson, V. Brabec and P. J. Sadler, Organometallic half-sandwich iridium anticancer complexes, *J. Med. Chem.*, 2011, **54**, 3011–3026, DOI: **10.1021/jm2000932**.

42 L. C. Brown, E. Ressegue and J. S. Merola, Rapid access to derivatized, dimeric, ring-substituted dichloro(cyclopentadienyl)rhodium(III) and iridium(III) complexes, *Organometallics*, 2016, **35**, 4014–4022, DOI: **10.1021/acs.organomet.6b00580**.

43 P. Štarha, Z. Dvorak and Z. Travnicek, Half-sandwich Ir(III) and Rh(III) 2,2′-dipyridylamine complexes: Synthesis, characterization and *in vitro* cytotoxicity against the ovarian carcinoma cells, *J. Organomet. Chem.*, 2018, **872**, 114–122, DOI: **10.1016/j.jorganchem.2018.07.035**.

44 Z. Liu, I. Romero-Canelon, B. Qamar, J. M. Hearn, A. Habtemariam, N. P. E. Barry, A. M. Pizarro, G. J. Clarkson and P. J. Sadler, The potent oxidant anticancer activity of organoiridium catalysts, *Angew. Chem., Int. Ed.*, 2014, **53**, 3941–3946, DOI: **10.1002/anie.201311161**.

45 R. Pettinari, F. Marchetti, C. Pettinari, F. Condello, A. Petrini, R. Scopelliti, T. Riedel and P. J. Dyson, Organometallic rhodium(III) and iridium(III) cyclopentadienyl complexes with curcumin and bisdemethoxycurcumin co-ligands, *Dalton Trans.*, 2015, **44**, 20523–20531, DOI: **10.1039/C5DT03037D**.

46 J. M. Cross, N. Gallagher, J. H. Gill, M. Jain, A. W. McNeillis, K. L. Rockley, F. H. Tscherny, N. J. Wirszycz, D. S. Yufit and J. W. Walton, Pyridylphosphinate metal complexes: Synthesis, structural characterization and biological activity, *Dalton Trans.*, 2016, **45**, 12807–12813, DOI: **10.1039/C6DT01264G**.

47 A. J. Blacker, M. J. Stirling and M. I. Page, Catalytic racemisation of chiral amines and application in dynamic

kinetic resolution, *Org. Process Res. Dev.*, 2007, **11**, 642–648, DOI: 10.1021/op060233w.

48 E. T. Chang, D. B. Green and K. R. Brereton, Microwave-assisted synthesis of pentamethylcyclopentadienyl iridium dihalide dimers, *Polyhedron*, 2022, **226**, 116089, DOI: 10.1016/j.poly.2022.116089.

49 H. Geisler, S. Harringer, D. Wenisch, R. Urban, M. A. Jakupec, W. Kandioller and B. K. Keppler, Systematic study on the cytotoxic potency of commonly used dimeric metal precursors in human cancer cell lines, *ChemistryOpen*, 2022, **11**, e202200019, DOI: 10.1002/open.202200019.

50 J. Patalenszki, L. Biro, A. C. Benyei, T. Radosova-Muchova, J. Kasparkova and P. Buglyo, Half-sandwich complexes of ruthenium, osmium, rhodium and iridium with DL-methionine or S-methyl-L-cysteine: A solid state and solution equilibrium study, *RSC Adv.*, 2015, **5**, 8094–8107, DOI: 10.1039/C4RA15649H.

51 P. L. Parajdi-Losonczi, P. Buglyo, H. Skakalova, J. Kasparkova, N. Lihi and E. Farkas, Half-sandwich type rhodium(III)-aminohydroxamate complexes: the role of the position of the amino group in metal ion binding, *New J. Chem.*, 2018, **42**, 7659–7670, DOI: 10.1039/C7NJ04711H.

52 L. Masaryk, I. Nemec, J. Kašpárková, V. Brabec and P. Štarha, Unexpected solution behaviour of ester-functionalized half-sandwich Ru(II) and Ir(III) complexes, *Dalton Trans.*, 2021, **50**, 8017–8028, DOI: 10.1039/D1DT00466B.

53 A. Casini, F. Edafe, M. Erlandsson, L. Gonsalvi, A. Ciancetta, N. Re, A. Ienco, L. Messori, M. Peruzzini and P. J. Dyson, Rationalization of the inhibition activity of structurally related organometallic compounds against the drug target cathepsin B by DFT, *Dalton Trans.*, 2010, **39**, 5556–5563, DOI: 10.1039/C003218B.

54 G. Ludwig, S. Mijatović, I. Randelović, M. Bulatović, D. Miljković, D. Maksimović-Ivanić, M. Korb, H. Lang, D. Steinborn and G. N. Kaluderović, Biological activity of neutral and cationic iridium(III) complexes with κ*P* and κ*P*,κ*S* coordinated $Ph_2PCH_2S(O)_xPh$ ($x$ = 0–2) ligands, *Eur. J. Med. Chem.*, 2013, **69**, 216–222, DOI: 10.1016/j.ejmech.2013.08.025.

55 G. Ludwig, I. Randelovic, D. Maksimovic-Ivanic, S. Mijatovic, M. Z. Bulatovic, D. Miljkovic, M. Korb, H. Lang, D. Steinborn and G. N. Kaluderovic, Anticancer potential of (pentamethylcyclopentadienyl)chloridoiridium(III) complexes bearing κ*P* and κ*P*,κ*S*-coordinated $Ph_2PCH_2CH_2CH_2S(O)xPh$ (x = 0–2) ligands, *ChemMedChem*, 2014, **9**, 1586–1593, DOI: 10.1002/cmdc.201300479.

56 H. Pruchnik, M. Latocha, A. Zielinska and F. P. Pruchnik, Rhodium(III) and iridium(III) pentamethylcyclopentadienyl complexes with tris(2-carboxyethyl)phosphine, properties and cytostatic activity, *J. Organomet. Chem.*, 2016, **822**, 74–79, DOI: 10.1016/j.jorganchem.2016.08.005.

57 S. Kozieł, U. K. Komarnicka, A. Ziółkowska, A. Skórska-Stania, B. Pucelik, M. Płotek, V. Sebastian, A. Bieńko, G. Stochel and A. Kyzioł, Anticancer potency of novel organometallic Ir(III) complexes with phosphine derivatives of fluoroquinolones encapsulated in polymeric micelles, *Inorg. Chem. Front.*, 2020, **7**, 3386–3401, DOI: 10.1039/D0QI00538J.

58 S. A. Kozieł, M. K. Lesiów, D. Wojtala, E. Dyguda-Kazimierowicz, D. Bieńko and U. K. Komarnicka, Interaction between DNA, albumin and apo-transferrin and iridium(III) complexes with phosphines derived from fluoroquinolones as a potent anticancer drug, *Pharmaceuticals*, 2021, **14**, 685, DOI: 10.3390/ph14070685.

59 U. K. Komarnicka, S. Kozieł, A. Skórska-Stania, A. Kyzioł and F. Tisato, Synthesis, physicochemical characterization and antiproliferative activity of phosphino Ru(II) and Ir(III) complexes, *Dalton Trans.*, 2022, **51**, 8605–8617, DOI: 10.1039/D2DT01055K.

60 U. K. Komarnicka, A. Niorettini, S. Kozieł, B. Pucelik, A. Barzowska, D. Wojtala, A. Ziółkowska, M. Lesiów, A. Kyzioł, S. Caramori, M. Porchia and A. Bieńko, Two out of Three Musketeers Fight against Cancer: Synthesis, physicochemical, and biological properties of phosphino $Cu^{I}$, $Ru^{II}$, $Ir^{III}$ complexes, *Pharmaceuticals*, 2022, **15**, 169, DOI: 10.3390/ph15020169.

61 D. B. Wojtala, U. K. Komarnicka, A. Kyzioł, S. Kozieł, M. Szmitka, M. Słowikowski, J. Kulczyńska and G. Stochel, Cellular mechanistic considerations on cytotoxic mode of action of phosphino Ru(II) and Ir(III) complexes, *Eur. J. Inorg. Chem.*, 2023, **26**, e202300515, DOI: 10.1002/ejic.202300515.

62 S. Kozieł, D. Wojtala, M. Szmitka, P. Kędzierski, D. Biénko and U. K. Komarnicka, Insights into the binding of half-sandwich phosphino Ir(III) and Ru(II) complexes to deoxyribonucleic acid, albumin and apo-transferrin: Experimental and theoretical investigation, *Spectrochim. Acta, Part A*, 2024, **304**, 123289, DOI: 10.1016/j.saa.2023.123289.

63 L. Wang, X. Liu, Y. Wu, X. He, X. Guo, W. Gao, L. Tan, X.-A. Yuan, J. Liu and Z. Liu, *In vitro* and *in vivo* antitumor assay of mitochondrially targeted fluorescent half-sandwich iridium(III) pyridine complexes, *Inorg. Chem.*, 2023, **62**, 3395–3408, DOI: 10.1021/acs.inorgchem.2c03333.

64 S. J. Lucas, R. M. Lord, A. M. Basri, S. J. Allison, R. M. Phillips, A. J. Blacker and P. C. McGowan, Increasing anti-cancer activity with longer tether lengths of group 9 Cp* complexes, *Dalton Trans.*, 2016, **45**, 6812–6815, DOI: 10.1039/C6DT00186F.

65 S. Adhikari, O. Hussain, R. M. Phillips and M. R. Kollipara, Half-sandwich $d^6$ metal complexes comprising of 2-substituted-1,8-naphthyridine ligands with unexpected bonding modes: Synthesis, structural and anti-cancer studies, *J. Organomet. Chem.*, 2018, **854**, 27–37, DOI: 10.1016/j.jorganchem.2017.11.011.

66 L. Dkhar, V. Banothu, E. Pinder, R. M. Phillips, W. Kaminsky and M. R. Kollipara, Ru, Rh and Ir metal complexes of pyridyl chalcone derivatives: Their potent antibacterial activity, comparable cytotoxicity potency and

 

selectivity to cisplatin, *Polyhedron*, 2020, **185**, 114606, DOI: 10.1016/j.poly.2020.114606.

67 S. Adhikari, O. Hussain, R. M. Phillips, W. Kaminsky and M. R. Kollipara, Neutral and cationic half-sandwich arene $d^6$ metal complexes containing pyridyl and pyrimidyl thiourea ligands with interesting bonding modes: Synthesis, structural and anti-cancer studies, *Appl. Organomet. Chem.*, 2018, **32**, e4476, DOI: 10.1002/aoc.4476.

68 A. Lapasam, O. Hussain, R. M. Phillips, W. Kaminsky and M. R. Kollipara, Synthesis, characterization and chemosensitivity studies of half-sandwich ruthenium, rhodium and iridium complexes containing $\kappa^1_{(S)}$, and $\kappa^2_{(N,S)}$ aroylthiourea ligands, *J. Organomet. Chem.*, 2019, **880**, 272–280, DOI: 10.1016/j.jorganchem.2018.11.020.

69 F. Schmitt, K. Donnelly, J. K. Muenzner, T. Rehm, V. Novohradsky, V. Brabec, J. Kasparkova, M. Albrecht, R. Schobert and T. Mueller, Effects of histidin-2-ylidene vs. imidazol-2-ylidene ligands on the anticancer and antivascular activity of complexes of ruthenium, iridium, platinum, and gold, *J. Inorg. Biochem.*, 2016, **163**, 221–228, DOI: 10.1016/j.jinorgbio.2016.07.021.

70 D. Truong, M. P. Sullivan, K. K. H. Tong, T. R. Steel, A. Prause, J. H. Lovett, J. W. Andersen, S. M. F. Jamieson, H. H. Harris, I. Ott, C. M. Weekley, K. Hummitzsch, T. Söhnel, M. Hanif, N. Metzler-Nolte, D. C. Goldstone and C. G. Hartinger, Potent inhibition of thioredoxin reductase by the Rh derivatives of anticancer M(arene/Cp*)(NHC)$Cl_2$ complexes, *Inorg. Chem.*, 2020, **59**, 3281–3289, DOI: 10.1021/acs.inorgchem.9b03640.

71 R. M. Lord, J. Holmes, F. N. Singer, A. Frith and C. E. Willans, Precious metal N-heterocyclic carbene-carbaboranyl complexes: Cytotoxic and selective compounds for the treatment of cancer, *J. Organomet. Chem.*, 2020, **907**, 121062, DOI: 10.1016/j.jorganchem.2019.121062.

72 B. Y. T. Lee, M. P. Sullivan, E. Yano, K. K. H. Tong, M. Hanif, T. Kawakubo-Yasukochi, S. M. F. Jamieson, T. Soehnel, D. C. Goldstone and C. G. Hartinger, Anthracenyl functionalization of half-sandwich carbene complexes: *In vitro* anticancer activity and reactions with biomolecules, *Inorg. Chem.*, 2021, **60**, 14636–14644, DOI: 10.1021/acs.inorgchem.1c01675.

73 D. Truong, N. Y. S. Lam, M. Kamalov, M. Riisom, S. M. F. Jamieson, P. W. R. Harris, M. A. Brimble, N. Metzler-Nolte and C. G. Hartinger, A solid support-based synthetic strategy for the site-selective functionalization of peptides with organometallic half-sandwich moieties, *Chem. – Eur. J.*, 2022, **28**, e202104049, DOI: 10.1002/chem.202104049.

74 M. Gras, B. Therrien, G. Suss-Fink, A. Casini, F. Edafe and P. J. Dyson, Anticancer activity of new organo-ruthenium, rhodium and iridium complexes containing the 2-(pyridine-2-yl)thiazole N,N-chelating ligand, *J. Organomet. Chem.*, 2010, **695**, 1119–1125, DOI: 10.1016/j.jorganchem.2010.01.020.

75 M. Gorol, H. W. Roesky, M. Noltemeyer and H.-G. Schmidt, ($\eta^5$-Pentamethylcyclopentadienyl)iridium(III) complexes with $\eta^2$-N,O and $\eta^2$-P,S ligands, *Eur. J. Inorg. Chem.*, 2005, 4840–4844, DOI: 10.1002/ejic.200500528.

76 V. Novohradsky, Z. Liu, M. Vojtiskova, P. J. Sadler, V. Brabec and J. Kasparkova, Mechanism of cellular accumulation of an iridium(III) pentamethylcyclopentadienyl anticancer complex containing a *C*,*N*-chelating ligand, *Metallomics*, 2014, **6**, 682–690, DOI: 10.1039/c3mt00341h.

77 V. Novohradsky, L. Zerzankova, J. Stepankova, A. Kisova, H. Kostrhunova, Z. Liu, P. J. Sadler, J. Kasparkova and V. Brabec, A dual-targeting, apoptosis-inducing organometallic half-sandwich iridium anticancer complex, *Metallomics*, 2014, **6**, 1491–1501, DOI: 10.1039/c4mt00112e.

78 M. Shao, X. Liu, Y. Sun, S. Dou, Q. Chen, X.-A. Yuan, L. Tian and Z. Liu, Preparation and the anticancer mechanism of configuration-controlled Fe(II)-Ir(III) heteronuclear metal complexes, *Dalton Trans.*, 2020, **49**, 12599–12609, DOI: 10.1039/D0DT02408B.

79 Y. Geldmacher, K. Splith, I. Kitanovic, H. Alborzinia, S. Can, R. Rubbiani, M. A. Nazif, P. Wefelmeier, A. Prokop, I. Ott, S. Wölfl, I. Neundorf and W. S. Sheldrick, Cellular impact and selectivity of half-sandwich organorhodium(III) anticancer complexes and their organoiridium(III) and trichloridorhodium(III) counterparts, *J. Biol. Inorg. Chem.*, 2012, **17**, 631–646, DOI: 10.1007/s00775-012-0883-2.

80 L. Guo, H. Zhang, M. Tian, Z. Tian, Y. Xu, Y. Yang, H. Peng, P. Liu and Z. Liu, Electronic effects on reactivity and anticancer activity by half-sandwich N,N-chelated iridium(III) complexes, *New J. Chem.*, 2018, **42**, 16183–16192, DOI: 10.1039/C8NJ03360A.

81 X. He, M. Tian, X. Liu, Y. Tang, C. F. Shao, P. Gong, J. Liu, S. Zhang, L. Guo and Z. Liu, Triphenylamine-appended half-sandwich iridium(III) complexes and their biological applications, *Chem. – Asian J.*, 2018, **13**, 1500–1509, DOI: 10.1002/asia.201800103.

82 X. He, X. Liu, Y. Tang, J. Du, M. Tian, Z. Xu, X. Liu and Z. Liu, Half-sandwich Iridium(III) complexes with triphenylamine-substituted dipyridine frameworks and bioactivity applications, *Dyes Pigm.*, 2019, **160**, 217–226, DOI: 10.1016/j.dyepig.2018.08.006.

83 P. Chellan, V. M. Avery, S. Duffy, K. M. Land, C. C. Tam, J. H. Kim, L. W. Cheng, I. Romero-Canelon and P. J. Sadler, Bioactive half-sandwich Rh and Ir bipyridyl complexes containing artemisinin, *J. Inorg. Biochem.*, 2021, **219**, 111408, DOI: 10.1016/j.jinorgbio.2021.111408.

84 L. Biancalana, H. Kostrhunova, L. K. Batchelor, M. Hadiji, I. Degano, G. Pampaloni, S. Zacchini, P. J. Dyson, V. Brabec and F. Marchetti, Hetero-bis-conjugation of bioactive molecules to half-sandwich ruthenium(II) and iridium(III) complexes provides synergic effects in cancer cell cytotoxicity, *Inorg. Chem.*, 2021, **60**, 9529–9541, DOI: 10.1021/acs.inorgchem.1c00641.

85 W. Ma, Z. Tian, S. Zhang, X. He, J. Li, X. Xia, X. Chen and Z. Liu, Lysosome targeted drugs: Rhodamine B modified

N^N-chelating ligands for half-sandwich iridium(III) anticancer complexes, *Inorg. Chem. Front.*, 2018, **5**, 2587–2597, DOI: 10.1039/C8QI00620B.

86 M. Kowalik, J. Masternak, M. Olszewski, N. Maciejewska, K. Kazimierczuk, J. Sitkowski, A. M. Dąbrowska, A. Chylewska and M. Makowski, Anticancer study on $Ir^{III}$ and $Rh^{III}$ half-sandwich complexes with the bipyridylsulfonamide ligand, *Inorg. Chem.*, 2024, **63**, 1296–1316, DOI: 10.1021/acs.inorgchem.3c03801.

87 M. Graf, J. Ochs, N. Metzler-Nolte, P. Mayer and H.-C. Böttcher, Synthesis, characterization and cytotoxic activities of half-sandwich pentamethylcyclopentadienyl iridium(III) complexes containing 4,4′-substituted 2,2′-bipyridine ligands, *Z. Anorg. Allg. Chem.*, 2023, **649**, e202200382, DOI: 10.1002/zaac.202200382.

88 S. Gadre, M. Manikandan, G. Chakraborty, A. Rayrikar, S. Paul, C. Patra and M. Patra, Development of a highly *in vivo* efficacious dual antitumor and antiangiogenic organoiridium complex as a potential anti-lung cancer agent, *J. Med. Chem.*, 2023, **66**, 13481–13500, DOI: 10.1021/acs.jmedchem.3c00704.

89 M. Kalidasan, S. Forbes, Y. Mozharivskyj, M. Ahmadi, Z. Ahmadihosseini, R. M. Phillips and M. R. Kollipara, Mononuclear half-sandwich cyclic-*p*-perimeter platinum group metal complexes having bithiazole ligands: Synthesis, molecular and anti-cancer studies, *Inorg. Chim. Acta*, 2014, **421**, 349–358, DOI: 10.1016/j.ica.2014.06.024.

90 L. Shadap, J. L. Tyagi, K. M. Poluri, E. Pinder, R. M. Phillips, W. Kaminsky and M. R. Kollipara, Synthesis, structural and *in vitro* functional studies of half-sandwich platinum group metal complexes having various bonding modes of benzhydrazone derivative ligands, *Polyhedron*, 2020, **176**, 114293, DOI: 10.1016/j.poly.2019.114293.

91 A. C. Matsheku, M. Y.-H. Chen, S. Jordaan, S. Prince, G. S. Smith and B. C. E. Makhubela, Acridine-containing $Ru^{II}$, $Os^{II}$, $Rh^{III}$ and $Ir^{III}$ half-sandwich complexes: Synthesis, structure and antiproliferative activity, *Appl. Organomet. Chem.*, 2017, **31**, e3852, DOI: 10.1002/aoc.3852.

92 P. Kumari, S. Ghosh, S. Acharya, P. Mitra, S. Roy, S. Ghosh, M. Maji, S. Singh and A. Mukherjee, Cytotoxic imidazolyl-mesalazine ester-based Ru(II) complexes reduce expression of stemness genes and induce differentiation of oral squamous cell carcinoma, *J. Med. Chem.*, 2023, **66**, 14061–14079, DOI: 10.1021/acs.jmedchem.3c01092.

93 N. Roy, U. Sen, S. R. Chaudhuri, V. Muthukumar, P. Moharana, P. Paira, B. Bose, A. Gauthaman and A. Moorthy, Mitochondria specific highly cytoselective iridium(III)–Cp* dipyridophenazine (dppz) complexes as cancer cell imaging agents, *Dalton Trans.*, 2021, **50**, 2268–2283, DOI: 10.1039/D0DT03586F.

94 A. Mondal, S. Shanavas, U. Sen, U. Das, N. Roy, B. Bose and P. Paira, Mitochondria-targeted half-sandwich iridium(III)-Cp*-arylimidazophenanthroline complexes as antiproliferative and bioimaging agents against triple negative breast cancer cells MDA-MB-468, *RSC Adv.*, 2022, **12**, 11953–11966, DOI: 10.1039/D2RA01036D.

95 B. Kar, S. Shanavas, A. H. Nagendra, U. Das, N. Roy, S. Pete, A. Sharma, S. De, S. K. Ashok Kumar, S. Vardhan, S. K. Sahoo, D. Panda, S. Shenoy, B. Bose and P. Paira, Iridium(III)–Cp*-(imidazo[4,5-*f*,][1,10]phenanthrolin-2-yl) phenol analogues as hypoxia active, GSH-resistant cancer cytoselective and mitochondria-targeting cancer stem cell therapeutic agents, *Dalton Trans.*, 2022, **51**, 5494–5514, DOI: 10.1039/D2DT00168C.

96 Y. Yang, Y. Gao, J. Zhao and S. Gou, An electron-accepting half-sandwich iridium(III) complex for the treatment of hypoxic tumors *via* synergetic chemo- and phototherapy, *Inorg. Chem. Front.*, 2024, **11**, 436–450, DOI: 10.1039/D3QI02047A.

97 I. Kacsir, A. Sipos, A. Bényei, E. Janka, P. Buglyó, L. Somsák, P. Bai and É. Bokor, Reactive oxygen species production is responsible for antineoplastic activity of osmium, ruthenium, iridium and rhodium half-sandwich type complexes with bidentate glycosyl heterocyclic ligands in various cancer cell models, *Int. J. Mol. Sci.*, 2022, **23**, 813, DOI: 10.3390/ijms23020813.

98 J. Li, L. Guo, Z. Tian, M. Tian, S. Zhang, K. Xu, Y. Qian and Z. Liu, Novel half-sandwich iridium(III) imino-pyridyl complexes showing remarkable *in vitro* anticancer activity, *Dalton Trans.*, 2017, **46**, 15520–15534, DOI: 10.1039/C7DT03265J.

99 D. Kong, M. Tian, L. Guo, X. Liu, S. Zhang, Y. Song, X. Meng, S. Wu, L. Zhang and Z. Liu, Novel iridium(III) iminopyridine complexes: synthetic, catalytic, and *in vitro* anticancer activity studies, *J. Biol. Inorg. Chem.*, 2018, **23**, 819–832, DOI: 10.1007/s00775-018-1578-0.

100 J. Li, L. Guo, Z. Tian, S. Zhang, Z. Xu, Y. Han, R. Li, Y. Li and Z. Liu, Half-sandwich iridium and ruthenium complexes: Effective tracking in cells and anticancer studies, *Inorg. Chem.*, 2018, **57**, 13552–13563, DOI: 10.1021/acs.inorgchem.8b02161.

101 Y. Yang, X. Ge, L. Guo, T. Zhu, Z. Tian, H. Zhang, Q. Du, H. Peng, W. Ma and Z. Liu, Zwitterionic and cationic half-sandwich iridium(III) ruthenium(II) complexes bearing sulfonate groups: synthesis, characterization and their different biological activities, *Dalton Trans.*, 2019, **48**, 3193–3197, DOI: 10.1039/C9DT00259F.

102 J. Li, Z. Tian, X. Ge, Z. Xu, Y. Feng and Z. Liu, Design, synthesis, and evaluation of fluorine and naphthyridine-based half-sandwich organoiridium/ruthenium complexes with bioimaging and anticancer activity, *Eur. J. Med. Chem.*, 2019, **163**, 830–839, DOI: 10.1016/j.ejmech.2018.12.021.

103 D. Kong, L. Guo, M. Tian, S. Zhang, Z. Tian, H. Yang, Y. Tian and Z. Liu, Lysosome-targeted potent half-sandwich iridium(III) α-diimine antitumor complexes, *Appl. Organomet. Chem.*, 2019, **33**, e4633, DOI: 10.1002/aoc.4633.

104 W. Ma, L. Guo, Z. Tian, S. Zhang, X. He, J. Li, Y. Yang and Z. Liu, Rhodamine-modified fluorescent half-sandwich iridium and ruthenium complexes: Potential application as bioimaging and anticancer agents, *Dalton Trans.*, 2019, **48**, 4788–4793, DOI: 10.1039/C9DT00999J.

105 W. Ma, S. Zhang, Z. Tian, Z. Xu, Y. Zhang, X. Xia, X. Chen and Z. Liu, Potential anticancer agent for selective damage to mitochondria or lysosomes: Naphthalimide-modified fluorescent biomarker half-sandwich iridium(III) and ruthenium(II) complexes, *Eur. J. Med. Chem.*, 2019, **181**, 111599, DOI: 10.1016/j.ejmech.2019.111599.

106 Y. Xie, S. Zhang, X. Ge, W. Ma, X. He, Y. Zhao, J. Ye, H. Zhang, A. Wang and Z. Liu, Lysosomal-targeted anticancer half-sandwich iridium(III) complexes modified with lonidamine amide derivatives, *Appl. Organomet. Chem.*, 2020, **34**, e5589, DOI: 10.1002/aoc.5589.

107 M. Łomzik, M. Hanif, A. Budniok, A. Błauż, A. Makal, D. M. Tchoń, B. Lešniewska, K. K. H. Tong, S. Movassaghi, T. Söhnel, S. M. F. Jamieson, A. Zafar, J. Reynisson, B. Rychlik, C. G. Hartinger and D. Plażuk, Metal-dependent cytotoxic and kinesin spindle protein inhibitory activity of Ru, Os, Rh, and Ir half-sandwich complexes of ispinesib-derived ligands, *Inorg. Chem.*, 2020, **59**, 14879–14890, DOI: 10.1021/acs.inorgchem.0c00957.

108 M. Łomzik, A. Błauż, D. Tchoń, A. Makal, B. Rychlik and D. Plażuk, Development of half-sandwich Ru, Os, Rh, and Ir complexes bearing the pyridine-2-ylmethanimine bidentate ligand derived from 7-chloroquinazolin-4(3*H*)-one with enhanced antiproliferative activity, *ACS Omega*, 2024, **9**, 18224–18237, DOI: 10.1021/acsomega.3c10482.

109 M. Łomzik, A. Błauż, M. Głodek, A. Makal, D. Tchoń, D. M. Ayine-Tora, C. Hartinger, B. Rychlik and D. Plażuk, Organometallic Ru, Os, Rh and Ir half-sandwich conjugates of ispinesib - impact of the organometallic group on the antimitotic activity, *Dalton Trans.*, 2023, **52**, 11859–11874, DOI: 10.1039/D3DT01217D.

110 R. Křikavová, M. Romanovová, Z. Jendželovská, M. Majerník, L. Masaryk, P. Zoufalý, D. Milde, J. Moncol, R. Herchel, R. Jendželovský and I. Nemec, Impact of the central atom and halido ligand on the structure, antiproliferative activity and selectivity of half-sandwich Ru(II) and Ir(III) complexes with a 1,3,4-thiadiazole-based ligand, *Dalton Trans.*, 2023, **52**, 12717–12732, DOI: 10.1039/D3DT01696J.

111 L. Masaryk, J. Orvoš, K. Słoczyńska, R. Herchel, J. Moncol, D. Milde, P. Halaš, R. Křikavová, P. Koczurkiewicz-Adamczyk, E. Pękala, R. Fischer, I. Šalitroš, I. Nemec and P. Štarha, Anticancer half-sandwich Ir(III) complex and its interaction with various biomolecules and their mixtures - a case study with ascorbic acid, *Inorg. Chem. Front.*, 2022, **9**, 3758–3770, DOI: 10.1039/D2QI00535B.

112 X. Hu, L. Guo, M. Liu, M. Sun, Q. Zhang, H. Peng, F. Zhang and Z. Liu, Formation of iridium(III) and rhodium(III) amine, imine, and amido complexes based on pyridine-amine ligands: Structural diversity arising from reaction conditions, substituent variation, and metal centers, *Inorg. Chem.*, 2022, **61**, 10051–10065, DOI: 10.1021/acs.inorgchem.2c00984.

113 L. Guo, P. Li, J. Li, Y. Gong, X. Li, Y. Liu, K. Yu and Z. Liu, Half-sandwich iridium(III), rhodium(III), and ruthenium(II) complexes chelating hybrid $sp^2$-N/$sp^3$-N donor ligands to achieve improved anticancer selectivity, *Inorg. Chem.*, 2023, **62**, 15118–15137, DOI: 10.1021/acs.inorgchem.3c02118.

114 U. Das and P. Paira, Synthesis, characterization, photophysical and electrochemical properties, and biomolecular interaction of 2,2′-biquinoline based phototoxic Ru(II)/Ir(II) complexes, *Dalton Trans.*, 2023, **52**, 12608–12617, DOI: 10.1039/D3DT01348K.

115 M. I. Acuña, A. R. Rubio, M. Martínez-Alonso, N. Busto, A. M. Rodríguez, N. Davila-Ferreira, C. Smythe, G. Espino, B. García and F. Domínguez, Targets, mechanisms and cytotoxicity of half-sandwich Ir(III) complexes are modulated by structural modifications on the benzazole ancillary ligand, *Cancers*, 2023, **15**, 107, DOI: 10.3390/cancers15010107.

116 S. J. Lucas, R. M. Lord, R. L. Wilson, R. M. Phillips, V. Sridharan and P. C. McGowan, Synthesis of iridium and ruthenium complexes with (*N*,*N*), (*N*,*O*) and (*O*,*O*) coordinating bidentate ligands as potential anti-cancer agents, *Dalton Trans.*, 2012, **15**, 13800–13802, DOI: 10.1039/C2DT32104A.

117 R. K. Gupta, R. Pandey, G. Sharma, R. Prasad, B. Koch, S. Srikrishna, P. Z. Li, Q. Xu and D. S. Pandey, DNA binding and anti-cancer activity of redox-active heteroleptic piano-stool Ru(II), Rh(III), and Ir(III) complexes containing 4-(2-methoxypyridyl)phenyldipyrromethene, *Inorg. Chem.*, 2013, **52**, 3687–3698, DOI: 10.1021/ic302196v.

118 G. Gupta, G. Sharma, B. Koch, S. Park, S. S. Lee and J. Kim, Syntheses, characterization and molecular structures of novel Ru(II), Rh(III) and Ir(III) complexes and their possible roles as antitumour and cytotoxic agents, *New J. Chem.*, 2013, **37**, 2573–2581, DOI: 10.1039/C3NJ00315A.

119 R. K. Gupta, G. Sharma, R. Pandey, A. Kumar, B. Koch, P.-Z. Li, Q. Xu and D. S. Pandey, DNA/protein binding, molecular docking, and *in vitro* anticancer activity of some thioether-dipyrrinato complexes, *Inorg. Chem.*, 2013, **52**, 13984–13996, DOI: 10.1021/ic401662d.

120 Z. Almodares, S. J. Lucas, B. D. Crossley, A. M. Basri, C. M. Pask, A. J. Hebden, R. M. Phillips and P. C. McGowan, Rhodium, iridium, and ruthenium half-sandwich picolinamide complexes as anticancer agents, *Inorg. Chem.*, 2014, **53**, 727–736, DOI: 10.1021/ic401529u.

121 A. R. Burgoyne, B. C. E. Makhubela, M. Meyer and G. S. Smith, Trinuclear half-sandwich $Ru^{II}$, $Rh^{III}$ and $Ir^{III}$ polyester organometallic complexes: Synthesis and *in vitro* evaluation as antitumor agents, *Eur. J. Inorg. Chem.*, 2015, 1433–1444, DOI: 10.1002/ejic.201403192.

122 M. Boge, C. Fowelin, P. Bednarski and J. Heck, Diaminohexopyranosides as ligands in half-sandwich ruthenium(II), rhodium(III), and iridium(III) complexes,

*Organometallics*, 2015, **34**, 1507–1521, DOI: 10.1021/om5013117.

123 A. Kumar, A. Kumar, R. K. Gupta, R. P. Paitandi, K. B. Singh, S. K. Trigun, M. S. Hundal and D. S. Pandey, Cationic Ru(II), Rh(III) and Ir(III) complexes containing cyclic π-perimeter and 2-aminophenyl benzimidazole ligands: Synthesis, molecular structure, DNA and protein binding, cytotoxicity and anticancer activity, *J. Organomet. Chem.*, 2016, **801**, 68–79, DOI: 10.1016/j.jorganchem.2015.10.008.

124 S. Thangavel, M. Paulpandi, H. B. Friedrich, K. Murugan, S. Kalva and A. A. Skelton, Synthesis, characterization, antiproliferative and molecular docking study of new half sandwich Ir(III), Rh(III) and Ru(II) complexes, *J. Inorg. Biochem.*, 2016, **159**, 50–61, DOI: 10.1016/j.jinorgbio.2016.02.006.

125 S. Adhikari, D. Sutradhar, S. L. Shepherd, R. M. Phillips, A. K. Chandra and M. R. Kollipara, Synthesis, structural, DFT calculations and biological studies of rhodium and iridium complexes containing azine Schiff-base ligands, *Polyhedron*, 2016, **117**, 404–414, DOI: 10.1016/j.poly.2016.06.001.

126 S. Adhikari, N. R. Palepu, D. Sutradhar, S. L. Shepherd, R. M. Phillips, W. Kaminsky, A. K. Chandra and M. R. Kollipara, Neutral and cationic half-sandwich arene ruthenium, Cp*Rh and Cp*Ir oximato and oxime complexes: Synthesis, structural, DFT and biological studies, *J. Organomet. Chem.*, 2016, **820**, 70–81, DOI: 10.1016/j.jorganchem.2016.08.004.

127 S. K. Tripathy, U. De, N. Dehury, P. Laha, M. K. Panda, H. S. Kim and S. Patra, Cyclometallated iridium complexes inducing paraptotic cell death like natural products: Synthesis, structure and mechanistic aspects, *Dalton Trans.*, 2016, **45**, 15122–15136, DOI: 10.1039/C6DT00929H.

128 S. B. Gajera, J. V. Mehta, P. Thakor, V. R. Thakkar, P. C. Chudasama, J. S. Patel and M. N. Patel, Half-sandwich iridium$^{III}$ complexes with pyrazole-substituted heterocyclic frameworks and their biological applications, *New J. Chem.*, 2016, **40**, 9968–9980, DOI: 10.1039/C6NJ02153K.

129 S. B. Gajera, J. V. Mehta and M. N. Patel, Design of multifunctional iridium$^{III}$ compounds as a potential therapeutic agents from basic molecular scaffolds, *ChemistrySelect*, 2016, **1**, 3966–3973, DOI: 10.1002/slct.201600882.

130 N. R. Palepu, S. Adhikari, R. J. Premkumar, A. K. Verma, S. L. Shepherd, R. M. Phillips, W. Kaminsky and M. R. Kollipara, Half-sandwich ruthenium, rhodium and iridium complexes featuring oxime ligands: Structural studies and preliminary investigation of *in vitro* and *in vivo* anti-tumour activities, *Appl. Organomet. Chem.*, 2017, **31**, e3640, DOI: 10.1002/aoc.3640.

131 P. Chellan, V. M. Avery, S. Duffy, J. A. Triccas, G. Nagalingam, C. Tam, L. W. Cheng, J. Liu, K. M. Land, G. J. Clarkson, I. Romero-Canelón and P. J. Sadler, Organometallic conjugates of the drug sulfadoxine for combatting antimicrobial resistence, *Chem. – Eur. J.*, 2018, **24**, 10078–10090, DOI: 10.1002/chem.201801090.

132 N. R. Palepu, R. J. Premkumar, A. K. Verma, K. Bhattacharjee, S. R. Joshi, S. Forbes, Y. Mozharivskyj and M. R. Kollipara, Antibacterial, *in vitro* antitumor activity and structural studies of rhodium and iridium complexes featuring the two positional isomers of pyridine carbaldehyde picolinic hydrazone ligand, *Arabian J. Chem.*, 2018, **11**, 714–728, DOI: 10.1016/j.arabjc.2015.10.011.

133 A. Gilewska, B. Barszcz, J. Masternak, K. Kazimierczuk, J. Sitkowski, J. Wietrzyk and E. Turlej, Similarities and differences in $d^6$ low-spin ruthenium, rhodium and iridium half-sandwich complexes: Synthesis, structure, cytotoxicity and interaction with biological targets, *J. Biol. Inorg. Chem.*, 2019, **24**, 591–606, DOI: 10.1007/s00775-019-01665-2.

134 N. R. Palepu, S. L. Nongbri, J. R. Premkumar, A. K. Verma, K. Bhattacharjee, S. R. Joshi, S. Forbes, Y. Mozharivskyj, R. Thounaojam, K. Aguan and M. R. Kollipara, Synthesis and evaluation of new salicylaldehyde-2-picolinylhydrazone Schiff base compounds of Ru(II), Rh(III) and Ir(III) as *in vitro* antitumor, antibacterial and fluorescence imaging agents, *J. Biol. Inorg. Chem.*, 2015, **20**, 619–638, DOI: 10.1007/s00775-015-1249-3.

135 A. Lapasam, E. Pinder, R. M. Phillips, W. Kaminsky and M. R. Kollipara, Synthesis, structure and bonding modes of pyrazine based ligands of Cp*Rh and Cp*Ir complexes: The study of *in vitro* cytotoxicity against human cell lines, *J. Organomet. Chem.*, 2019, **899**, 120887, DOI: 10.1016/j.jorganchem.2019.120887.

136 M.-M. Wang, X.-L. Xue, X.-X. Sheng, Y. Su, Y.-Q. Kong, Y. Qian, J.-C. Bao, Z. Su and H.-K. Liu, Unveiling the anticancer mechanism for half-sandwich and cyclometalated Ir(III)-based complexes with functionalized α-lipoic acid, *RSC Adv.*, 2020, **10**, 5392–5398, DOI: 10.1039/C9RA10357K.

137 L. Shadap, V. Banothu, E. Pinder, R. M. Phillips, W. Kaminsky and M. R. Kollipara, *In vitro* biological evaluation of half-sandwich platinum-group metal complexes containing benzothiazole moiety, *J. Coord. Chem.*, 2020, **73**, 1538–1553, DOI: 10.1080/00958972.2020.1777547.

138 A. C. Carrasco, V. Rodriguez-Fanjul and A. M. Pizarro, Activation of the Ir-N(pyridine) bond in half-sandwich tethered iridium(III) complexes, *Inorg. Chem.*, 2020, **59**, 16454–16466, DOI: 10.1021/acs.inorgchem.0c02287.

139 L. Dkhar, A. K. Verma, V. Banothu, W. Kaminsky and M. R. Kollipara, Ruthenium, rhodium, and iridium complexes featuring coumarin hydrazone derivatives: Synthesis, characterization, and preliminary investigation of their anticancer and antibacterial activity, *Appl. Organomet. Chem.*, 2022, **36**, e6589, DOI: 10.1002/aoc.6589.

140 W. K. Chu, C. K. Rono and B. C. E. Makhubela, Synthesis, structural elucidation, and cytotoxicity studies of new tria-

 

zolyl half-sandwich $Ru^{II}$, $Os^{II}$, $Rh^{III}$ and $Ir^{III}$ complexes, *Eur. J. Inorg. Chem.*, 2024, **27**, e202300541, DOI: **10.1002/ejic.202300541**.

141 C. G. L. Nongpiur, A. K. Verma, M. M. Ghate, K. M. Poluri, W. Kaminsky and M. R. Kollipara, Synthesis, cytotoxicity and antibacterial activities of ruthenium, rhodium and iridium metal complexes containing diazafluorene functionalized ligands, *J. Mol. Struct.*, 2023, **1285**, 135474, DOI: **10.1016/j.molstruc.2023.135474**.

142 L. T. Babu and P. Paira, CuAAC "click"-derived luminescent 2-(2-(4-(4-(pyridin-2-yl)-1*H*-1,2,3-triazol-1-yl)butoxy) phenyl)benzo[*d*]thiazole-based Ru(II)/Ir(III)/Re(I) complexes as anticancer agents, *ACS Omega*, 2023, **8**, 32382–32395, DOI: **10.1021/acsomega.3c01639**.

143 L. Yang, S. Bose, A. H. Ngo and L. H. Do, Innocent but deadly: Nontoxic organoiridium catalysts promote selective cancer cell death, *ChemMedChem*, 2017, **12**, 292–299, DOI: **10.1002/cmdc.201600638**.

144 U. Sliwinska, F. P. Pruchnik, S. Ułaszewski, M. Latocha and D. Nawrocka-Musiał, Properties of $\eta^5$-pentamethylcyclopentadienyl rhodium(III) and iridium(III) complexes with quinolin-8-ol and their cytostatic activity, *Polyhedron*, 2010, **29**, 1653–1659, DOI: **10.1016/j.poly.2010.02.013**.

145 S. Wirth, C. J. Rohbogner, M. Cieslak, J. Kazmierczak-Baranska, S. Donevski, B. Nawrot and I.-P. Lorenz, Rhodium(III) and iridium(III) complexes with 1,2-naphthoquinone-1-oximate as a bidentate ligand: Synthesis, structure, and biological activity, *J. Biol. Inorg. Chem.*, 2010, **15**, 429–440, DOI: **10.1007/s00775-009-0615-4**.

146 X. He, J. Chen, L. Wei, M. Kandawa-Shultz, G. Shao and Y. Wang, Antitumor activity of iridium/ruthenium complexes containing nitro-substituted quinoline ligands *in vivo* and *in vitro*, *Dyes Pigm.*, 2023, **213**, 111146, DOI: **10.1016/j.dyepig.2023.111146**.

147 H. Hao, X. Liu, X. Ge, Y. Zhao, X. Tian, T. Ren, Y. Wang, C. Zhao and Z. Liu, Half-sandwich iridium(III) complexes with α-picolinic acid frameworks and antitumor applications, *J. Inorg. Biochem.*, 2019, **192**, 52–61, DOI: **10.1016/j.jinorgbio.2018.12.012**.

148 R. M. Lord, A. J. Hebden, C. M. Pask, I. R. Henderson, S. J. Allison, S. L. Shepherd, R. M. Phillips and P. C. McGowan, Hypoxia-sensitive metal β-ketoiminato complexes showing induced single-strand DNA breaks and cancer cell death by apoptosis, *J. Med. Chem.*, 2015, **58**, 4940–4953, DOI: **10.1021/acs.jmedchem.5b00455**.

149 R. M. Lord, M. Zegke, I. R. Henderson, C. M. Pask, H. J. Shepherd and P. C. McGowan, β-Ketoiminato iridium(III) organometallic complexes: Selective cytotoxicity towards colorectal cancer cells HCT116 *p53*−/−, *Chem. – Eur. J.*, 2019, **25**, 495–500, DOI: **10.1002/chem.201804901**.

150 M. Sawkmie, M. Bhattacharyya, V. Banothu, W. Kaminsky, P. M. Gannon, S. Majaw and M. R. Kollipara, Ruthenium, rhodium, and iridium complexes featuring fluorenyl benzohydrazone derivatives: Synthesis and preliminary investigation of their anticancer and antibacterial activity, *J. Mol. Struct.*, 2023, **1291**, 135994, DOI: **10.1016/j.molstruc.2023.135994**.

151 L. Wang, C. Huang, F. Hu, W. Cui, Y. Li, J. Li, J. Zong, X. Liu, X.-A. Yuana and Z. Liu, Preparation and antitumor application of *N*-phenylcarbazole/triphenylamine-modified fluorescent half-sandwich iridium(III) Schiff base complexes, *Dalton Trans.*, 2021, **50**, 15888–15899, DOI: **10.1039/D1DT02959B**.

152 A. R. Burgoyne, C. H. Kaschula, M. I. Parker and G. S. Smith, Synthesis and anticancer evaluation of mono- and trinuclear halfsandwich rhodium(III) and iridium(III) complexes based on *N*,*O*-salicylaldiminato-sulfonated scaffolds, *J. Organomet. Chem.*, 2017, **846**, 100–104, DOI: **10.1016/j.jorganchem.2017.05.058**.

153 A. R. Burgoyne, C. H. Kaschula, M. I. Parker and G. S. Smith, Tripodal half-sandwich rhodium and iridium complexes containing sulfonate and pyridinyl entities as antitumor agents, *Eur. J. Inorg. Chem.*, 2017, 5379–5386, DOI: **10.1002/ejic.201700704**.

154 Z. Liu, L. Salassa, A. Habtemariam, A. M. Pizarro, G. J. Clarkson and P. J. Sadler, Contrasting reactivity and cancer cell Cytotoxicity of isoelectronic organometallic iridium(III) complexes, *Inorg. Chem.*, 2011, **50**, 5777–5783, DOI: **10.1021/ic200607j**.

155 A. J. Millett, A. Habtemariam, I. Romero-Canelon, G. J. Clarkson and P. J. Sadler, Contrasting anticancer activity of half-sandwich iridium(III) complexes bearing functionally diverse 2-phenylpyridine ligands, *Organometallics*, 2015, **34**, 2683–2694, DOI: **10.1021/acs.organomet.5b00097**.

156 J. Ruiz, V. Rodriguez, N. Cutillas, K. G. Samper, M. Capdevila, O. Palacios and A. Espinosa, Novel *C*,*N*-chelate rhodium(III) and iridium(III) antitumor complexes incorporating a lipophilic steroidal conjugate and their interaction with DNA, *Dalton Trans.*, 2012, **41**, 12847–12856, DOI: **10.1039/C2DT31654D**.

157 V. Koch, A. Meschkov, W. Feuerstein, J. Pfeifer, O. Fuhr, M. Nieger, U. Schepers and S. Braese, Synthesis, characterization, and biological properties of steroidal ruthenium(II) and iridium(III) complexes based on the androst-16-en-3-ol framework, *Inorg. Chem.*, 2019, **58**, 15917–15926, DOI: **10.1021/acs.inorgchem.9b02402**.

158 Z. Liu, A. Habtemariam, A. M. Pizarro, G. J. Clarkson and P. J. Sadler, Organometallic iridium(III) cyclopentadienyl anticancer complexes containing C,N-chelating ligands, *Organometallics*, 2011, **30**, 4702–4710, DOI: **10.1021/om2005468**.

159 W. Ma, X. Ge, Z. Xu, S. Zhang, X. He, J. Li, X. Xia, X. Chen and Z. Liu, Theranostic lysosomal targeting anticancer and antimetastatic agents: Half-sandwich iridium(III) rhodamine complexes, *ACS Omega*, 2019, **4**, 15240–15248, DOI: **10.1021/acsomega.9b01863**.

160 S. Chen, X. Liu, Z. Tian, X. Ge, H. Hao, Y. Hao, Y. Zhang, Y. Xie, L. Tian and Z. Liu, Triphenylamine and carbazole-modified $iridium^{III}$ 2-phenylpyridine complexes: Synthesis, anticancer application and targeted research,

*Appl. Organomet. Chem.*, 2019, **33**, e5053, DOI: 10.1002/aoc.5053.

161 X. Liu, S. Chen, X. Ge, Y. Zhang, Y. Xie, Y. Hao, D. Wu, J. Zhao, X.-A. Yuan, L. Tian and Z. Liu, Dual functions of iridium(III) 2-phenylpyridine complexes: Metastasis inhibition and lysosomal damage, *J. Inorg. Biochem.*, 2020, **205**, 110983, DOI: 10.1016/j.jinorgbio.2019.110983.

162 Z. Liu, I. Romero-Canelon, A. Habtemariam, G. J. Clarkson and P. J. Sadler, Potent half-sandwich iridium(III) anticancer complexes containing C^N-chelated and pyridine ligands, *Organometallics*, 2014, **33**, 5324–5333, DOI: 10.1021/om500644f.

163 J. M. Zimbron, K. Passador, B. Gatin-Fraudet, C.-M. Bachelet, D. Plazuk, L.-M. Chamoreau, C. Botuha, S. Thorimbert and M. Salmain, Synthesis, photophysical properties, and living cell imaging of theranostic half-sandwich iridium-4,4-difluoro-4-bora-3*a*,4*a*-diaza-*s*-indacene (BODIPY) dyads, *Organometallics*, 2017, **36**, 3435–3442, DOI: 10.1021/acs.organomet.7b00250.

164 J. J. Conesa, A. C. Carrasco, V. Rodriguez-Fanjul, Y. Yang, J. L. Carrascosa, P. Cloetens, E. Pereiro and A. M. Pizarro, Unambiguous intracellular localization and quantification of a potent iridium anticancer compound by correlative 3D cryo X-ray imaging, *Angew. Chem., Int. Ed.*, 2020, **59**, 1270–1278, DOI: 10.1002/anie.201911510.

165 A. C. Carrasco, V. Rodriguez-Fanjul, A. Habtemariam and A. M. Pizarro, Structurally strained half-sandwich iridium (III) complexes as highly potent anticancer agents, *J. Med. Chem.*, 2020, **63**, 4005–4021, DOI: 10.1021/acs.jmedchem.9b02000.

166 G. S. Yellol, A. Donaire, J. G. Yellol, V. Vasylyeva, C. Janiak and J. Ruiz, On the antitumor properties of novel cyclometalated benzimidazole Ru(II), Ir(III) and Rh(III) complexes, *Chem. Commun.*, 2013, **49**, 11533–11535, DOI: 10.1039/C3CC46239K.

167 J. Yellol, S. A. Perez, A. Buceta, G. Yellol, A. Donaire, P. Szumlas, P. J. Bednarski, G. Makhloufi, C. Janiak, A. Espinosa and J. Ruiz, Novel C,N-cyclometalated benzimidazole ruthenium(II) and iridium(III) complexes as antitumor and antiangiogenic agents: A structure-activity relationship study, *J. Med. Chem.*, 2015, **58**, 7310–7327, DOI: 10.1021/acs.jmedchem.5b01194.

168 S. Mukhopadhyay, R. K. Gupta, R. P. Paitandi, N. K. Rana, G. Sharma, B. Koch, L. K. Rana, M. S. Hundal and D. S. Pandey, Synthesis, structure, DNA/protein binding, and anticancer activity of some half-sandwich cyclometalated Rh(III) and Ir(III) complexes, *Organometallics*, 2015, **34**, 4491–4506, DOI: 10.1021/acs.organomet.5b00475.

169 Z.-d. Mou, N. Deng, F. Zhang, J. Zhang, J. Cen and X. Zhang, "Half-sandwich" Schiff-base Ir(III) complexes as anticancer agents, *Eur. J. Med. Chem.*, 2017, **138**, 72–82, DOI: 10.1016/j.ejmech.2017.06.027.

170 Y. Yang, L. Guo, Z. Tian, Y. Gong, H. Zheng, S. Zhang, Z. Xu, X. Ge and Z. Liu, Novel and versatile imine-N-heterocyclic carbene half-sandwich iridium(III) complexes as lysosome-targeted anticancer agents, *Inorg. Chem.*, 2018, **57**, 11087–11098, DOI: 10.1021/acs.inorgchem.8b01656.

171 Y. Yang, L. Guo, X. Ge, S. Shi, Y. Gong, Z. Xu, X. Zheng and Z. Liu, Structure-activity relationships for highly potent half-sandwich organoiridium(III) anticancer complexes with C^N-chelated ligands, *J. Inorg. Biochem.*, 2019, **191**, 1–7, DOI: 10.1016/j.jinorgbio.2018.11.007.

172 Y. Han, X. Liu, Z. Tian, X. Ge, J. Li, M. Gao, Y. Li, Y. Liu and Z. Liu, Half-sandwich iridium(III) benzimidazole-appended imidazolium-based *N*-heterocyclic carbene complexes and antitumor application, *Chem. – Asian J.*, 2018, **13**, 3697–3705, DOI: 10.1002/asia.201801323.

173 K. K. H. Tong, M. Hanif, S. Movassaghi, M. P. Sullivan, J. H. Lovett, K. Hummitzsch, T. Söhnel, S. M. F. Jamieson, S. K. Bhargava, H. H. Harris and C. G. Hartinger, Triazolyl-functionalized N-heterocyclic carbene half-sandwich compounds: Coordination mode, reactivity and *in vitro* anticancer activity, *ChemMedChem*, 2021, **16**, 3017–3026, DOI: 10.1002/cmdc.202100311.

174 K. K. H. Tong, M. Riisom, E. Leung, M. Hanif, T. Sohnel, S. M. F. Jamieson and C. G. Hartinger, Impact of coordination mode and ferrocene functionalization on the anticancer activity of N-heterocyclic carbene half-sandwich complexes, *Inorg. Chem.*, 2022, **61**, 17226–17241, DOI: 10.1021/acs.inorgchem.2c02832.

175 J. Kralj, A. Bolje, D. S. Polancec, I. Steiner, T. Grzan, A. Tupek, N. Stojanovic, S. Hohloch, D. Urankar, M. Osmak, B. Sarkar, A. Brozovic and J. Košmrlj, Half-sandwich Ir(III) and Os(II) complexes of pyridyl-mesoionic carbenes as potential anticancer agents, *Organometallics*, 2019, **38**, 4082–4092, DOI: 10.1021/acs.organomet.9b00327.

176 C. K. Rono, W. K. Chu, J. Darkwa, D. Meyer and B. C. E. Makhubela, Triazolyl $Ru^{II}$, $Rh^{III}$, $Os^{II}$, and $Ir^{III}$ complexes as potential anticancer agents: Synthesis, structure elucidation, cytotoxicity, and DNA model interaction studies, *Organometallics*, 2019, **38**, 3197–3211, DOI: 10.1021/acs.organomet.9b00440.

177 R. Ramos, J. M. Zimbron, S. Thorimbert, L.-M. Chamoreau, A. Munier, C. Botuha, A. Karaiskou, M. Salmain and J. Sobczak-Thépot, Insights into the antiproliferative mechanism of (C^N)-chelated half-sandwich iridium complexes, *Dalton Trans.*, 2020, **49**, 17635–17641, DOI: 10.1039/D0DT03414B.

178 R. Ramos, J.-F. Gilles, R. Morichon, C. Przybylski, B. Caron, C. Botuha, A. Karaiskou, M. Salmain and J. Sobczak-Thépot, Cytotoxic BODIPY-appended half-sandwich iridium(III) complex forms protein adducts and induces ER stress, *J. Med. Chem.*, 2021, **64**, 16675–16686, DOI: 10.1021/acs.jmedchem.1c01335.

179 R. Ramos, A. Karaiskou, C. Botuha, S. Amhaz, M. Trichet, F. Dingli, J. Forté, F. Lam, A. Canette, C. Chaumeton, M. Salome, T. Chenuel, C. Bergonzi, P. Meyer, S. Bohic, D. Loew, M. Salmain and J. Sobczak-Thépot, Identification of cellular protein targets of a half-sandwich iridium(III) complex reveals its dual mechanism of

 

action via both electrophilic and oxidative stresses, *J. Med. Chem.*, 2024, **67**, 6189–6206, DOI: 10.1021/acs.jmedchem.3c02000.

180 C. Gonzalo-Navarro, E. Zafon, J. A. Organero, F. A. Jalón, J. C. Lima, G. Espino, A. M. Rodríguez, L. Santos, A. J. Moro, S. Barrabés, J. Castro, J. Camacho-Aguayo, A. Massaguer, B. R. Manzano and G. Durá, Ir(III) half-sandwich photosensitizers with a π-expansive ligand for efficient anticancer photodynamic therapy, *J. Med. Chem.*, 2024, **67**, 1783–1811, DOI: 10.1021/acs.jmedchem.3c01276.

181 P. Štarha, Z. Trávníček, H. Crlíková, J. Vančo, J. Kašpárková and Z. Dvořák, Half-sandwich Ir(III) complex of *N*1-pyridyl-7-azaindole exceeds cytotoxicity of cisplatin at various human cancer cells and 3D multicellular tumor spheroids, *Organometallics*, 2018, **37**, 2749–2759, DOI: 10.1021/acs.organomet.8b00415.

182 N. Raja, N. Devika, G. Gupta, V. L. Nayak, A. Kamal, N. Nagesh and B. Therrien, Biological activities of pyrenyl-derived thiosemicarbazone half-sandwich complexes, *J. Organomet. Chem.*, 2015, **794**, 104–114, DOI: 10.1016/j.jorganchem.2015.06.036.

183 W. Su, B. Peng, P. Li, Q. Xiao, S. Huang, Y. Gu and Z. Lai, Synthesis, structure and antiproliferative activity of organometallic iridium(III) complexes containing thiosemicarbazone ligands, *Appl. Organomet. Chem.*, 2017, **31**, e3610, DOI: 10.1002/aoc.3610.

184 W. Su, Z. Luo, S. Dong, X. Chen, J. Xiao, B. Peng and P. Li, Novel half-sandwich rhodium(III) and iridium(III) photosensitizers for dual chemo- and photodynamic therapy, *Photodiagn. Photodyn. Ther.*, 2019, **26**, 448–454, DOI: 10.1016/j.pdpdt.2019.04.028.

185 S. Adhikari, O. Hussain, R. M. Phillips, W. Kaminsky and M. R. Kollipara, Synthesis, structural and chemosensitivity studies of arene $d^6$ metal complexes having N-phenyl-N'-(pyridyl/pyrimidyl)thiourea derivatives, *Appl. Organomet. Chem.*, 2018, **32**, e4362, DOI: 10.1002/aoc.4362.

186 K. K. H. Tong, M. Hanif, J. H. Lovett, K. Hummitzsch, H. H. Harris, T. Soehnel, S. M. F. Jamieson and C. G. Hartinger, Thiourea-derived chelating ligands and organometallic compounds and investigations into anticancer activity, *Molecules*, 2020, **25**, 3661, DOI: 10.3390/molecules25163661.

187 J. Arshad, K. K. H. Tong, S. Movassaghi, T. Sohnel, S. M. F. Jamieson, M. Hanif and C. G. Hartinger, Impact of the metal center and leaving group on the anticancer activity of organometallic complexes of pyridine-2-carbothioamide, *Molecules*, 2021, **26**, 833, DOI: 10.3390/molecules26040833.

188 Y. Yang, L. Guo, Z. Tian, X. Ge, Y. Gong, H. Zheng, S. Shi and Z. Liu, Lysosome-targeted phosphine-imine half-sandwich iridium(III) anticancer complexes: Synthesis, characterization, and biological activity, *Organometallics*, 2019, **38**, 1761–1769, DOI: 10.1021/acs.organomet.9b00080.

189 X. Hu, L. Guo, M. Liu, Q. Zhang, Y. Gong, M. Sun, S. Feng, Y. Xu, Y. Liu and Z. Liu, Increasing anticancer activity with phosphine ligation in zwitterionic half-sandwich iridium(III), rhodium(III), and ruthenium(II) complexes, *Inorg. Chem.*, 2022, **61**, 20008–20025, DOI: 10.1021/acs.inorgchem.2c03279.

190 W. Su, X. Wang, X. Lei, Q. Xiao, S. Huang and P. Li, Synthesis, characterization, cytotoxic activity of half-sandwich rhodium(III), and iridium(III) complexes with curcuminoids, *J. Organomet. Chem.*, 2017, **833**, 54–60, DOI: 10.1016/j.jorganchem.2017.01.028.

191 A. Petrini, R. Pettinari, F. Marchetti, C. Pettinari, B. Therrien, A. Galindo, R. Scopelliti, T. Riedel and P. J. Dyson, Cytotoxic half-sandwich Rh(III) and Ir(III) β-diketonates, *Inorg. Chem.*, 2017, **56**, 13600–13612, DOI: 10.1021/acs.inorgchem.7b02356.

192 G. Gupta, S. Cherukommu, G. Srinivas, S. W. Lee, S. H. Mun, J. Jung, N. Nagesh and C. Y. Lee, BODIPY-based Ru(II) and Ir(III) organometallic complexes of avobenzone, a sunscreen material: Potent anticancer agents, *J. Inorg. Biochem.*, 2018, **189**, 17–29, DOI: 10.1016/j.jinorgbio.2018.08.009.

193 C. M. Hackl, M. S. Legina, V. Pichler, M. Schmidlehner, A. Roller, O. Dömötör, E. A. Enyedy, M. A. Jakupec, W. Kandioller and B. K. Keppler, Thiomaltol-based organometallic complexes with 1-methylimidazole as leaving group: Synthesis, stability, and biological behavior, *Chem. – Eur. J.*, 2016, **22**, 17269–17281, DOI: 10.1002/chem.201603206.

194 S. Harringer, B. Happl, M. Ozenil, C. Kast, M. Hejl, D. Wernitznig, A. A. Legin, A. Schweikert, N. Gajic, A. Roller, G. Koellensperger, M. A. Jakupec, W. Kandioller and B. K. Keppler, Synthesis, modification, and biological evaluation of a library of novel water-soluble thiopyridone-based organometallic complexes and their unexpected (biological) behavior, *Chem. – Eur. J.*, 2020, **26**, 5419–5433, DOI: 10.1002/chem.201905546.

195 S. Harringer, D. Wernitznig, N. Gajic, A. Diridl, D. Wenisch, M. Hejl, M. A. Jakupec, S. Theiner, G. Koellensperger, W. Kandioller and B. K. Keppler, Introducing *N*-, *P*- and *S*-donor leaving groups: An investigation of the chemical and biological properties of ruthenium, rhodium and iridium thiopyridone piano stool complexes, *Dalton Trans.*, 2020, **49**, 15693–15711, DOI: 10.1039/D0DT03165H.

196 S. Harringer, M. Matzinger, N. Gajic, M. Hejl, M. A. Jakupec, W. Kandioller and B. K. Keppler, First insights into the novel class of organometallic compounds bearing a bidentate selenopyridone coordination motif: Synthesis, characterization, stability and biological investigations, *Inorg. Chim. Acta*, 2020, **513**, 119919, DOI: 10.1016/j.ica.2020.119919.

197 Q. Du, L. Guo, M. Tian, X. Ge, Y. Yang, X. Jian, Z. Xu, Z. Tian and Z. Liu, Potent half-sandwich iridium(III) and ruthenium(II) anticancer complexes containing a P^O-chelated ligand, *Organometallics*, 2018, **37**, 2880–2889, DOI: 10.1021/acs.organomet.8b00402.

198 Q. Du, Y. Yang, L. Guo, M. Tian, X. Ge, Z. Tian, L. Zhao, Z. Xu, J. Li and Z. Liu, Fluorescent half-sandwich phosphine-sulfonate iridium(III) and ruthenium(II) complexes as potential lysosome-targeted anticancer agents, *Dyes Pigm.*, 2019, **162**, 821–830, DOI: **10.1016/j.dyepig.2018.11.009**.

199 Y. Zhang, S. Zhang, Z. Tian, J. Li, Z. Xu, S. Li and Z. Liu, Phenoxide chelated Ir(III) N-heterocyclic carbene complexes: Synthesis, characterization, and evaluation of their *in vitro* anticancer activity, *Dalton Trans.*, 2018, **47**, 13781–13787, DOI: **10.1039/C8DT03159B**.

200 Z. Xu, Y. Zhang, S. Zhang, X. Jia, G. Zhong, Y. Yang, Q. Du, J. Li and Z. Liu, Novel half-sandwich iridium ÔC (carbene)-complexes: *In vitro* and *in vivo* tumor growth suppression and pro-apoptosis via ROS-mediated cross-talk between mitochondria and lysosomes, *Cancer Lett.*, 2019, **447**, 75–85, DOI: **10.1016/j.canlet.2019.01.018**.

201 J. J. Li, Z. Tian, S. Zhang, Z. Xu, X. Mao, Y. Zhou and Z. Liu, Organometallic ruthenium and iridium phosphorus complexes: Synthesis, cellular imaging, organelle targeting and anticancer applications, *Appl. Organomet. Chem.*, 2019, **33**, e4685, DOI: **10.1002/aoc.4685**.

202 J. Li, Z. Tian, Z. Xu, S. Zhang, Y. Feng, L. Zhang and Z. Liu, Highly potent half-sandwich iridium and ruthenium complexes as lysosome-targeted imaging and anticancer agents, *Dalton Trans.*, 2018, **47**, 15772–15782, DOI: **10.1039/C8DT02963F**.

203 J. Li, M. Tian, Z. Tian, S. Zhang, C. Yan, C. Shao and Z. Liu, Half-sandwich iridium(III) and ruthenium(II) complexes containing P-P-chelating ligands: A new class of potent anticancer agents with unusual redox features, *Inorg. Chem.*, 2018, **57**, 1705–1716, DOI: **10.1021/acs.inorgchem.7b01959**.

204 C. Wang, J. Liu, Z. Tian, M. Tian, L. Tian, W. Zhao and Z. Liu, Half-sandwich iridium N-heterocyclic carbene anticancer complexes, *Dalton Trans.*, 2017, **46**, 6870–6883, DOI: **10.1039/C7DT00575J**.

205 J. Zhang, J. Liu, X. Liu, B. Liu, S. Song, X. He, C. Che, M. Si, G. Yang and Z. Liu, Lysosome-targeted chemotherapeutics: Anticancer mechanism of N-heterocyclic carbene iridium(III) complex, *J. Inorg. Biochem.*, 2020, **207**, 111063, DOI: **10.1016/j.jinorgbio.2020.111063**.

206 Y. Han, Z. Tian, S. Zhang, X. Liu, J. Li, Y. Li, Y. Liu, M. Gao and Z. Liu, Half-sandwich Iridium$^{III}$ N-heterocyclic carbene antitumor complexes and biological applications, *J. Inorg. Biochem.*, 2018, **189**, 163–171, DOI: **10.1016/j.jinorgbio.2018.09.009**.

207 M. Ali Nazif, J.-A. Bangert, I. Ott, R. Gust, R. Stoll and W. S. Sheldrick, Dinuclear organoiridium(III) mono- and bis-intercalators with rigid bridging ligands: Synthesis, cytotoxicity and DNA binding, *J. Inorg. Biochem.*, 2009, **103**, 1405–1414, DOI: **10.1016/j.jinorgbio.2009.08.003**.

208 M. Ali Nazif, R. Rubbiani, H. Alborzinia, I. Kitanovic, S. Woelfl, I. Ott and W. S. Sheldrick, Cytotoxicity and cellular impact of dinuclear organoiridium DNA intercalators and nucleases with long rigid bridging ligands, *Dalton Trans.*, 2012, **41**, 5587–5598, DOI: **10.1039/C2DT00011C**.

209 P. Chellan, K. M. Land, A. Shokar, A. Au, S. H. An, D. Taylor, P. J. Smith, T. Riedel, P. J. Dyson, K. Chibale and G. S. Smith, Synthesis and evaluation of new polynuclear organometallic Ru(II), Rh(III) and Ir(III) pyridyl ester complexes as *in vitro* antiparasitic and antitumor agents, *Dalton Trans.*, 2014, **43**, 513–526, DOI: **10.1039/C3DT52090K**.

210 S. Parveen, M. Hanif, E. Leung, K. K. H. Tong, A. Yang, J. Astin, G. H. De Zoysa, T. R. Steel, D. Goodman, S. Movassaghi, T. Söhnel, V. Sarojini, S. M. F. Jamieson and C. G. Hartinger, Anticancer organorhodium and -iridium complexes with low toxicity *in vivo* but high potency *in vitro*: DNA damage, reactive oxygen species formation, and haemolytic activity, *Chem. Commun.*, 2019, **55**, 12016–12019, DOI: **10.1039/C9CC03822A**.

211 P. Štarha, J. Hošek, Z. Trávníček and Z. Dvořák, Cytotoxic dimeric half-sandwich Ru(II), Os(II) and Ir(III) complexes containing the 4,4′-biphenyl-based bridging ligands, *Appl. Organomet. Chem.*, 2020, **34**, e5785, DOI: **10.1002/aoc.5785**.

212 R. Payne, P. Govender, B. Therrien, C. M. Clavel, P. J. Dyson and G. S. Smith, Neutral and cationic multinuclear half-sandwich rhodium and iridium complexes coordinated to poly(propyleneimine) dendritic scaffolds: Synthesis and cytotoxicity, *J. Organomet. Chem.*, 2013, **729**, 20–27, DOI: **10.1016/j.jorganchem.2013.01.009**.

213 L. C. Sudding, R. Payne, P. Govender, F. Edafe, C. M. Clavel, P. J. Dyson, B. Therrien and G. S. Smith, Evaluation of the *in vitro* anticancer activity of cyclometalated half-sandwich rhodium and iridium complexes coordinated to naphthaldimine-based poly(propyleneimine) dendritic scaffolds, *J. Organomet. Chem.*, 2014, **774**, 79–85, DOI: **10.1016/j.jorganchem.2014.10.003**.

214 A. R. Burgoyne, C. H. Kaschula, M. I. Parker and G. S. Smith, *In vitro* cytotoxicity of half-sandwich platinum group metal complexes of a cationic alkylated phosphaadamantane ligand, *Eur. J. Inorg. Chem.*, 2016, 1267–1273, DOI: **10.1002/ejic.201501458**.

215 P. Govender, T. Riedel, P. J. Dyson and G. S. Smith, Regulating the anticancer properties of organometallic dendrimers using pyridylferrocene entities: Synthesis, cytotoxicity and DNA binding studies, *Dalton Trans.*, 2016, **45**, 9529–9539, DOI: **10.1039/C6DT00849F**.

216 A. B. P. Rao, A. Uma, T. Chiranjeevi, M. S. Bethu, J. V. Rao, D. K. Deb, B. Sarkar, W. Kaminsky and M. R. Kollipara, The *in vitro* antitumor activity of oligonuclear polypyridyl rhodium and iridium complexes against cancer cells and human pathogens, *J. Organomet. Chem.*, 2016, **824**, 131–139, DOI: **10.1016/j.jorganchem.2016.10.018**.

217 G. Gupta, A. Garci, B. S. Murray, P. J. Dyson, G. Fabre, P. Trouillas, F. Giannini, J. Furrer, G. Suss-Fink and B. Therrien, Synthesis, molecular structure, computational study and in vitro anticancer activity of dinuclear thiolatobridged pentamethylcyclopentadienyl Rh(III) and Ir(III) complexes, *Dalton Trans.*, 2013, **42**, 15457–15463, DOI: **10.1039/C3DT51991K**.

218 J. P. Johnpeter, G. Gupta, J. M. Kumar, G. Srinivas, N. Nagesh and B. Therrien, Biological studies of chalcogenolato-bridged dinuclear half-sandwich complexes, *Inorg. Chem.*, 2013, **52**, 13663–13673, DOI: 10.1021/ic4022307.

219 G. Gupta, B. S. Murray, P. J. Dyson and B. Therrien, Highly cytotoxic trithiolato-bridged dinuclear Rh(III) and Ir(III) complexes, *J. Organomet. Chem.*, 2014, **767**, 78–82, DOI: 10.1016/j.jorganchem.2014.05.021.

220 G. Gupta, B. S. Murray, P. J. Dyson and B. Therrien, Synthesis, molecular structure and cytotoxicity of molecular materials based on water soluble half-sandwich Rh(III) and Ir(III) tetranuclear metalla-cycles, *Materials*, 2013, **6**, 5352–5366, DOI: 10.3390/ma6115352.

221 G. Gupta, J. M. Kumar, A. Garci, N. Rangaraj, N. Nagesh and B. Therrien, Anticancer activity of half-sandwich Rh(III) and Ir(III) metalla-prisms containing lipophilic side chains, *ChemPlusChem*, 2014, **79**, 610–618, DOI: 10.1002/cplu.201300425.

222 G. Gupta, J. M. Kumar, A. Garci, N. Nagesh and B. Therrien, Exploiting natural products to build metalla-assemblies: The anticancer activity of embelin-derived Rh(III) and Ir(III) metalla-rectangles, *Molecules*, 2014, **19**, 6031–6046, DOI: 10.3390/molecules19056031.

223 G. Gupta, E. Denoyelle-Di-Muro, J. P. Mbakidi, S. Leroy-Lhez, V. Sol and B. Therrien, Delivery of porphin to cancer cells by organometallic Rh(III) and Ir(III) metalla-cages, *J. Organomet. Chem.*, 2015, **787**, 44–50, DOI: 10.1016/j.jorganchem.2015.03.035.

224 G. Gupta, G. S. Oggu, N. Nagesh, K. K. Bokara and B. Therrien, Anticancer activity of large metalla-assemblies built from half-sandwich complexes, *CrystEngComm*, 2016, **18**, 4952–4957, DOI: 10.1039/C6CE00139D.

225 L. Masaryk, P. Koczurkiewicz-Adamczyk, D. Milde, I. Nemec, K. Sloczynska, E. Pękala and P. Štarha, Dinuclear half-sandwich Ir(III) complexes containing 4,4′-methylenedianiline-based ligands: Synthesis, characterization, cytotoxicity, *J. Organomet. Chem.*, 2021, **938**, 121748, DOI: 10.1016/j.jorganchem.2021.121748.

226 T. R. Steel, K. K. H. Tong, T. Sohnel, S. M. F. Jamieson, L. J. Wright, J. D. Crowley, M. Hanif and C. G. Hartinger, Homodinuclear organometallics of ditopic N,N-chelates: Synthesis, reactivity and in vitro anticancer activity, *Inorg. Chim. Acta*, 2021, **518**, 120220, DOI: 10.1016/j.ica.2020.120220.

227 E. Řezníčková, O. Bárta, D. Milde, V. Kryštof and P. Štarha, Anticancer dinuclear Ir(III) complex activates Nrf2 and interferes with NAD(H) in cancer cells, *J. Inorg. Biochem.*, 2025, **262**, 112704, DOI: 10.1016/j.jinorgbio.2024.112704.

228 N. Msimango, A. Welsh, S. Prince and G. S. Smith, Synthesis and anticancer evaluation of trinuclear N-N quinolyl-benzimidazole-based PGM complexes, *Inorg. Chem. Commun.*, 2022, **144**, 109840, DOI: 10.1016/j.inoche.2022.109840.

229 H. Sepehrpour, W. Fu, Y. Sun and P. J. Stang, Biomedically relevant self-assembled metallacycles and metallacages, *J. Am. Chem. Soc.*, 2019, **141**, 14005–14020, DOI: 10.1021/jacs.9b06222.

230 H. Tang, G. C. Saunders, O. Raymond, X. Ma and W. Henderson, Pyrrole thioamide complexes of organo-rhodium(III), -iridium(III) and -ruthenium(II), *Inorg. Chim. Acta*, 2020, **506**, 119545, DOI: 10.1016/j.ica.2020.119545.

231 M. Shao, M. Yao, X. Liu, C. Gao, W. Liu, J. Guo, J. Zong, X. Sun and Z. Liu, *In vitro* and *in vivo* of triphenylamine-appended fluorescent half-sandwich iridium(III) thiosemicarbazones antitumor complexes, *Inorg. Chem.*, 2021, **60**, 17063–17073, DOI: 10.1021/acs.inorgchem.1c02250.

232 X. Liu, A. Lv, P. Zhang, J. Chang, R. Dong, M. Liu, J. Liu, X. Huang, X. Yuan and Z. Liu, Anticancer application of half-sandwich iridium(III) ferrocene-thiosemicarbazide Schiff base complexes, *Dalton Trans.*, 2024, **53**, 552–563, DOI: 10.1039/D3DT02879H.

233 S. B. Kavukcu, H. K. Ensarioğlu, H. Karabıyık, H. S. Vatansever and H. Türkmen, Cell death mechanism of organometallic ruthenium(II) and iridium(III) arene complexes on HepG2 and Vero cells, *ACS Omega*, 2023, **8**, 37549–37563, DOI: 10.1021/acsomega.3c05898.

234 R. Stodt, S. Gencaslan, A. Frodl, C. Schmidt and W. S. Sheldrick, Functional mono- and dinuclear peptide complexes featuring chemospecific κS- or $\eta^6$-coordination of organometallic half-sandwich fragments, *Inorg. Chim. Acta*, 2003, **355**, 242–253, DOI: 10.1016/S0020-1693(03)00345-1.

235 S. Gençaslan and W. S. Sheldrick, Bifunctional bioorganometallic iridium(III)–platinum(II) complexes incorporating both intercalative and covalent DNA binding capabilities, *Eur. J. Inorg. Chem.*, 2005, 3840–3849, DOI: 10.1002/ejic.200500223.

236 W. Nkoana, D. Nyoni, P. Chellan, T. Stringer, D. Taylor, P. J. Smith, A. T. Hutton and G. S. Smith, Heterometallic half-sandwich complexes containing a ferrocenyl motif: Synthesis, molecular structure, electrochemistry and antiplasmodial evaluation, *J. Organomet. Chem.*, 2014, **752**, 67–75, DOI: 10.1016/j.jorganchem.2013.11.025.

237 R. P. Paitandi, R. K. Gupta, R. S. Singh, G. Sharma, B. Koch and D. S. Pandey, Interaction of ferrocene appended Ru(II), Rh(III) and Ir(III) dipyrrinato complexes with DNA/protein, molecular docking and antitumor activity, *Eur. J. Med. Chem.*, 2014, **84**, 17–29, DOI: 10.1016/j.ejmech.2014.06.052.

238 I. Cassells, T. Stringer, A. T. Hutton, S. Prince and G. S. Smith, Impact of various lipophilic substituents on ruthenium(II), rhodium(III) and iridium(III) salicylaldimine-based complexes: Synthesis, in vitro cytotoxicity studies and DNA interactions, *J. Biol. Inorg. Chem.*, 2018, **23**, 763–774, DOI: 10.1007/s00775-018-1567-3.

239 X. Ge, S. Chen, X. Liu, Q. Wang, L. Gao, C. Zhao, L. Zhang, M. Shao, X.-A. Yuan, L. Tian and Z. Liu, Ferrocene-appended iridium(III) complexes: Configuration regulation, anticancer application, and mechanism

research, *Inorg. Chem.*, 2019, **58**, 14175–14184, DOI: 10.1021/acs.inorgchem.9b02227.

240 Z. Wang, Z. Lv, X. Liu, Y. Wu, J. Chang, R. Dong, C. Li, X.-A. Yuan and Z. Liu, Anticancer application of ferrocene appended configuration-regulated half-sandwich iridium (III) pyridine complexes, *J. Inorg. Biochem.*, 2022, **237**, 112010, DOI: 10.1016/j.jinorgbio.2022.112010.

241 J. Liu, Y. Wu, G. Yang, Z. Liu and X. Liu, Mitochondrial targeting half-sandwich iridium(III) and ruthenium(II) dppf complexes and *in vitro* anticancer assay, *J. Inorg. Biochem.*, 2023, **239**, 112069, DOI: 10.1016/j.jinorgbio.2022.112069.

242 X. Liu, Z. Wang, X. Zhang, X. Lv, Y. Sun, R. Dong, G. Li, X. Ren, Z. Ji, X.-A. Yuan and Z. Liu, Configurationally regulated half-sandwich iridium(III)-ferrocene heteronuclear metal complexes: Potential anticancer agents, *J. Inorg. Biochem.*, 2023, **249**, 112393, DOI: 10.1016/j.jinorgbio.2023.112393.

243 B. Bertrand, G. Gontard, C. Botuha and M. Salmain, Pincer-based heterobimetallic Pt(II)/Ru(II), Pt(II)/Ir(III) and Pt(II)/Cu(I) complexes: Synthesis and evaluation of antiproliferative properties, *Eur. J. Inorg. Chem.*, 2020, **2020**, 3370–3377, DOI: 10.1002/ejic.202000717.

244 N. Roy, U. Sen, P. Moharana, L. T. Babu, B. Kar, S. Vardhan, S. K. Sahoo, B. Bose and P. Paira, 2,2′-Bipyrimidine-based luminescent Ru(II)/Ir(III)–arene monometallic and homo- and hetero-bimetallic complexes for therapy against MDA-MB-468 and Caco-2 cells, *Dalton Trans.*, 2021, **50**, 11725–11729, DOI: 10.1039/D1DT01556G.

245 N. Roy, S. Shanavas, B. Kar, L. Thilak Babu, U. Das, S. Vardhan, S. K. Sahoo, B. Bose, V. Rajagopalan and P. Paira, G2/M-Phase-inhibitory mitochondrial-depolarizing Re(I)/Ru(II)/Ir(III)-2,2′-bipyrimidine-based heterobimetallic luminescent complexes: An assessment of *in vitro* antiproliferative activity and bioimaging for targeted therapy toward human TNBC cells, *ACS Omega*, 2023, **8**, 12283–12297, DOI: 10.1021/acsomega.2c08285.

246 U. K. Komarnicka, S. Koziel, B. Pucelik, A. Barzowska, M. Siczek, M. Malik, D. Wojtala, A. Niorettini, A. Kyziol, V. Sebastian, P. Kopel, S. Caramori and A. Bieńko, Liposomal binuclear Ir(III)-Cu(II) coordination compounds with phosphino-fluoroquinolone conjugates for human prostate carcinoma treatment, *Inorg. Chem.*, 2022, **61**, 19261–19273, DOI: 10.1021/acs.inorgchem.2c03015.

247 W. D. J. Tremlett, K. K. H. Tong, T. R. Steel, S. Movassaghi, M. Hanif, S. M. F. Jamieson, T. Sohnel and C. G. Hartinger, Hydroxyquinoline-derived anticancer organometallics: Introduction of amphiphilic PTA as an ancillary ligand increases their aqueous solubility, *J. Inorg. Biochem.*, 2019, **199**, 110768, DOI: 10.1016/j.jinorgbio.2019.110768.

248 W.-Y. Zhang, S. Banerjee, G. M. Hughes, H. E. Bridgewater, J.-I. Song, B. G. Breeze, G. J. Clarkson, J. P. C. Coverdale, C. Sanchez-Cano, F. Ponte, E. Sicilia and P. J. Sadler, Ligand-centred redox activation of inert organoiridium anticancer catalysts, *Chem. Sci.*, 2020, **11**, 5466–5480, DOI: 10.1039/D0SC00897D.

249 P. Štarha, A. Habtemariam, I. Romero-Canelón, G. J. Clarkson and P. J. Sadler, Hydrosulfide adducts of organo-iridium anticancer complexes, *Inorg. Chem.*, 2016, **55**, 2324–2331, DOI: 10.1021/acs.inorgchem.5b02697.

250 P. Štarha, Z. Trávníček, B. Drahoš, R. Herchel and Z. Dvořák, Cell-based studies of the first-in-class half-sandwich Ir(III) complex containing histone deacetylase inhibitor 4-phenylbutyrate, *Appl. Organomet. Chem.*, 2018, **32**, e4246, DOI: 10.1002/aoc.4246.

251 L. Tabrizi, The discovery of half-sandwich iridium complexes containing lidocaine and (pyren-1-yl)ethynyl derivatives of phenylcyanamide ligands for photodynamic therapy, *Dalton Trans.*, 2017, **46**, 7242–7252, DOI: 10.1039/C7DT01091E.

252 B. P. R. Aradhyula, M. Kalidasan, K. Gangele, D. K. Deb, S. L. Shepherd, R. M. Phillips, K. M. Poluri and M. R. Kollipara, Synthesis, structural and biological studies of some half-sandwich $d^6$-metal complexes with pyrimidine-based ligands, *ChemistrySelect*, 2017, **2**, 2065–2076, DOI: 10.1002/slct.201601926.

253 H. Amouri, J. Moussa, A. K. Renfrew, P. J. Dyson, M. N. Rager and L. M. Chamoreau, Discovery, structure, and anticancer activity of an iridium complex of diselenobenzoquinone, *Angew. Chem., Int. Ed.*, 2010, **49**, 7530–7533, DOI: 10.1002/anie.201002532.

254 Q. Du, L. Guo, X. Ge, L. Zhao, Z. Tian, X. Liu, F. Zhang and Z. Liu, Serendipitous synthesis of five-coordinated half-sandwich aminoimine iridium(III) and ruthenium(II) complexes and their application as potent anticancer agents, *Inorg. Chem.*, 2019, **58**, 5956–5965, DOI: 10.1021/acs.inorgchem.9b00282.

255 J. Gao, L. Guo, Y. Wu, Y. Cheng, X. Hu, J. Liu and Z. Liu, 16-Electron half-sandwich rhodium(III), iridium(III), and ruthenium(II) complexes as lysosome-targeted anticancer agents, *Organometallics*, 2021, **40**, 3999–4010, DOI: 10.1021/acs.organomet.1c00572.

256 L. Guo, P. Li, J. Li, Y. Gong, X. Li, T. Wen, X. Wu, X. Yang and Z. Liu, Potent half-sandwich 16-/18-electron iridium (III) and ruthenium(II) anticancer complexes with readily available amine–imine ligands, *Inorg. Chem.*, 2023, **62**, 21379–21395, DOI: 10.1021/acs.inorgchem.3c03471.

257 M. Azmanova, J. Soldevila-Barreda, H. Bani Hani, R. M. Lord, A. Pitto-Barry, S. M. Picksley and N. P. E. Barry, Anticancer activity of electron-deficient metal complexes against colorectal cancer *in vitro* models, *ChemMedChem*, 2019, **14**, 1887–1893, DOI: 10.1002/cmdc.201900528.

258 Y. Yang, L. Guo, X. Ge, T. Zhu, W. Chen, H. Zhou, L. Zhao and Z. Liu, The fluorine effect in zwitterionic half-sandwich iridium(III) anticancer complexes, *Inorg. Chem.*, 2020, **59**, 748–758, DOI: 10.1021/acs.inorgchem.9b03006.

259 A. De Palo, D. Draca, M. G. Murrali, S. Zacchini, G. Pampaloni, S. Mijatovic, D. Maksimovic-Ivanic and F. Marchetti, A comparative analysis of the *in vitro* anti-

 

cancer activity of iridium(III){$\eta^5$-$C_5Me_4R$} complexes with variable R groups, *Int. J. Mol. Sci.*, 2021, **22**, 7422, DOI: 10.3390/ijms22147422.

260 H. Zhang, L. Guo, Z. Tian, M. Tian, S. Zhang, Z. Xu, P. Gong, X. Zheng, J. Zhao and Z. Liu, Significant effects of counteranions on the anticancer activity of iridium(III) complexes, *Chem. Commun.*, 2018, **54**, 4421–4424, DOI: 10.1039/C8CC01326H.

261 X. Duan, D. Liu, C. Chan and W. Lin, Polymeric micelle-mediated delivery of DNA-targeting organometallic complexes for resistant ovarian cancer treatment, *Small*, 2015, **11**, 3962–3972, DOI: 10.1002/smll.201500288.

262 J. M. Hearn, I. Romero-Canelon, B. Qamar, Z. Liu, I. Hands-Portman and P. J. Sadler, Organometallic iridium(III) anticancer complexes with new mechanisms of action: NCI-60 screening, mitochondrial targeting, and apoptosis, *ACS Chem. Biol.*, 2013, **8**, 1335–1343, DOI: 10.1021/cb400070a.

263 J. M. Hearn, G. M. Hughes, I. Romero-Canelon, A. F. Munro, B. Rubio-Ruiz, Z. Liu, N. O. Carragher and P. J. Sadler, Pharmaco-genomic investigations of organo-iridium anticancer complexes reveal novel mechanism of action, *Metallomics*, 2018, **10**, 93–107, DOI: 10.1039/c7mt00242d.

264 S. J. Berners-Price, T. A. Frenkiel, U. Frey, J. D. Ranford and P. J. Sadler, Hydrolysis products of cisplatin: pKa determinations via[$^1$H, $^{15}$N] NMR spectroscopy, *J. Chem. Soc., Chem. Commun.*, 1992, 789–791, DOI: 10.1039/C39920000789.

265 L. Dadci, H. Elias, U. Frey, A. Hoernig, U. Koelle, A. E. Merbach, H. Paulus and J. S. Schneider, .pi.-Arene aqua complexes of cobalt, rhodium, iridium, and ruthenium: Preparation, structure, and kinetics of water exchange and water substitution, *Inorg. Chem.*, 1995, **34**, 306–315, DOI: 10.1021/ic00105a048.

266 I. Ritacco, N. Russo and E. Sicilia, DFT investigation of the mechanism of action of organoiridium(III) complexes as anticancer agents, *Inorg. Chem.*, 2015, **54**, 10801–10810, DOI: 10.1021/acs.inorgchem.5b01832.

267 S. Berger, J. Fiedler, R. Reinhardt and W. Kaim, Metal vs ligand reduction in complexes of dipyrido[3,2-a:2′,3′-c] phenazine and related ligands with $[(C_5Me_5)ClM]^+$ (M = Rh or Ir): Evidence for potential rather than orbital control in the reductive cleavage of the metal–chloride bond, *Inorg. Chem.*, 2004, **43**, 1530–1538, DOI: 10.1021/ic0351388.

268 W.-Y. Zhang, S. Banerjee, C. Imberti, G. J. Clarkson, Q. Wang, Q. Zhong, L. S. Young, I. Romero-Canelon, M. Zeng, A. Habtemariam and P. J. Sadler, Strategies for conjugating iridium(III) anticancer complexes to targeting peptides *via* copper-free click chemistry, *Inorg. Chim. Acta*, 2020, **503**, 119396, DOI: 10.1016/j.ica.2019.119396.

269 G. Gupta, A. Das, N. B. Ghate, T. Kim, J. Y. Ryu, J. Lee, N. Mandal and C. Y. Lee, Novel BODIPY-based Ru(II) and Ir(III) metallarectangles: Cellular localization of compounds and their antiproliferative activities, *Chem. Commun.*, 2016, **52**, 4274–4277, DOI: 10.1039/C6CC00046K.

270 C. Mari, H. Huang, R. Rubbiani, M. Schulze, F. Wuerthner, H. Chao and G. Gasser, Evaluation of perylene bisimide-based $Ru^{II}$ and $Ir^{III}$ complexes as photosensitizers for photodynamic therapy, *Eur. J. Inorg. Chem.*, 2017, **2017**, 1745–1752, DOI: 10.1002/ejic.201600516.

271 G. Gupta, P. Kumari, J. Y. Ryu, J. Lee, S. M. Mobin and C. Y. Lee, Mitochondrial localization of highly fluorescent and photostable BODIPY-based ruthenium(II), rhodium (III), and iridium(III) metal complexes, *Inorg. Chem.*, 2019, **58**, 8587–8595, DOI: 10.1021/acs.inorgchem.9b00898.

272 G. Gupta, A. Das, S. W. Lee, J. Y. Ryu, J. Lee, N. Nagesh, N. Mandal and C. Y. Lee, BODIPY-based Ir(III) rectangles containing bis-benzimidazole ligands with highly selective toxicity obtained through self-assembly, *J. Organomet. Chem.*, 2018, **868**, 86–94, DOI: 10.1016/j.jorganchem.2018.04.034.

273 G. Gupta, A. Das, J. Lee, N. Mandal and C. Y. Lee, Multinuclear Ir-BODIPY complexes: Synthesis and binding studies, *Inorg. Chem. Commun.*, 2020, **113**, 107759, DOI: 10.1016/j.inoche.2019.107759.

274 R. P. Paitandi, S. Mukhopadhyay, R. S. Singh, V. Sharma, S. M. Mobin and D. S. Pandey, Anticancer activity of iridium(III) complexes based on a pyrazole-appended quinoline-based BODIPY, *Inorg. Chem.*, 2017, **56**, 12232–12247, DOI: 10.1021/acs.inorgchem.7b01693.

275 M. Kokoschka, J.-A. Bangert, R. Stoll and W. S. Sheldrick, Sequence-selective organoiridium DNA bis-intercalators with flexible dithiaalkane linker chains, *Eur. J. Inorg. Chem.*, 2010, 1507–1515, DOI: 10.1002/ejic.200901123.

276 I. Romero-Canelon and P. J. Sadler, Next-generation metal anticancer complexes: Multitargeting *via* redox modulation, *Inorg. Chem.*, 2013, **52**, 12276–12291, DOI: 10.1021/ic400835n.

277 H. T. H. Nguyen and L. H. Do, Organoiridium-quinone conjugates for facile hydrogen peroxide generation, *Chem. Commun.*, 2020, **56**, 13381–13384, DOI: 10.1039/D0CC04970K.

278 J. J. Soldevila-Barreda and P. J. Sadler, Approaches to the design of catalytic metallodrugs, *Curr. Opin. Chem. Biol.*, 2015, **25**, 172–183, DOI: 10.1016/j.cbpa.2015.01.024.

279 Z. Yu and J. A. Cowan, Catalytic metallodrugs: Substrate-selective metal catalysts as therapeutics, *Chem. – Eur. J.*, 2017, **23**, 14113–14127, DOI: 10.1002/chem.201701714.

280 E. Steckhan, S. Herrmann, R. Ruppert, E. Dietz, M. Frede and E. Spika, Analytical study of a series of substituted (2,2′-bipyridyl)(pentamethylcyclopentadienyl) rhodium and -iridium complexes with regard to their effectiveness as redox catalysts for the indirect electrochemical and chemical reduction of $NAD(P)^+$, *Organometallics*, 1991, **10**, 1568–1577, DOI: 10.1021/om00051a056.

281 J. Canivet, G. Süss-Fink and P. Štěpnička, Water-soluble phenanthroline complexes of rhodium, iridium and ruthenium for the regeneration of NADH in the enzymatic

reduction of ketones, *Eur. J. Inorg. Chem.*, 2007, 4736–4742, DOI: 10.1002/ejic.200700505.

282 S. Betanzos-Lara, Z. Liu, A. Habtemariam, A. M. Pizarro, B. Qamar and P. J. Sadler, Organometallic ruthenium and iridium transfer-hydrogenation catalysts using coenzyme NADH as a cofactor, *Angew. Chem., Int. Ed.*, 2012, **51**, 3897–3900, DOI: 10.1002/anie.201108175.

283 Z. Liu, R. J. Deeth, J. S. Butler, A. Habtemariam, M. E. Newton and P. J. Sadler, Reduction of quinones by NADH catalyzed by organoiridium complexes, *Angew. Chem., Int. Ed.*, 2013, **52**, 4194–4197, DOI: 10.1002/anie.201300747.

284 H. Komatsu, N. Velychkivska, A. B. Shatan, Y. Shindo, K. Oka, K. Ariga, J. P. Hill and J. Labuta, Kinetic study of NADPH activation using ubiquinone-rhodol fluorescent probe and an $Ir^{III}$ complex promoter at the cell interior, *RSC Adv.*, 2023, **13**, 34012–34019, DOI: 10.1039/D3RA05412H.

285 T. Stringer, D. R. Melis and G. S. Smith, N,O-Chelating quinoline-based half-sandwich organorhodium and -iridium complexes: synthesis, antiplasmodial activity and preliminary evaluation as transfer hydrogenation catalysts for the reduction of $NAD^+$, *Dalton Trans.*, 2019, **48**, 13143–13148, DOI: 10.1039/C9DT02030F.

286 D. R. Melis, C. B. Barnett, L. Wiesner, E. Nordlander and G. S. Smith, Quinoline-triazole half-sandwich iridium(III) complexes: Synthesis, antiplasmodial activity and preliminary transfer hydrogenation studies, *Dalton Trans.*, 2020, **49**, 11543–11555, DOI: 10.1039/D0DT01935F.

287 G. Noctor, G. Queval, A. Mhamdi, S. Chaouch and C. H. Foyer, Glutathione, *Arabidopsis Book*, 2011, vol. 9, pp. e0142. DOI: 10.1199/tab.0142.

288 N. Z. Homer, J. Reglinski, R. Sowden, C. M. Spickett, R. Wilson and J. J. Walker, Dimethylsulfoxide oxidizes glutathione *in vitro* and in human erythrocytes: Kinetic analysis by $^1H$ NMR, *Cryobiology*, 2005, **50**, 317–324, DOI: 10.1016/j.cryobiol.2005.04.002.

289 I. Tolbatov and A. Marrone, Reactivity of N-heterocyclic carbene half-sandwich Ru-, Os-, Rh-, and Ir-based complexes with cysteine and selenocysteine: A computational study, *Inorg. Chem.*, 2022, **61**, 746–754, DOI: 10.1021/acs.inorgchem.1c03608.

290 A. Nemirovski, I. Vinograd, K. Takrouri, A. Mijovilovich, A. Rompel and D. Gibson, New reduction pathways for *ctc*-$[PtCl_2(CH_3CO_2)_2(NH_3)(Am)]$ anticancer prodrugs, *Chem. Commun.*, 2010, **46**, 1842–1844, DOI: 10.1039/B925721G.

291 Y. Qi, Z. Liu, H. Li, P. J. Sadler and P. B. O'Connor, Mapping the protein-binding sites for novel iridium(III) anticancer complexes using electron capture dissociation, *Rapid Commun. Mass Spectrom.*, 2013, **27**, 2028–2032, DOI: 10.1002/rcm.6643.

292 C. A. Wootton, A. J. Millett, A. F. Lopez-Clavijo, C. K. C. Chiu, M. P. Barrow, G. J. Clarkson, P. J. Sadler and P. B. O'Connor, Structural analysis of peptides modified with organo-iridium complexes, opportunities from multimode fragmentation, *Analyst*, 2019, **144**, 1575–1581, DOI: 10.1039/C8AN02094A.

293 R. Das, U. Das, N. Roy, C. Mukherjee, S. U and P. Paira, A Glance on target specific PDT active cyclometalated iridium complexes, *Dyes Pigm.*, 2024, **226**, 112134, DOI: 10.1016/j.dyepig.2024.112134.

294 B. F. Hohlfeld, B. Gitter, C. J. Kingsbury, K. J. Flanagan, D. Steen, G. D. Wieland, N. Kulak, M. O. Senge and A. Wiehe, Dipyrrinato-iridium(III) complexes for application in photodynamic therapy and antimicrobial photodynamic inactivation, *Chem. – Eur. J.*, 2021, **27**, 6440–6459, DOI: 10.1002/chem.202004776.

295 Z. Cai, H. Zhang, Y. Wei, Y. Wei, Y. Xie and F. Cong, Reduction- and pH-sensitive hyaluronan nanoparticles for delivery of iridium(III) anticancer drugs, *Biomacromolecules*, 2017, **18**, 2102–2117, DOI: 10.1021/acs.biomac.7b00445.

296 S. C. Larnaudie, J. C. Brendel, I. Romero-Canelon, C. Sanchez-Cano, S. Catrouillet, J. Sanchis, J. P. C. Coverdale, J. Song, A. Habtemariam, P. J. Sadler, K. A. Jolliffe and S. Perrier, Cyclic peptide-polymer nanotubes as efficient and highly potent drug delivery systems for organometallic anticancer complexes, *Biomacromolecules*, 2018, **19**, 239–247, DOI: 10.1021/acs.biomac.7b00445.

297 C. Weng, L. Shen, J. W. Teo, Z. C. Lim, B. S. Loh and W. H. Ang, Targeted antibacterial strategy based on reactive oxygen species generated from dioxygen reduction using an organoruthenium complex, *JACS Au*, 2021, **1**, 1348–1354, DOI: 10.1021/jacsau.1c00262.

298 A. T. Odularu, P. A. Ajibade, J. Z. Mbese and O. O. Oyedeji, Developments in platinum-group metals as dual antibacterial and anticancer agents, *J. Chem.*, 2019, **2019**, 5459461, DOI: 10.1155/2019/5459461.

299 A. Frei, Metal complexes, an untapped source of antibiotic potential?, *Antibiotics*, 2020, **9**, 90, DOI: 10.3390/antibiotics9020090.

300 A. B. P. Rao, K. Gulati, N. Joshi, D. K. Deb, D. Rambabu, W. Kaminsky, K. M. Poluri and M. R. Kollipara, Synthesis and biological studies of ruthenium, rhodium and iridium metal complexes with pyrazole-based ligands displaying unpredicted bonding modes, *Inorg. Chim. Acta*, 2017, **462**, 223–235, DOI: 10.1016/j.ica.2017.03.037.

301 G. W. Karpin, D. M. Morris, M. T. Ngo, J. S. Merola and J. O. Falkinham III, Transition metal diamine complexes with antimicrobial activity against *Staphylococcus aureus* and methicillin-resistant *S. aureus* (MRSA), *MedChemComm*, 2015, **6**, 1471–1478, DOI: 10.1039/C5MD00228A.

302 L. Shadap, S. Diamai, V. Banothu, D. P. S. Negi, U. Adepally, W. Kaminsky and M. R. Kollipara, Half sandwich platinum group metal complexes of thiourea derivative ligands with benzothiazole moiety possessing antibacterial activity and colorimetric sensing: Synthesis and characterisation, *J. Organomet. Chem.*, 2019, **884**, 44–54, DOI: 10.1016/j.jorganchem.2019.01.019.

303 L.-i. Rylands, A. Welsh, K. Maepa, T. Stringer, D. Taylor, K. Chibale and G. S. Smith, Structure-activity relationship

 

studies of antiplasmodial cyclometallated ruthenium(II), rhodium(III) and iridium(III) complexes of 2-phenylbenzimidazoles, *Eur. J. Med. Chem.*, 2019, **161**, 11–21, DOI: 10.1016/j.ejmech.2018.10.019.

304 C. M. DuChane, L. C. Brown, V. S. Dozier and J. S. Merola, Synthesis, characterization, and antimicrobial activity of $Rh^{III}$ and $Ir^{III}$ β-diketonato piano-stool compounds, *Organometallics*, 2018, **37**, 530–538, DOI: 10.1021/acs.organomet.7b00742.

305 P. Chellan, K. M. Land, A. Shokar, A. Au, S. H. An, D. Taylor, P. J. Smith, K. Chibale and G. S. Smith, Di- and trinuclear ruthenium-, rhodium-, and iridium-functionalized pyridyl aromatic ethers: A new class of antiparasitic agents, *Organometallics*, 2013, **32**, 4793–4804, DOI: 10.1021/om400493k.

306 F. Chen, J. Moat, D. McFeely, G. Clarkson, I. J. Hands-Portman, J. P. Furner-Pardoe, F. Harrison, C. G. Dowson and P. J. Sadler, Biguanide iridium(III) complexes with potent antimicrobial activity, *J. Med. Chem.*, 2018, **61**, 7330–7344, DOI: 10.1021/acs.jmedchem.8b00906.

307 G. W. Karpin, J. S. Merola and J. O. Falkinham, Transition metal-α-amino acid complexes with antibiotic activity against *Mycobacterium spp.*, *Antimicrob. Agents Chemother.*, 2013, **57**, 3434–3436, DOI: 10.1128/aac.00452-13.

308 E. Ekengard, K. Kumar, T. Fogeron, C. de Kock, P. J. Smith, M. Haukka, M. Monari and E. Nordlander, Pentamethylcyclopentadienylrhodium and -iridium complexes containing (N^N and N^O) bound chloroquine analog ligands: synthesis, characterization and antimalarial properties, *Dalton Trans.*, 2016, **45**, 3905–3917, DOI: 10.1039/C5DT03739E.

309 N. Baartzes, A. Jordaan, D. F. Warner, J. Combrinck, D. Taylor, K. Chibale and G. S. Smith, Antimicrobial evaluation of neutral and cationic iridium(III) and rhodium(III) aminoquinoline-benzimidazole hybrid complexes, *Eur. J. Med. Chem.*, 2020, **206**, 112694, DOI: 10.1016/j.ejmech.2020.112694.

310 T. Stringer, M. A. S. Quintero, L. Wiesner, G. S. Smith and E. Nordlander, Evaluation of PTA-derived ruthenium(II) and iridium(III) quinoline complexes against chloroquine-sensitive and resistant strains of the *Plasmodium falciparum* malaria parasite, *J. Inorg. Biochem.*, 2019, **191**, 164–173, DOI: 10.1016/j.jinorgbio.2018.11.018.

311 C. M. DuChane, G. W. Karpin, M. Ehrich, J. O. Falkinham and J. S. Merola, Iridium piano stool complexes with activity against *S. aureus* and MRSA: it is past time to truly think outside of the box, *MedChemComm*, 2019, **10**, 1391–1398, DOI: 10.1039/C9MD00140A.

312 P. A. Vekariya, P. S. Karia, J. V. Vaghasiya, S. Soni, E. Suresh and M. N. Patel, Evolution of rhodium(III) and iridium(III) chelates as metallonucleases, *Polyhedron*, 2016, **110**, 73–84, DOI: 10.1016/j.poly.2016.01.050.

313 L. Shadap, J. L. Tyagi, K. M. Poluri, S. Novikov, C.-W. T. Lo, Y. Mozharivskyj and M. R. Kollipara, Insights to the strained thiocarbamate derivative complexes of platinum group metals induced by azide as a co-ligand: Characterization and biological studies, *J. Organomet. Chem.*, 2020, **920**, 121345, DOI: 10.1016/j.jorganchem.2020.121345.

314 C. G. L. Nongpiur, L. Dkhar, D. K. Tripathi, K. M. Poluri, W. Kaminsky and M. R. Kollipara, Half-sandwich platinum group metal complexes containing coumarin-*N*-acylhydrazone hybrid ligands: Synthesis and biological evaluation studies, *Inorg. Chim. Acta*, 2021, **525**, 120459, DOI: 10.1016/j.ica.2021.120459.

315 A. Lapasam, L. Shadap, D. K. Tripathi, K. M. Poluri, W. Kaminsky and M. R. Kollipara, Arene ruthenium, rhodium and iridium complexes containing N∩O chelating ligands: synthesis, antibacterial and antioxidant studies, *J. Coord. Chem.*, 2021, **74**, 2365–2379, DOI: 10.1080/00958972.2021.1963439.

316 L. Shadap, N. Agarwal, V. Chetry, K. M. Poluri, W. Kaminsky and M. R. Kollipara, Arene ruthenium, rhodium and iridium complexes containing benzamide derivative ligands: Study of interesting bonding modes, antibacterial, antioxidant and DNA binding studies, *J. Organomet. Chem.*, 2021, **937**, 121731, DOI: 10.1016/j.jorganchem.2021.121731.

317 C. G. L. Nongpiur, D. F. Diengdoh, V. Banothu, P. M. Gannon, W. Kaminsky and M. R. Kollipara, Variable coordination behavior of rhodium metal complexes towards thiourea derivative ligands in comparison to its ruthenium and iridium analogs: Synthesis and biological studies, *J. Organomet. Chem.*, 2023, **999**, 122823, DOI: 10.1016/j.jorganchem.2023.122823.

318 C. G. L. Nongpiur, C. Soh, D. F. Diengdoh, A. K. Verma, R. Gogoi, V. Banothu, W. Kaminsky and M. R. Kollipara, 3-Acetyl-coumarin-substituted thiosemicarbazones and their ruthenium, rhodium and iridium metal complexes: An investigation of the antibacterial, antioxidant and cytotoxicity activities, *J. Organomet. Chem.*, 2023, **998**, 122788, DOI: 10.1016/j.jorganchem.2023.122788.

319 L. Dkhar, V. Banothu, K. M. Poluri, W. Kaminsky and M. R. Kollipara, Platinum group complexes containing salicylaldehyde based thiosemicarbazone ligands: Their synthesis, characterization, bonding modes, antibacterial and antioxidant studies, *J. Organomet. Chem.*, 2020, **918**, 121298, DOI: 10.1016/j.jorganchem.2020.121298.

320 L. Dkhar, H. Gupta, K. M. Poluri, P. M. Gannon, W. Kaminsky and M. R. Kollipara, Influence of counterions on the formation of supramolecular platinum group metal complexes containing pyridyl thioamide derivatives: antioxidant and antimicrobial studies, *New J. Chem.*, 2022, **46**, 19241–19253, DOI: 10.1039/D2NJ03108F.

321 C. G. L. Nongpiur, A. K. Verma, R. K. Singh, M. M. Ghate, K. M. Poluri, W. Kaminsky and M. R. Kollipara, Half-sandwich ruthenium(II), rhodium(III) and iridium(III) fluorescent metal complexes containing pyrazoline based ligands: DNA binding, cytotoxicity and antibacterial activities, *J. Inorg. Biochem.*, 2023, **238**, 112059, DOI: 10.1016/j.jinorgbio.2022.112059.

322 H. Liu, Y. Qu and X. Wang, Amyloid β-targeted metal complexes for potential applications in Alzheimer's disease, *Future Med. Chem.*, 2018, **10**, 679–701, DOI: **10.4155/fmc-2017-0248**.

323 G. S. Yellol, J. G. Yellol, V. B. Kenche, X. M. Liu, K. J. Barnham, A. Donaire, C. Janiak and J. Ruiz, Synthesis of 2-pyridyl-benzimidazole iridium(III), ruthenium(II), and platinum(II) complexes. Study of the activity as inhibitors of amyloid-β aggregation and neurotoxicity evaluation, *Inorg. Chem.*, 2015, **54**, 470–475, DOI: **10.1021/ic502119b**.

324 R.-S. Shyu, T. Khamrang, J.-R. Sheu, C.-W. Hsia, M. Velusamy, C.-H. Hsia, D.-S. Chou and C.-C. Chang, Ir-6: a novel iridium(III) organometallic derivative for inhibition of human platelet activation, *Bioinorg. Chem. Appl.*, 2018, **2018**, 8291393, DOI: **10.1155/2018/8291393**.